POLITECNICO DI MILANO

Scuola di Ingegneria Industriale e dell'Informazione

Dipartimento di Chimica, Materiali e Ingegneria Chimica "Giulio Natta"

Master's Degree in Chemical Engineering

Adduct of carbon black with serinol pyrrole.
From flocculation studies to its use as reinforcing filler in elastomer nanocomposites.

Supervisor: Prof. Maurizio Stefano **GALIMBERTI**

Co-supervisor: Francesco **Moriggi**

Master's Thesis by:

Valerio Arosio

ID number: 953713

Academic year 2022-2023

To my

family

Table of contents

List of Figures

List of Tables

List of Abbreviations

6PPD: (1,3-dimethyl butyl)-N'-Phenyl-p-phenylenediamine

BET: Brunauer Emmett Teller

BR: Synthetic poly (1,4-butadiene)

CB: Carbon Black

CB-PyC: adduct between carbon black and pyrrole compound

CB-SP: adduct between carbon black and serinol pyrrole compound

DA: Diels-Alder

DSC: differential scanning calorimetry

GC: gas chromatography

GC-MS: gas chromatography-mass spectrometry

HD: 2,5-hexanedione

IR: isoprene rubber (cis-1,4-polyisoprene)

MH: highest achievable torque

ML: lowest achievable torque

NMR: nuclear magnetic resonance

NR: Natural rubber

phc: parts per hundred carbon

phr: parts per hundred rubber

PyC: Pyrrole compound(s)

SP: serinol pyrrole

t_{90}: optimal vulcanization time

Tg: polymer's glass transition temperature

t_{S1}: scorch time

TBBS: N–tert-butyl-2-benzothiazyl sulfenamide

TGA: thermogravimetric analysis

Abstract

This thesis demonstrates that the functionalization of CB with SP has a clear effect on the properties of a rubber composite and, more in general, of a composite based on a lipophilic matrix.

Furnace CB was functionalized with serinol pyrrole (SP) and elastomeric composites were prepared with CB and CB-SP as such and with their mixtures. Composites were as well prepared in paraffin oil. Flocculation studies were performed, by applying literature protocols and a novel protocol developed during the thesis.

The functionalization reduced the surface area of CB. The reduction of surface area appeared to have the prevailing effect up to a certain level of SP: reduction of Payne Effect. The effect of the OH groups becomes evident above a certain level of SP. The mentioned level of SP likely depends on the type of CB and of the matrix.

The effect of SP on the composite's properties was observed to be dependent on the chemical composition of the surrounding: the reduction of the Payne effect was promoted by so called small ingredients of the composite, in particular the polar ingredients. Lower Payne effect was in particular obtained in the vulcanized composite.

This thesis reveals the potentiality of the functionalization of CB with OH groups, which are grafted on the CB surface. These results were obtained on the basis of supramolecular interactions. The next step clearly appears to be the use of a suitable coupling agent, to covalently link CB and the polymer chains.

Chapter 0

Introduction

Rubbers

The huge world of rubbers affects many aspects of the everyday life. The 70 % of the compound consumption is related to the tyre industry, while the rest is for the production of adhesives, footwear and gloves. The use of rubbers is wide thanks to the broad variety of properties given by each different type of structure and composition.[1]

The key property of rubbers is the entropic elasticity whose characteristics are related to the crosslinking system obtained through the vulcanization. This process, discovered by Charles Goodyear in the 1839, allows the rubber to have good dynamic-mechanical properties due to the chemical bonds formed between the polymer chains.

To enhance the mechanical properties of rubbers and to allow them to fulfill the requirements of demanding applications, such as the one in tyre, reinforcing fillers are added. Composites with higher static and dynamic-mechanical properties are obtained. Carbon Black and silica are the most diffused, industrially applied reinforcing fillers for elastomeric composites.

In conclusion, a competitive rubber material is made by a rubber matrix, appropriately crosslinked, loaded with at least a reinforcing filler.

The network of crosslinking

There are many types of crosslinking systems. The one of interest for the tyre compounds is sulphur-based. In this system, some chemicals, such as sulphenamides and thiazoles, help sulphur to form sulphur bridges between the polymer chains. This crosslinking process, known as vulcanization, is characterized by a fast kinetic.

The crosslinking network is not enough to satisfy the requests of the technical applications so reinforcement is mandatory to prepare high-performances compounds.

The mechanical reinforcement and the reinforcing fillers

The characteristics of mechanical reinforcement are related to the characteristics of the filler: the particle dimensions, which steer the surface area, the structure of the filler, i.e. the voids in the particles' aggregates, the surface properties of the filler, which are responsible for the interactions which will be established among the filler particles and with the polymer chains.

Silica (an acidic filler) is characterized by polar groups which are able to generate strong interactions among the filler particles. To develop a positive interaction with the polymer chains, a coupling agent

is needed. Moreover, amines (called secondary accelerators) are used to allow an efficient vulcanization which is mandatory to obtain the dynamic-mechanical properties and a high productivity required by the tyre industry.[2] The ability of the silica/coupling agent system to react with the rubber chains forming strong interactions is the reason for which they are nowadays the preferred choice in the tyre field. Indeed, the silica-rubber bond prevents the formation of the filler network. It is well known that the formation and disruption of the filler network, i.e. the filler networking phenomenon, is source of energy dissipation. On the other side many disadvantages arise from the use of silica: the filler-filler interaction makes the composites more viscous, the composites' shelf life is problematic, and the presence of the coupling agent increases the adhesion to the metal parts of the mixing machines. Last but not least, silica compounds release ethanol which is burnt in factories, producing carbon dioxide.

It would be thus desirable to replace silica with another filler, such as Carbon Black, which reduces the reported drawbacks.

Many different types of CB exist to satisfy each level of reinforcement and properties improvement required by any rubber applications. CB grades with high surface area and structure do exist. The main disadvantage of carbon black is the absence of functional groups on its surface, which could establish covalent interactions with the polymer chains.[3] The possibility to substitute silica as the filler in rubber compounds goes through the modification of the surface of CB, by introducing functional groups on its surface, able to establish chemical bonds with the polymer chains.

Needless to say, carbon black is not *per se* a sustainable filler, from the environmental point of view: it comes from oil and requires much energy to be produced. However, new generations of carbon materials, potentially suitable to replace CB, are appearing on the scene of the reinforcing fillers: biochar, char from end of life tyre compounds, char from end of life thermoplastic materials. These new carbon materials are characterized by large particle size and low surface area. Hence, they are not the ideal reinforcing fillers. Their reinforcing ability could be enhanced by introducing on the surface functional groups able to eact with composites environments, mainly with the polymer chains. A learning curve for the functionalization of a carbon material, developed on CB, would be thus greatly beneficial.

Functionalization of sp^2 carbon allotropes

Both in the academic world and in industry, particular attention has been dedicated to the modification of the surface activity of Carbon Black. Many techniques have been developed[4] with the objective to introduce various functional groups. Among them, the OH functional group could be able to react with the sulphur based silanes during the vulcanization process and then with the rubber chains.

The focus of this thesis is on CB as the sp^2 carbon allotrope, functionalized with OH groups. The functionalization should be performed with a method in line with the basic principles of green chemistry.

Objective of the thesis

The objectives of this thesis were:

- to functionalize CB with the OH functional group, through a sustainable process, meaning sustainable essentially from the environmental point of view, performing the functionalization reaction in line with the basic principles of green chemistry
- to study the effect of the OH functional groups on the self assembling of the CB aggregates, performing flocculation studies in masterbatches obtained through non productive mixing, i.e. in the absence of vulcanizers

The OH groups should favor the aggregation and this aspect should be elucidated, in the absence of chemical reactions involving the OH groups, essentially during the vulcanization step.

- to perform flocculation studies in oil, to investigate the possibility of using a simple method for studying the self assembling ability of CB, without preparing the rubber composite
- to use the functionalized CB as filler in rubber compounds, exploiting the ability of the OH groups to react with other ingredients of the compound

What has been done

The functionalization of CB

The functionalization of CB was performed by using a methodology developed by the group where this thesis was done: the pyrrole methodology.

The pyrrole methodology consists in the reaction, promoted by either thermal or mechanical energy, of an sp^2 carbon allotrope with a pyrrole compound. This methodology, which will be described in detail in Chapter 3, allows to obtain the formation of a covalent bond between the carbon substrate and the pyrrole ring in a two steps mechanism sketched in **Figure 0.1**.[3]

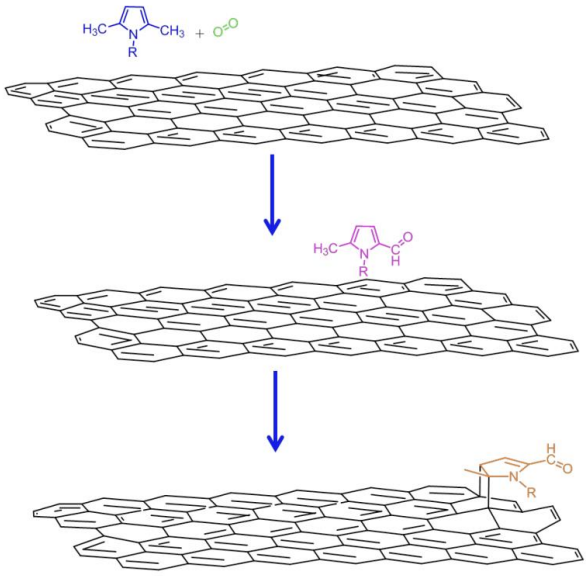

Figure 0.1 Representation of Pyrrole method steps: 1ST pyrrole oxidation, 2ND Diels-Alder reaction

The reaction can be performed by simply mixing carbon black and the pyrrole compound, giving then either thermal or mechanical energy, without using solvent of catalyst.
In this thesis, serinol pyrrole (SP), whose structure is in **Figure 0.2**, was used.

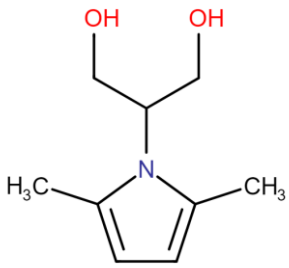

Figure 0.2 The molecular structure of Serinol Pyrrole

The use of serinol pyrrole allows the introduction of OH functional groups.
The functionalization was carried out by using thermal energy.
The preparation of CB-SP adduct was done according to the principles of green chemistry. Dangerous and noxious reagents were not used. The reaction was made between beeds of industrial CB and serinol pyrrole. The yield of the functionalization was calculated.

The flocculation studies in a rubber matrix

The adduct CB-SP has OH groups on its surface. These functional groups could give rise to interactions which in turn could lead to the formation of filler network. As a matter of fact, CB-SP is a polar filler and it is reasonable to expect a behavior similar to the one of silica, although the extent of polarity is remarkably lower. On the other side, the functionalization could lead to the reduction of surface area. A lower surface area would hinder the filler particles' interactions and should thus reduce the extent of the filler network.

In order to investigate the influence of SP on the filler – filler interaction, pristine CB and CB-SP were added to the rubber matrix, with poly(1,4-cis-isoprene) as the rubber. The total amount of filler was fixed at 50 phr and CB and CB-SP were used in different relative ratios.

Flocculation studies were performed. The flocculation of CB and CB-SP was investigated by using the procedure proposed by Tunnicliffe[5]. The composite was kept at high temperature, to cancel the thermo-mechanical history. A strain sweep experiment was then performed by applying a strain from 0.1 % to 10 %, to check the extent of the filler network. Finally, the sample was kept at high and constant temperature, at constant frequency and at a fixed strain value in order to investigate the re-formation of the filler network. The discussion of the results will be the subject of Chapter 8.

The flocculation studies in oil

Oil was used as the matrix to perform flocculation studies. The reason for using the oil were: (i) to study the role played by the filler: the results are reproduced, whatever the matrix is? It is worth noting that the amount of the filler is well above its percolation threshold. Hence, the filler should play the key role. (ii) to have a simpler and quicker test to check the behaviour of CB-PyC. Indeed, many PyC were prepared in the group where this thesis was done and the investigation of the behaviour of the CB-PyC adduct in a lipophilic (rubber) matrix is an important objective.

Dispersions of CB and CB-SP in paraffin oil were prepared, by using a speed-mixer. The total filler content was kept constant: 50 pho (per hundred oil). The pristine CB was replaced with CB-SP, at different relative ratios. The procedure proposed by Robertson[6] was first used and optimization of the procedure was studied, by grinding CB and CB-SP before preparing the mixtures.

The flocculation of CB in these compounds was then evaluated with the same method used for the composites in IR matrix.

The results are in Chapter 9.

CB/SP in a rubber compound

The preparation of rubber composites with a total CB content and different relative amounts of CB and CB-SP were prepared. The preparation was carried out via melt blending in a Brabender® type internal mixer, in two steps. The first one was the so called unproductive mixing. In the second step, vulcanization agents were added. Flocculation study was performed on the uncured composites. Composites were then crosslinked with a sulphur based system. Dynamic-mechanical characterization, in the shear and in the axial mode, was performed.

Results will be discussed in Chapter 10.

The experimental part is presented in Chapter 11. Needless to say, the experiments were at the basis of the collection and elaboration of the results. The experimental part is presented at the end of the thesis, by adopting the traditional style of the Group where this thesis was done.

References

[1] Kauffman, George B. (1989). "Charles Goodyear—Inventor of Vulcanization." Education in Chemistry 26(6).

[2] R. A. Jones, G. P. Bean. The Chemistry of Pyrroles, vol. 34. Academic Press Inc. (London) LTD, (1977).

[3] M. Galimberti, V. Barbera, S. Guerra, A. Bernardi. Facile functionalization of sp2 carbon allotropes with a biobased Janus molecule. Rubber Chemistry and Technology, Vol. 90, No. 2, pp. 285–307 (2017).

[4] Donnet, Jean-Baptiste (ed.). Carbon black: science and technology. Routledge, 2018.

[5] Tunnicliffe, L.B.; Kadlcak, J.; Morris, M.D.; Shi, Y.; Thomas, A.G.; Busfield, J.J.C. Flocculation and viscoelastic behaviour in carbon black-filled natural rubber. Macromol. Mater. Eng. 2014, 299, 1474–1483, doi:10.1002/mame.201400117.

[6] N. Warasitthinon, A.C. Genix, M. Sztucki, J. Oberdisse, C. G. Robertson. The Payne Effect: Primarily Polymer-Related Or Filler-Related Phenomenon? Rubber Chemistry and Technology 1 October 2019; 92 (4): 599–611

Section I – State of art

Chapter 1
The world of rubber

1.1 Introduction

Rubber is a common elastomer which main properties are the high deformability and the ability of recovering quickly and forcibly its initial shape. There are two types of rubber: the natural rubber (coming mainly from the Hevea Brasiliense's three) and the synthetic one. As shown in **Figure 1.1**, the rubber industry is nowadays mainly concentrated in Asia, while in the past it tooks place in Europe and North America.[1] The main applications are in tyre industry, chemical industry and as latex with an overall consumption of about 35 million of ton per year.[2]

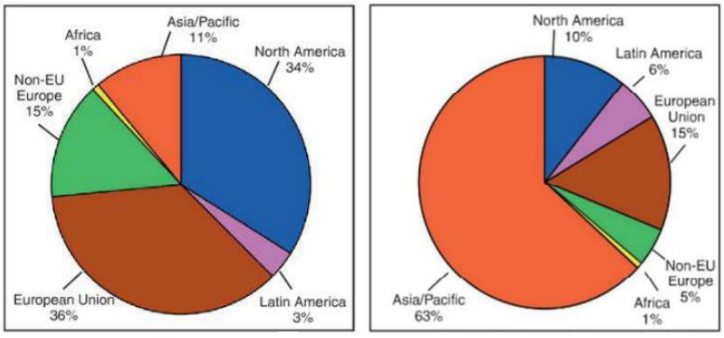

Figure 1.1 The evolution rubber consumption in industry from 1960 to 2019

To be considered a rubber, an elastomeric polymer has to be a high molecular weight molecule with many entanglements and slightly crosslinked with the typical value of Young modulus in the range of 10^3 kPA and its elongation strain at break in the order of 10^3 %. The glass transition temperature (Tg) of the material must be below the room temperature to guarantee the right flexibility to the chains during the exercise: typical Tg are in the range of 233 – 253 K. So the rubber has to be predominantly amorphous and characterized by a random coil structure when it is undeformed.

1.2 Natural rubber

Natural rubber (NR) is a low Tg (-70 °C) polymer made by cis-1,4-polyisoprene (94 %) obtained by coagulation of Taraxacum Kok-Saghyz, Guayule and Hevea Brasiliensis latexes. The main differences between NR and synthetic cis-1,4-polyisoprene is that in natural the cis-1,4 configuration

is higher (more than 99,9 %) and there is a 6% of impurities such as proteins, lipids and other low molecular weight carbohydrates.[3]

The regular structure (**Figure 1.2**) with unsaturated double bonds and the composition is responsible of good chain mobility and mechanical strength, high elasticity, resilience, tear and abrasion resistance, good reactivity towards light, heat ozone and oxygen and low hysteresis. Low permeability, low aging resistance and difficult processability are the bad features that have to be faced during the use of NR.[4],[5],[6]

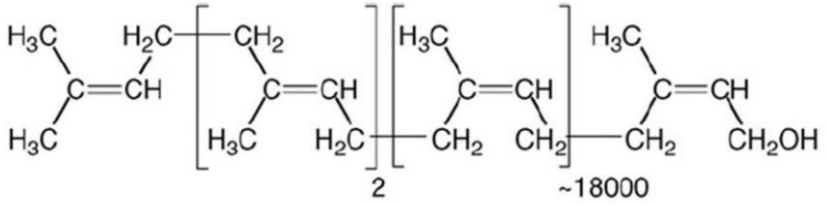

Figure 1.2 Natural rubber chemical structure

The vulcanization process involved for the natural rubber is the sulfur based one, which is used in general for all the unsaturated rubbers.

1.3 Isoprene rubber

Isoprene rubber (IR) is the synthetic version of the natural rubber previously described. It is designed to have properties as close as possible to the one of NR.

In the past the stereoregular synthesis was a problem because the IR obtained in laboratory didn't have high cis-1,4 structure (**Figure 1.2**), which was required to allow the rubber to crystallize under strain. In 1962, Goodyear introduced a Ziegler-Natta catalyst based on titanium-aluminum reaction which was able to produce an isoprene rubber with a content of cis-1,4 structure of 98.5 %.

Nowadays, synthetic polyisoprene rubber shows characteristics a little bit lower than the one of NR, but closer (**Table 1.1**)

Table 1.1 NR-IR main properties comparison

	NR	**IR**
Tg (°C)	-70	-70
Hardness range (IRHD)	30 - 100	35 – 100
Tensile strength (MPa)	24	21
Tear and abrasion resistance	Very good	Good

Depending on the amount and type of reinforcement, fields of application of IR are multiple. It is used in rubber bands, baby bottle nipples, extruded hose as pure, while, if charged with black fillers, it is applied in tires, pipe gaskets, shock absorber bushings industry.
In the last years synthetic isoprene rubber use is increased due to the fact that it doesn't contain proteins present in NR which can cause allergy.

1.4 Theory of rubber elasticity

One of the preferred ways to define the rubber elasticity is the ability of rubbers to achieve a complete recoverability after deformation.
During the application of an external deformation, most of crystalline solids show a little shift of the atomic positions induced by the external force with a consequent increase of enthalpic energy. Then to restore the equilibrium position, represented by the minimum of energy, the system decreases its enthalpy for the elastic recovery: this behaviour is called "enthalpic elasticity".
On the other hand, rubbers present an entropic elasticity coming from the polymer random coil conformation and to the crosslinks present in the structure. In this case the external force induces an alignment of the polymer chains which correspond to a decrease of entropy. Under stress in the absence of crosslinks, there is a rearrangement of the chains to restore the initial entropy which ends with a non-recovered shape (**Figure 1.3.a**) while in the presence of crosslinks the entropy is recovered by going back to the equilibrium position by restoring the random coil configuration (**Figure 1.3.b**). This phenomenon is called entropic elasticity and its nature is strongly related to the crosslinks network which forces the polymer chains to slip one with the each other and not independently.[2], [11]

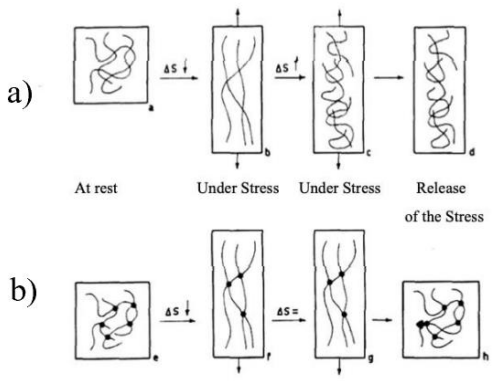

Figure 1.3 Representation of the entropic elasticity behaviour: a) un-crosslinked, b) crosslinked

This behaviour is described by several approaches: the Thermodynamic (based on the macroscopic evidences) and the Statistical (focused on the rubber molecular structure) are reported in the following sections.

1.4.1 *Thermodynamic approach*

As said before, this approach points the attention of the overall macroscopic system that can be considered made by an external force *f* applied on a rubber strip. The work done on the system can be evaluated through the following expression:

$$dW = -PdV + fdL$$

Since the applied force induce a variation in the internal energy *dU*, the Gibbs free energy can be written as:

$$dG = fdL + VdP - SdT$$

To analyze the contributions of the enthalpic elasticity and the entropic one, it is possible to assume that the elastic force is given by the sum of two contribution: f_H (related to the enthalpy) and f_S (the one of the entropy). The resulting equation is known as the elasticity equation of state at constant pressure:

$$f = \left.\frac{\partial G}{\partial L}\right|_{T;P} = f_H + f_S = \left.\frac{\partial H}{\partial L}\right|_{T;P} - T\left.\frac{\partial S}{\partial L}\right|_{P;L} = \left.\frac{\partial H}{\partial L}\right|_{T;P} + T\left.\frac{\partial f}{\partial L}\right|_{P;L}$$

Considering an ideal rubber where the enthalpic contribution is negligible, the elastic force becomes:

$$f \sim -T\left.\frac{\partial S}{\partial L}\right|_{P;L} \sim +T\left.\frac{\partial f}{\partial L}\right|_{P;L}$$

Due to the last expression the expected behaviour of the elastic force with respect to the temperature at constant pressure is linear. On this basis the restoring force has to increase with the temperature which is true for high deformations, when rubber chain behaviour is close to the ideal one, as shown in the following σ/T plot (**Figure 1.4)**.

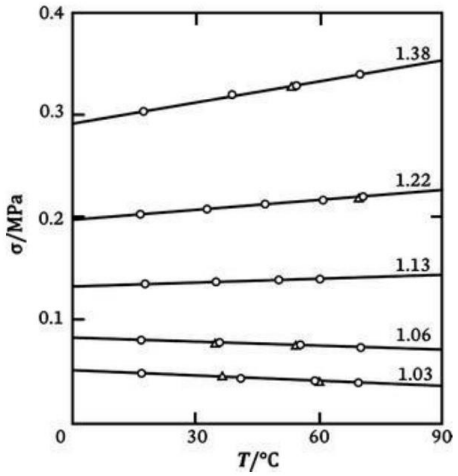

Figure 1.4 Stress vs T at constant length for different elongations.

For small deformations the slope becomes negative. This is related to the fact that the enthalpic contribution is no more negligible. This phenomenon is called thermoelastic inversion and proves that the ideal rubber approximation is valid only if ∂L is not too low (avoiding small deformations).[2],[12]

1.4.2 *Statistical approach*

The statistical approach can explain rubber elasticity considering the deformation of a single chain and the one of the elastic network.[2] This method requires the identification of four main assumptions:

1. the entropy is function only of the system available conformations;
2. the previous conformations are described through a Gaussian distribution function related to the quadratic mean of end-to-end distance;
3. the single chain deformation is proportional to the macroscopic one (the so called "affine deformation assumption");
4. During the deformation the volume remains constant.

Assuming λ as the uniaxial deformation ration and G, the rubber modulus, proportional to the density of crosslinks (ν'), to R, the gas constant and to the temperature, it is possible to write the constitutive equation of the rubber elasticity as:

$$\sigma = G\left(\lambda - \frac{1}{\lambda^2}\right)$$

From this equation two evidences can be denoted. First of all, an increasing of temperature correspond to a higher stress for a given strain (this is related to the decreasing of probability of the compactness

of the conformations and so to a raise in entropy). Also a greater value of crosslinks density leads to higher stress for a constant strain which allows to have an improvement of mechanical properties by increasing the crosslinks.

Comparing now the real and the theoretical trends of the stress/strain plot (**Figure 1.5**), for low deformations ($\lambda < 1{,}5$) the two curves fit well, while for bigger values there is a consistent discrepancy. This variation of behaviours can be described by means of inadequacy of Gaussian statistics for the real case ad high strains, or by the failure of affine assumption hypothesis at high deformations. Also the omission of entanglements, loops, dangling bonds and the crystallization under strain that occurs in real rubber can be the source of this unfitting trends.[2],[12],[13]

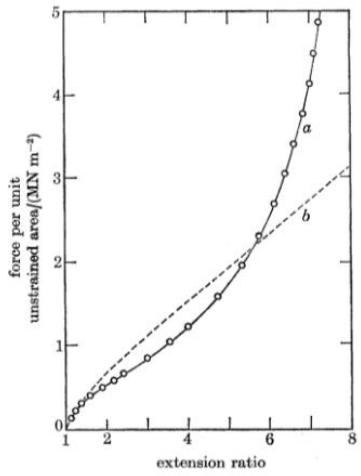

Figure 1.5 Comparison between the stress/strain curve for the real rubber and the theoretical one.

References

[1] P. M.Visakh et. Al. Advances in elastomers I: Blends and interpenetrating networks, 2013.

[2] M. Galimberti, Course of "Chemistry for elastomer composites", Polytechnic University of Milan, 2020.

[3] A.D. Robets, Natural rubber science and technology, Oxford University Press, 1988.

[4] G. R. Hamed, Rubber Chem. Technol, 54, 403, (1981).

[5] A. G. Thomas, J. M. Whittle, Rubber Chem. Technol, 43, 222, (1970).

[6] A. N. Gent, Zhang L. Q, Rubber Chem. Technol., 75, 923-934, (2002).

[7] D. Feldman & A. Barbalata, Springer Science & Business Media, (1996).

[8] L. Friebe, O. Nuyken and W. Obrecht, Adv. Polym. Sci, 204, 1, (2006).

[9] Treads en el Polybutadiene, RubberTechCenter de Lanxess.

[10] J. A. Kent, Handbook of Industrial Chemistry and Biotechnology (11 ed.), Springer, (2006).

[11] Mark JE. Rubber elasticity. J Chem Educ. 1981;58(11):898.

[12] S. E. Turri, Course of "Advanced chemistry for materials engineering", Polytechnic University of Milan, 2018.

[13] L. R. Treloar, The mechanics of rubber elasticity. The royal society publishing, 1976, 301-330.

Chapter 2
Carbon allotropes

2.1 Introduction

The sixth place of the periodic table is occupied by Carbon which is the second abundant element in the human body and the fourth in the universe.[1] With its electronic ground state configuration, $1s^2 2s^2 2p^2$, it is the fundamental element of the organic chemistry because it is able to combine its orbitals giving rise to the hybridized sp^1, sp^2, sp^3. Thanks to the similar energy of the 2s-orbitals and the 2p-orbitals, these configurations of the electronic density can be obtained conferring on Carbon the ability to link a wide range of atoms and also with itself to form many different structures from the common pencil graphite to the precious diamond.[2]

2.2 sp^3 hybridization

The combination of 2s-orbital with three 2p-orbitals leads to four hybridized sp^3 orbitals (**Figure 2.1**). If a structure made of only carbon atoms is considered, four identical σ bonds, tetrahedrally oriented, can be highlighted. This molecular shape is characterized by four carbon atoms that surround each carbon atom. The atoms are covalently linked giving rise to the diamond allotrope which is a natural mineral with a huge hardness and thermal conductivity.[3]

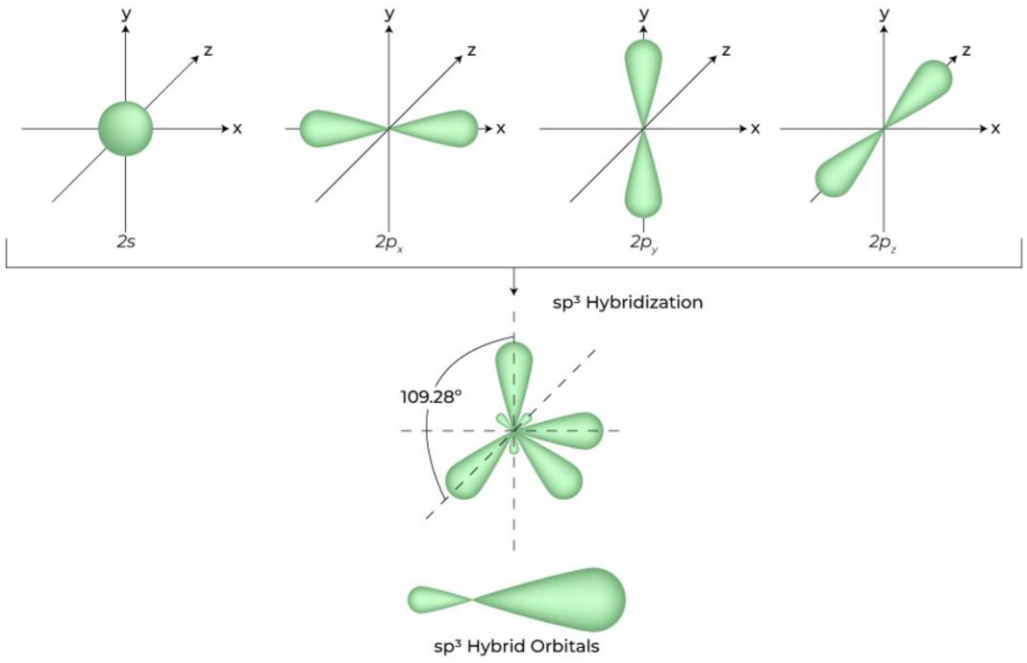

Figure 2.1 sp^3 hybridization

2.3 sp^2 hybridization

sp2 hybridized orbitals come from the combination of the 2s-orbitals and two 2p-orbitals. This configuration, characterized by a planar shape (the trigonal planar geometry), presents three identical orbitals (**Figure 2.2**).

The bonds that can be formed are both of type σ and π which allow to the formation of the six atoms aromatic ring allotrope. This particular repeating unit leads to many different structures.[4] The principals are:

- *fullerene* (carbon atoms are arranged in a quasi-spherical shape made by hexagons and pentagons);
- *carbon nanotubes* (CNT, made by single or multi walled cylinders of graphitic sheets);
- *graphite* (with its multilayer planar hexagonal condensed ring structure it is the most thermodynamically stable form of carbon);
- *graphene* (this is the monolayer buiding block of graphite and if rolled generates single wall CNT);
- *carbon black* (carbon is arranged is nanometric particles with very high surface area constitute by graphitic layers in an onion-like structure).[5]

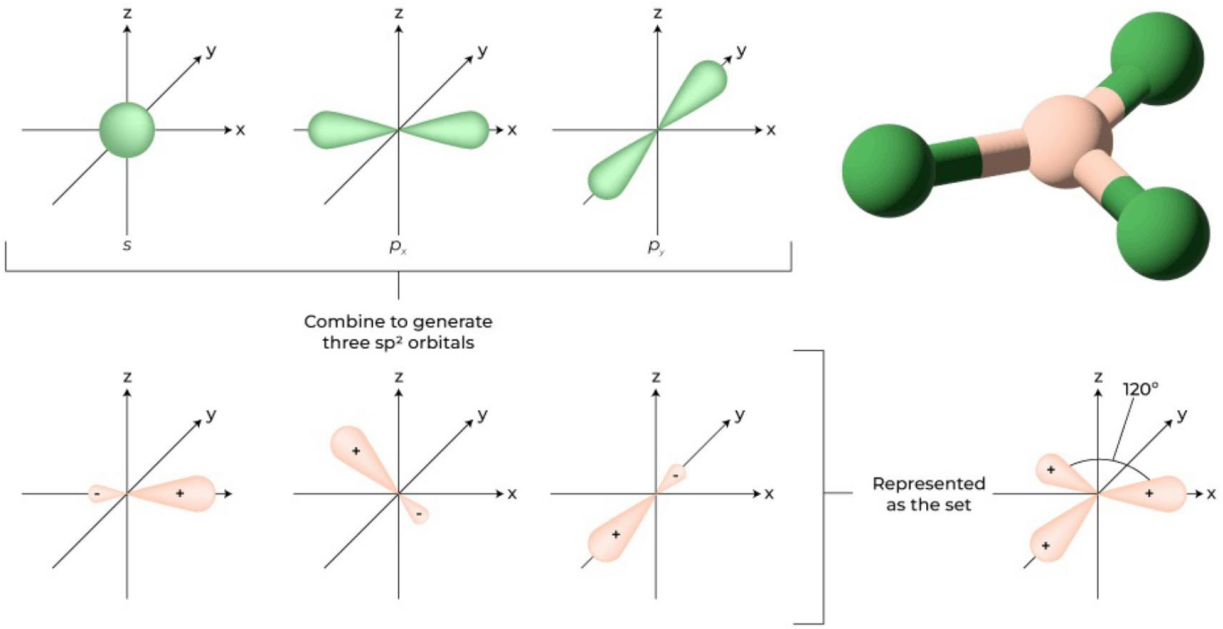

Figure 2.2 sp^2 hybridization

2.3.1 *Carbon Black*

The particular structure of Carbon Black (CB) nanoparticles previously described is responsible to the high filler-filler and filler-polymer interactions that can be obtained between CB and rubber. The instaured network improves the dynamic-mechanical properties, such as strength, rolling and abrasion resistance, of the material making CB an outstanding candidate for the industry, in particular the tyre one, to be used as reinforcing filler.[5] The graphitic layers (**Figure 2.3c**) constituting the structure of Carbon Black give to the particles a less crystalline behaviour with respect to the graphite one and presents three levels of aggregation.

The first one is the primary nanoparticle (**Figure 2.3b**). Its diameter is below 100 nm[6] and can be modified through the production methods to obtain the required application dimension.[7]

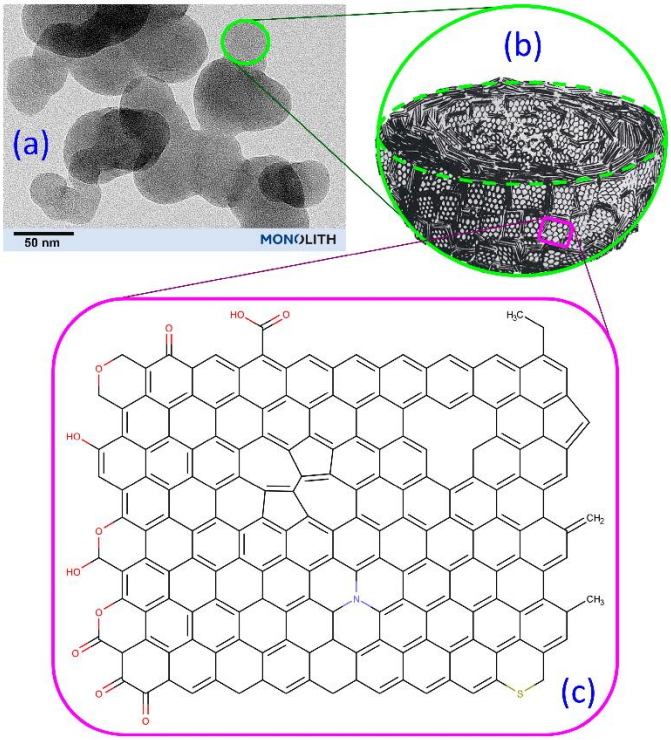

Figure 2.3 CB nanoparticle structure and morphology [8]

The second level of the filler structure is the result of the coagulation of CB nanoparticles forming the so-called *aggregates* (**Figure 2.3a**). The length of this macroparticle is one or two orders of magnitude higher than the first level (**Figure 2.4**).[4] Carbon Black aggregates are the smallest dispersible objects in the polymer matrix, remaining unbroken also during the rubber processing. For this reason, this constitutes the finest reinforcing unit and their structure determines the strength of the reinforcement.

The last aggregation level is generated by the Van der Waals forces instaured between aggregates. This complex is named agglomerate (**Figure 2.4**) and it can be easily broken because of the weakness of its constitutive forces.[4],[9]

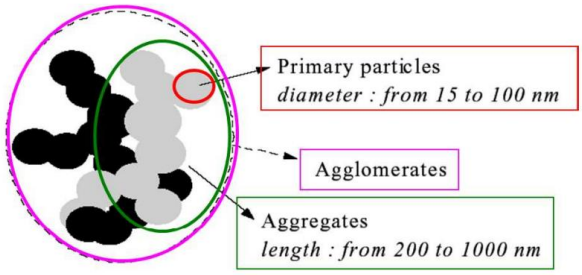

Figure 2.4 Complessive filler structure.[4]

The last portion of the nanofiller complex is made by the voids in between the particles. They are responsible to the adsorption of hydrophobic substances and therefore in which the occluded rubber interacts with carbon black resulting in a more rigid material. In the chapter 4 it will be explained the relevance of the interaction between voids and rubber and its influence on the reinforcing behaviour. Carbon Black is mainly produced via *thermal oxidative process* (about 98 %) taking place in a closed furnace at high temperature or in an open system named gas black process or channel black process. In the first case feedstock is made by natural gas and aromatic oils based on coal tar or crude oil. For the open system case, instead, coal tar distillates and natural gas are the raw materials. Finally, a little amount of industrial CB is produced by *thermal decomposition* (in continuous or discontinuous) through thermal black process, starting from natural gas, or via acetylene black process, involving acetylene as feed. Both of these processes are done in a closed system.[10]

2.4 sp hybridization

The combination of one2p-orbital and the 2s-orbital give birth to the sp (or sp^1) hybridized orbital (**Figure 2.5**).

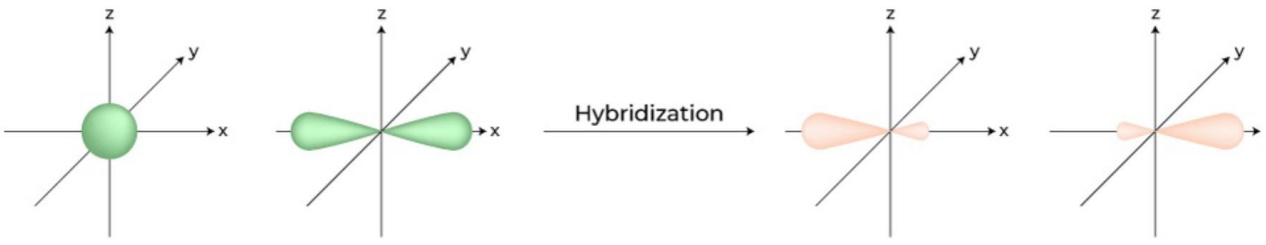

Figure 2.5 sp hybridization

The resulting configuration is a planar, ideally infinite, one-dimension chain of carbon atoms linked by a sequence of triple and single bonds, the α-carbyne, or by a repetition of double bonds, the β-carbyne or cumene (**Figure 2.6**).[11] Both of these structures are highly reactive because of the delocalization of the π-electrons which makes carbyne very unstable. Due to this fact, these types of chain tend to crosslinks and to react with other atoms. The suggested limit is of about 50 consecutive alkynes for a carbyne molecule.

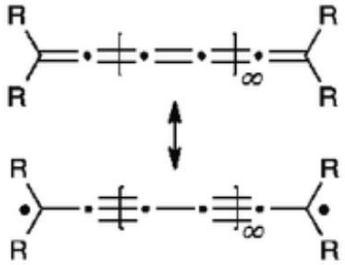

Figure 2.6 Structure of carbyne: α-carbyne (below) and β-carbyne (above)

References

[1] J. B. Reece, & Campbell, Campbell biology. Boston: Benjamin Cummings / Pearson, 2011.

[2] Bitao Pan et al., Carbyne with finite length: The one-dimensional sp carbon, Science Advances, Vol 1, 2015.

[3] N. Brandt, S. Chudinov, Ya.G. Ponomarev. Semimetals Graphite and Its Compounds, Vol. 20.1, 1988.

[4] M. Galimberti, Course of "Chemistry for elastomer composites", Polytechnic University of Milan, 2020.

[5] N. Probst, E. Grivei, Structure and electrical properties of carbon black, Carbon, Volume 40, Issue 2, 2002.

[6] G. R. Hamed, Rubber Chem. Technol, 73, 524, (2000).

[7] Advanced in Polyolefin nanocomposites, Edited by Vikas Mittal, CRC Press, (2011), 12.

[8] C. G. Robertson, N. J. Hardman. Nature of Carbon Black Reinforcement of Rubber: Perspective on the Original Polymer Nanocomposite. Polymers 2021, 13, 538.

[9] S. E. Turri, Course of "Advanced chemistry for materials engineering", Polytechnic University of Milan, 2018.

[10] J. B. Donnet, R. C. Bansal, M. J. Wang Carbon Black Second revision, Science and Technology.

[11] Heimann RB, Evsyukov SE, Kavan L. Carbyne and carbynoid structures. Vol 21. Springer Science & Business Media; 1999.

Chapter 3
Functionalization of carbon black

3.1 Introduction

To improve carbon-based material properties, a growing research field exploits the surface modifications of carbon allotropes to face the market and material requests and enlarge their fields of application. These manipulations, named functionalization, are made through many methods such as covalent or non-covalent modifications including hydrogen bonding, π – π, π – cation/anion and Van der Waals interactions.[1]

This chapter is about the state of art of the functionalization of carbon black to increase its dispersibility in polar media. In the last century, deep studies were made by researchers to achieve a better *oxidation of CB*. Comparing the process involving nitric acid with the in situ oxidation of CB using O_2 and argon at 350 °C, it is observed the formation of epoxides (cyclic ethers).[2] Through this, it is possible to obtain OH groups on the surface of carbon black that can be exploited to perform the *silanization of oxidized CB*. Here, depending on the type of silane agent, dual fille systems (such as X50S) can be synthesized and added to the rubber composites to increase filler-polymer compatibility.[3],[4] On of the most recent functionalization is the "pyrrole methodology".[5] In this work, serinol pyrrole (2-(2,5-dimethyl-1H-pyrrol-1-yl)propane-1,3-diol) is used to prepare high performances functionalized CB filler for rubber compound to substitute the pristine one in the composites.

3.2 Non covalent functionalization

There are many types of non-covalent functionalizations (**Figure 3.1**). In all cases the electronic configuration and the properties of the carbon allotrope are not altered by the functional groups of the chemical agents involved due to their less invasive introduction in the system compared to the covalent approach.

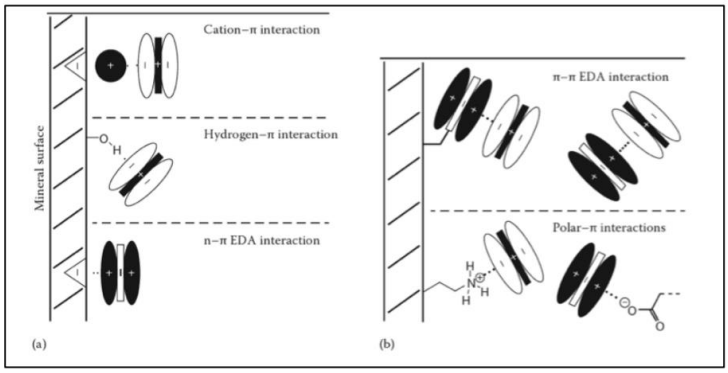

Figure 3.1 Representation of some non-covalent interaction involving aromatics and π-system[1]

3.2.1 *π-π interaction*

The overlapping of the p-orbitals of a system made by a π-acceptor and π-donor particles is called π-π interaction. This type of weak bond, that can take place for instance between an aromatic molecule and a sp^2 carbon allotrope, has a significant impact in the change in solubility of the carbon material without modifying the electronic band structure and its crystalline domain.[6],[7] On the other hand electrical and thermal conductivity are only weakly affected by non-covalent functionalization.

3.2.2 *Cation-π interaction*

This type of interaction is the one involved in the motion of ions through the selective membrane technology[8]. It is established between the π electron cloud of the carbon allotrope and the cation.

3.3 Covalent functionalization

Covalent functionalization is a strong perturbation of the carbon system by the formation of a covalent bond with an organic molecule which can end with the disruption of the hybridization. The modification of the material properties is significant.

To establish this bonds, intrinsic enhanced chemical reactive sites have to be present. They are called defects of the carbon atoms and they can be of three types:

- *unsaturated bonds* (lack of bonding between carbon atoms due to vacations, dislocations and atoms in interstitial positions);
- *re-hybridization defects* (thanks to the presence of different hybridizations in the same allotrope);
- *topological defects* (they can lead to deformations and change in chirality due to the presence of pentagons in the hexagonal cell structure).

Both the carbon allotrope and the agent must have functional groups such as -COOH, -OH and $-NH_2$ on the surface to make the covalent bonds through the following reactions: free-radical reaction, carboxylation, amidation, fluorination, diazonium and Bingel reactions. Strong chemical agents such as aryl diazonium salts, benzoyl peroxide, styrene, nitrenes and carbenes are required for this kind of functionalization.[1]

In this thesis work the functionalization method applied is based on the Diels-Alder reaction and it is detailed described in the following paragraph.

3.4 Pyrrole methodology

This process is a sustainable two-step modification of carbon allotropes through insertion of a active pyrrole substance thanks to the use of only mixing and thermal energy. This kind of functionalization

does not require solvents or catalysts[9] and involves the defects present on the carbon atoms due to their chemical reactivity.[10] The only one condition for the formation of these chemical bonds is the presence both on the carbon allotrope surface and on the pyrrole of the following functional groups: -COOH, -OH and/or -NH_2.[11] Hence, the first step of this mechanism is indeed the *oxidation of the pyrrole* (**Figure 3.1**). This reaction take place directly in proximity of the CB surface that acts as catalyst.

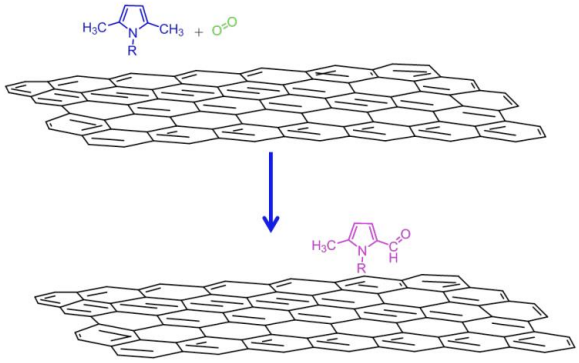

Figure 3.2 Hypothesized mechanism of pyrrole methodology oxidation of generic PyC.[12]

The second step (**Figure 3.2**) is the Diels-Alder reaction that occurs between the oxidized pyrrole as the dienophile and the carbon black graphitic surface as the diene.[13] The features of this particular reaction used to insert functional groups on CB surface are reported in the following paragraph.

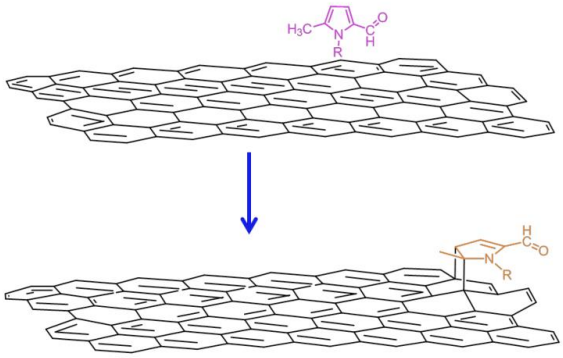

Figure 3.3 Hypothesized mechanism of pyrrole methodology Diels-Alder.[12]

3.4.1 *Diels-Alder reaction*

Diels-Alder reaction (DA) takes place between a substituted alkene, the so-called dienophile, with at least one π-bond and a conjugated diene, i.e. represented by a portion of the aromatic rings of the graphitic layer of carbon black. The reaction path, briefly sketched in the **Figure 3.3**, involves a concerted mechanism in which three π-bonds are broken forming one π-bond and two σ-bonds: the

reaction is indeed thermodynamically favoured. The resulting cyclic adduct is obtained without passing through intermediate of reaction.

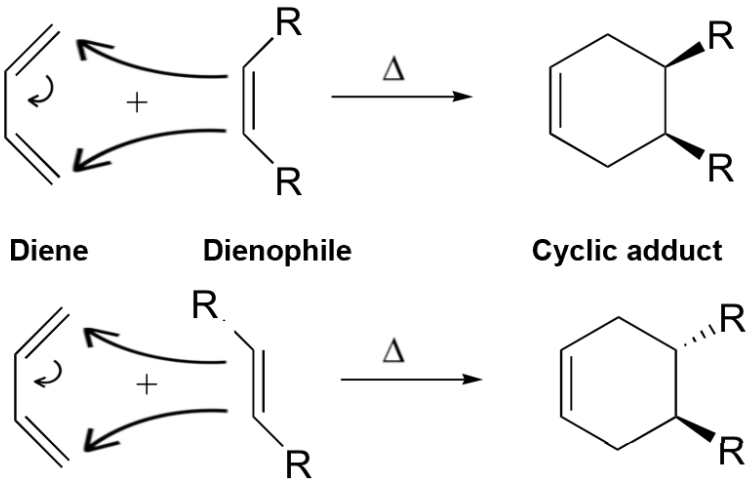

Figure 3.4 DA generic concerted mechanism representation.

This **Figure 3.4** shows also that DA reaction has a good regio- and stereoselectivity therefore it can be a good choice to introduce functionalities on carbon allotrope peripherical positions without affecting surface bulk properties.

The pyrrole methodology is a solid-state process with an air flux for the first step. Heat and agitation are provided for the Diels-Alder reaction with a maximum functionalization yields achieved for values of temperature in between 150 °C and 180 °C.[12]

References

[1] V.K Thakur, M.K. Thakur. Chemical Functionalization of Carbon Nanomaterials: Chemistry and Applications (1st ed.). CRC Press, 2015.

[2] P. E. Fanning and M. A. Vannice. Carbon, 31, 721, (1993)

[3] L. Bokobza and O. Rapoport. Macromolecular Symposia, 194, 125, (2003).

[4] N. Nugay and B. Erman, J. Appl. Polym. Sci., 79, 366, (2001).

[5] G. Leonardi, A. Valerio, V. Barbera, A. Truscello, G. Terraneo, M. Galimberti, R. Sebastiano, A. Citterio. Synthesis of pyrrole derivatives of serinol for functionalization of carbon allotropes (2017).

[6] M. Galimberti, V. Barbera, S. Guerra, et al. Biobased janus molecule for the facile preparation of water solutions of few layer graphene sheets. RSC Advances. 2015;5(99):81142-81152.

[7] M. Galimberti, V. Barbera, S. Guerra, A. Bernardi. Facile functionalization of sp2 carbon allotropes with a biobased janus molecule. Rubber Chemistry and Technology. 2017;90(2):285-307.

[8] J. P. Gallivan, D. A. Dougherty, Proc. Natl. Acad. Sci. USA, 1999, 96, 9459-9464.

[9] M. Galimberti, V. Barbera, S. Guerra, A. Bernardi. Facile functionalization of sp2 carbon allotropes with a biobased janus molecule. Rubber Chemistry and Technology. 2017;90(2).
[10] I. Y. Jeon et Al., Edge-carboxylated graphene nanosheets via ball milling PNAS April10, 2012 vol.109 no.15, 5593.
[11] Vinay Deep Punetha et. Al. Functionalization of carbon nanomaterials for advanced polymer nanocomposites: A comparison study between CNT and graphene. Progress in Polymer Science, 2017, 67, 1-47.
[12] Barbera, V., Brambilla, L., Milani, A., Palazzolo, A., Castiglioni, C., Vitale, A., ... & Galimberti, M. (2019). Domino Reaction for the Sustainable Functionalization of Few-Layer Graphene. Nanomaterials, 9(1), 44.
[13] V. Barbera, A. Bernardi, A. Palazzolo, A. Rosengart, L. Brambilla, M. Galimberti. Facile and sustainable functionalization of graphene layers with pyrrole compounds. Pure and Applied Chemistry. 2018;90(2):253-270.

Chapter 4
Theory of the rubber reinforcement

4.1 Introduction

As anticipated in the previous chapters, rubbers have to be reinforced to improve material strength and stiffness without losing elastic properties. To do this, reinforcing fillers are added to the vulcanized rubber obtaining elastomeric composites with increasing performances with respect to the amount and structure of the employed fillers.

According to the reinforcing ability, which depends on the size of the particles, it is possible to divide fillers in four categories:

- *reinforcing* (0.01 – 0.1 μm)
- *semi-reinforcing* (0.1 – 1 μm)
- *diluents* (1 - 10 μm)
- *degradants* (above 10 μm)

The first type is the one used in the rubber industry, in particular carbon black and silica.[1] Also zinc oxide, silicates, and carbonates can be present in some composites for specific applications.[2] In this thesis the attention is pointed on the improvement of the interaction between rubber and CB by its functionalization with serinol pyrrole and on a study on the compatibility of these reinforcing fillers with the rubber and oil matrices.

4.2 Nanostructure reinforcing fillers

In the chapter 2 the morphology of a nanofiller structure was presented as the result of the coagulation of the filler particles in aggregates and the voids in between them. This system is named **structure**: the higher is the voids amount, the higher is the structure. Since the occluded rubber interacts with fillers in the voids, the structure influences the reinforcing behaviour, mainly at high strain.[2]

The application of reinforcing nanofillers allows the composites to increase of at least one order of magnitude its tensile strength, its stress at given elongation and the modulus. Also tear, fatigue and abrasion resistance become higher.[3]

The mechanism of reinforcement is affected by three main factors: *filler morphology*, *dispersibility* and *surface physics* and *chemistry*.[4]

4.2.1 *Filler morphology*

As written at the beginning of this paragraph, the authors of the theory of reinforcement explain that the degree of disorder of the aggregation of the primary filler particles is at the base of the determination of the occluded rubber and the real filler volume.[4] This entangled polymer fraction, trapped in the aggregates voids, behaves as the near filler particles giving to the material an improvement of the mechanical properties.[2] Therefore, it is possible to conclude that a greater anisotropy of the aggregates confers a higher reinforcement.

The other relevant parameter related to the morphology of the system is the aggregate **surface area** which strictly depends on the particles size. Smaller filler dimensions correspond to bigger value of available contact area between filler and rubber. This ends up to an increase of filler-polymer interaction and so to a theoretical better reinforcement.[2] The problem is that also the filler-filler interactions are higher with a reduction of the particles size that causes a bad dispersibility of the filler in the rubber matrix.[5]

4.2.2 *Dispersibility*

Due to depletion forces, chemical incompatibility and different surface energies, it is difficult to obtain a homogeneous dispersion of filler in polymeric latex, but it is mandatory to improve dynamic-mechanical properties of the material. Filler structure and surface energy are the main influencing factors of the dispersibility: high degree of dispersion is usually registered for high filler structure and similar surface energies. Also the disruption of the agglomerates system leads to a well dispersed filler network.[5],[6] In this thesis work the effects of grinding and rotary mixing are studied.

4.2.3 *Surface properties*

The interaction between polymer and filler is founded on the physical absorption of the elastomeric chain on the particle surface and on the covalent bonds that can be instaured between rubber and chemical active sites of the reinforcing material.

Focusing on carbon black, on the physical point of view, some defects are present on the graphitized surface. These amorphous vacancies can give birth to strong interactions between polymer and filler. On the other hand, considering the surface chemical nature of CB, oxidized species take place and they are responsible to lesser material performances.[4] Also organic and mineral impurities can be deposited during the manufacturing process. They don't affect significantly the reinforcement, but speed up the vulcanization process.[1],[4] To improve the chemical affinity functionalized carbon black can be introduced in the polymer composite.

4.3 Elastomer reinforcement

The reinforcement of elastomers due to the addition of fillers depends both on polymer and filler properties. The influencing factors previously described in this chapter impact on the loaded composite differently with respect to the amplitude of the applied deformation.

4.3.1 *Small and moderate deformation reinforcement: the Payne effect*

Applying a dynamic-mechanical stress (i.e. sinusoidal at constant frequency) on an elastomer-filler composite, it is possible to measure the complex shear modulus, whose trend is represented in the **Figure 4.1** and described by the following general expression:

$$G^* = G' + iG^{"}$$

G' and G" are easily devived.

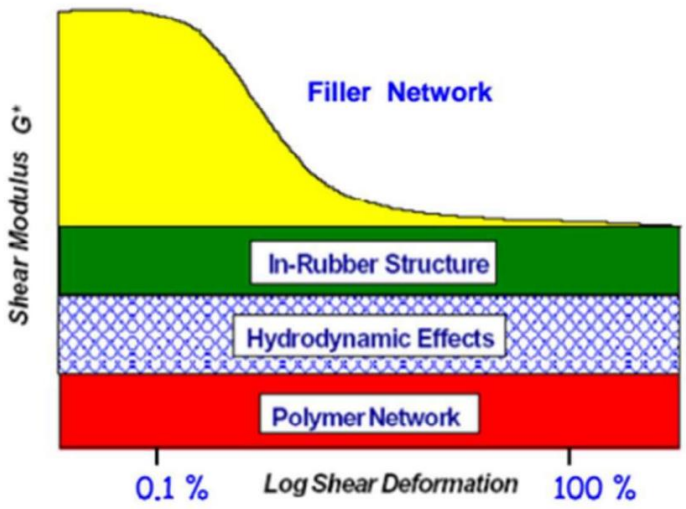

Figure 4.1 Trend of loaded composites' shear modulus vs log of shear deformation

In this **Figure 4.1**, it can be seen that the overall modulus is given by the sum of different contributions. Three of them are independent from the strain amplitude, while the one related to the filler network is strongly relevant only for small deformations.

The *polymer network* contribution depends on entanglements, crystallinity domain and rigid bonds domain. The *hydrodynamic effects* one comes from the presence of the occluded rubber adsorbed on the rigid filler surface that can't be deformed while the rest of the elastomer is subjected to the strain amplitude due to the high stress. For these two contributions, the shear modulus is function of the volume fraction through the next expression:

$$G^* = G_0^* \left(1 + 0{,}67 * f * x + 1{,}62 * f^2 * x^2 \right)$$

G_0^* is the modulus for the unloaded rubber calculated under the same stress, f is the geometrical factor (which takes into account the deviation from perfect spherical shape) and x is the filler volume fraction.

The *in-rubber structure* contribution depends on the amount of the occluded rubber which behaves as the filler increasing the rigid fraction. The G* equation remains the same, but the filler volume fraction x is replaced by a higher value x_c.

The last and real related to the filler nature contribution is the one of the *filler network.* For small deformations (strain less than 10 %) the elastic response is due to the filler surface: the higher the content and/or the smaller the particles, the greater is the reinforcement. After this point the filler network is destroyed with a relevant dependence of the modulus on the structure of the filler. G' and G" decrease due to the progressive desorption of the polymer chains with an overall fall of the shear modulus till the effect of the reinforcement is no more relevant. This phenomenon is called **Payne effect**.[2]

4.3.2 *Large deformation reinforcement*

Since for high deformation, applying a sinusoidal stress, there is no sinusoidal strain, to evaluate the deformation response a quasi-static uniaxial extension test is used (**Figure 4.2**).[2]

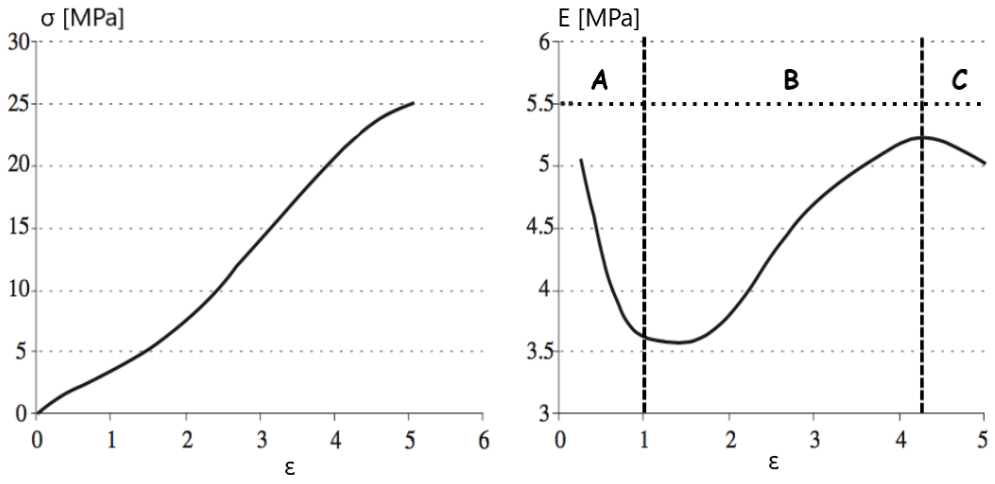

Figure 4.2 Quasi-axial stress strain curve (left) and Young modulus vs strain trend (right)

For strain below 100 % (region A of **Figure 4.2**) the behaviour of the modulus is explained by the Payne effect. Then, for ε > 100 % (region B), the increasing of the Young modulus can be justified by the paradox of elastomers.[2] Rigid fillers are defined undeformable so, during a macroscopic

deformation, the local stress induced is higher. Due to this fact, the elongation at break (region C) should be theoretically lower. The observed composite behaviour (**Figure 4.3**) is, instead, the opposite thanks to the so-called **strain amplitude effect**.[4]

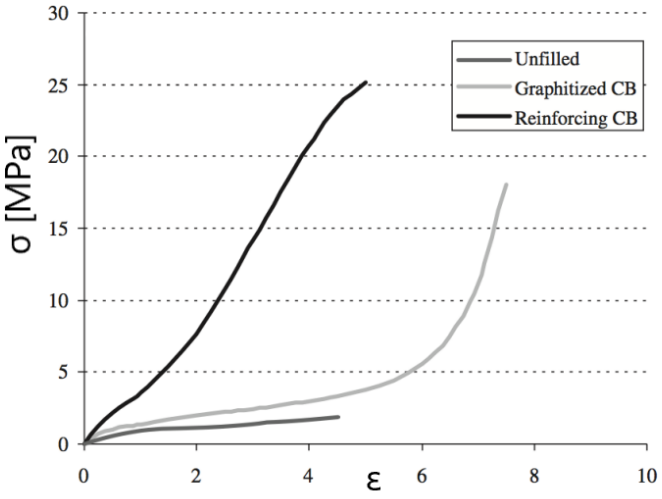

Figure 4.3 Stress-strain curves of unloaded, graphitized CB and reinforcing CB

This increase of the elongation at break is the result of the continuous adsorption-desorption process of the rubber chains that link the filler particles. As shown in the **Figure 4.4**, at large deformations this ends up with a homogenization of these short segments ensuring a local distribution of stresses achieving a higher fracture strain.[7]

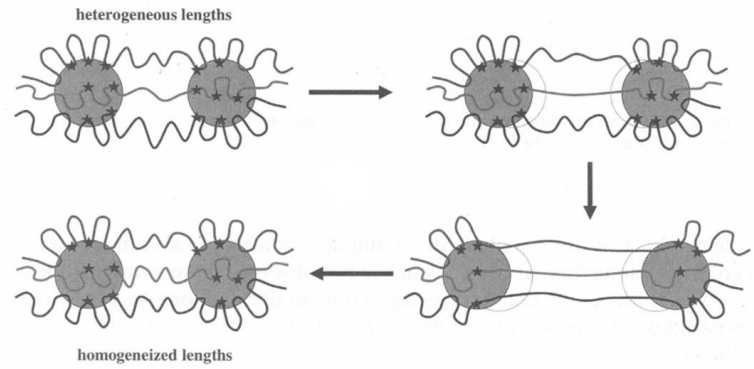

Figure 4.4 Homogeneization of polymer chains in between filler particles.[2]

References

[1] S. E. Turri, Course of "Advanced chemistry for materials engineering", Polytechnic University of Milan, 2018.

[2] M. Galimberti, Course of "Chemistry for elastomer composites", Polytechnic University of Milan, 2020.

[3] A Salim, A Hassan, H Ismail, Polymer-Plastics Technology and Engineering, 2018, 57(6).

[4] J. B. Donnet, E. Custodero, Chapter 8 - Reinforcement of Elastomers by Particulate Fillers, Editor(s): J. E. Mark, E. Burak, C. M. Roland, The Science and Technology of Rubber (Fourth Edition), Academic Press, 2013.

[5] C. G. Robertson, N. J. Hardman. Nature of Carbon Black Reinforcement of Rubber: Perspective on the Original Polymer Nanocomposite. Polymers 2021, 13, 538.

[6] N. Warasitthinon, A. C. Genix, M. Sztucki, J. Oberdisse, C. G. Robertson. The Payne Effect: Primarily Polymer-Related or Filler-Related Phenomenon?: Rubber Chemistry and Technology (2019) 92 (4): 599–611.

[7] J.B Donnet, E. Custodero. in The Science and Technology of Rubber Third Ed.; Mark, J.E.; Erman, B.; Eirich, F.R. Eds. Elsevier Academic Press 2005, Chapter 8, 367-400.

Chapter 5
Vulcanization: the importance of crosslinking network

5.1 Introduction

To be employed in the industrial world, a rubber has to be vulcanized in order to decrease its plasticity to have an higher elastic response. In this chemical process, giving heat in presence of vulcanization agents, the network of crosslinking is formed: covalent bonds are established between polymer chains as shown in the following **Figure 5.1**:

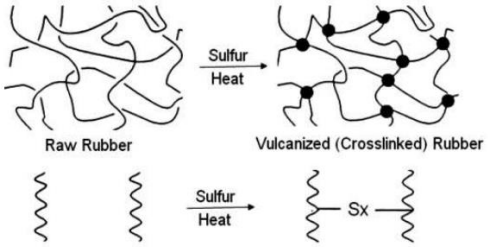

Figure 5.1 Conceptual representation of network generation.

The higher the degree of crosslinking is, the greater the retractile force and the lower the amount of permanent deformation are when tensile loads are removed.[1]

5.2 Process features

Vulcanization is carried out by adding to the rubber vulcanizing agents and additives, such as accelerators and dispersants, while mixing under pressure and heating. Temperature and process conditions strictly depends on the crosslinking methods.

5.2.1 *Vulcanizing agents*

The most used vulcanizing agents are peroxides and sulfur.[1] The first one is characterized by a radical mechanism of reaction that requires specific temperature conditions and involves the hydrogen extraction from rubber chains forming polymeric radicals. The links between elastomeric chains is obtaining through the combination of these radicals (**Figure 5.2**). Therefore, this method is applied for completely satured chains.

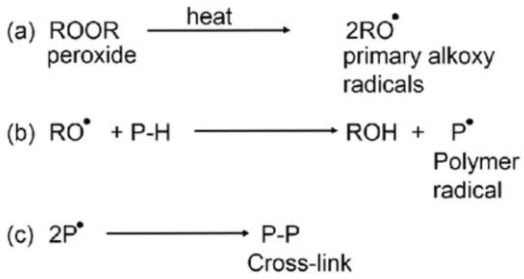

Figure 5.2 Scheme of generic peroxide vulcanization reaction.[2]

For unsaturated polymers, instead, vulcanization occurs via sulfur-based mechanism. In this process cyclic octamer elemental sulfur (S_8) is open starting from 140 °C. The linear sulfide segments are then able to react with the double bonds of the rubber chains: the crosslinking network is established thanks to formation of the C-S_X-C bond (**Figure 5.3**). The lower the sulfides chain is (small x), the higher is the thermal stability of the material which can be tuned varying the concentration of sulfur and of the accelerants.[3]

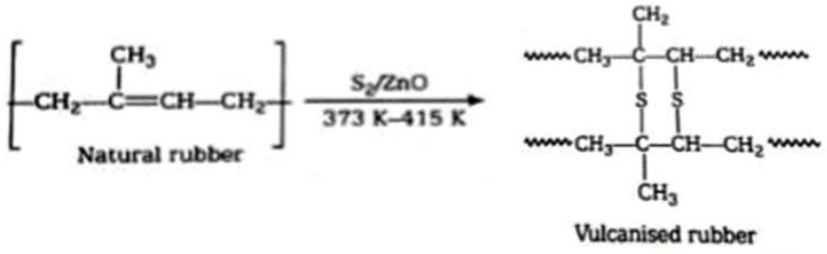

Figure 5.3 Scheme of generic sulfur vulcanization reaction with NR.

As anticipated in **Figure 5.3**, zinc oxide (ZnO) is added to improve sulfur decomposition. Also stearic acid is used to increase ZnO solubility in rubber matrix and organic accelerants (as TBBS and 6PPD) are employed to increase the reaction kinetics. Only thanks to these additions the sulfur-based vulcanization results economically practicable.[1]

5.2.2 *Curing curve*

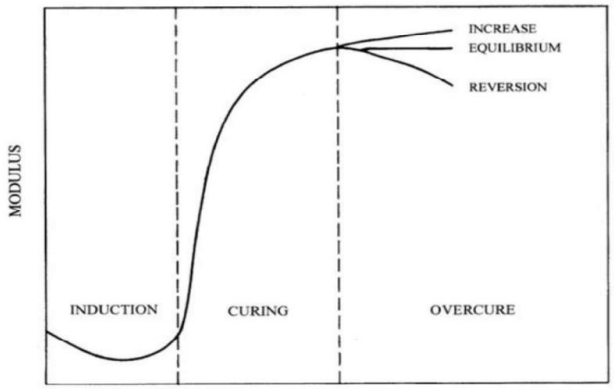

Figure 5.4 Qualitative rubber curing curve

Figure 5.4 represents qualitatively the vulcanization curing of rubbers. The curve is the measurement of the evolution of the dynamic modulus (or torque) in time and it is divided in three zone.

The first one is the **induction** zone in which the modulus wanes because crosslinking has not yet begun. After reaching the minimum, associated with the polymer viscosity, the modulus start to increase entering the curing phenomenon.

The **curing** zone is the time range in which crosslinking network rises in the rubber matrix. Since the curve is related to the vulcanization kinetics, the faster the networking process is the greater is the slope.

The last zone is the **overcure** one. Here three different scenarios can be highlighted: an further increasing, the most common plateau (due to equilibrium) and, in case of polysulfides bonds breakdown, reversion. This last case should be avoided because material undergoes worse mechanical properties.[1]

5.2.3 *Parameters of the process*

The most indicative parameters to analyze the vulcanization process are the ones obtained from the curing curve, the degree of curing, α(t), and the vulcanization rate.

The following list resume the main curing parameters:

- *minimum torque* (M_L) that is the lowest possible torque value. It gives an idea of the composite viscosity;
- *maximum torque* (M_H) which is reached at the highest crosslinking level at the process temperature;

- *delta torque* (ΔS). It is the difference between M_H and M_L representing the crosslinking density;
- *scorch time* (t_{S1}) that is the time needed to increase the torque value of 1;
- *optimal curing time* (t_{90}) which is the time at which the 90% of M_H is obtained.

The *degree of curing* can be determined through rheometer test or as the integral of the DCS tecnique curve related to a single curing reaction event.
In the first case α(t) is proportional to the rubber stiffness and it depends on the crosslinking density.[1] Its expression is:

$$\alpha(t) = \frac{M_t - M_0}{M_\infty - M_0}$$

where M_t is the torque at time at which the degree of curing is evaluated, M_∞ is the torque value at the end of the process and M_0 is the torque at the beginning.
On the other hand, α(t) is function of the heat of reaction as the enthalpy evaluated at time t with respect to the total curing released enthalpy as written in the following formula:[1]

$$\alpha(t) = \frac{\Delta H(t)}{\Delta H_{TOT}}$$

The last parameter here reported is the *vulcanization rate*. This is the derivative of the degree of curing in time and it is the result of two contributions:

- $k(T) = k_0 e^{-\frac{E_{ATT}}{RT}}$, that represents the temperature dependence like the Arrhenius law;
- $f(\alpha) = \alpha^m (1-\alpha)^n$, where $0 \leq m \leq 1$ and $n \geq 1$ [1]

The combined expression is:

$$\frac{d\alpha(t)}{dt} = k(T) f(\alpha)$$

5.3 Vulcanization effects

The sulfur and additives amount and the curing time influences the mechanical properties by decreasing plasticity and hysteresis, increasing elasticity, tensile strength, hardness and reducing elongation and permanent deformations.[5]

On the other end, reticulation increases the density of the elastomeric compound due to the crosslinking network. This prevents the motion of dispersed molecules of gas and liquid which correspond to lower permeability.

Also chemical properties are affected. The permeability by the common solvents of the rubber-filler vulcanized composite decrease considerably making material chemically stable with a higher resistance to ageing effect.[6]

References

[1] M. Galimberti, Course of "Chemistry for elastomer composites", Polytechnic University of Milan, 2020.

[2] M. Azevedo, A. M. Monks, R. Kerschbaumer, C. Holzer. Peroxide-based crosslinking of solid silicone rubber, part II: The counter-intuitive influence of dicumylperoxide concentration on crosslink effectiveness and related network structure. May 2023.

[3] A.Y. Coran, Chapter 7 - Vulcanization, Editor(s): J. E. Mark, E. Burak, C. M. Roland, The Science and Technology of Rubber (Fourth Edition), Academic Press, 2013.

[4] S. E. Turri, Course of "Advanced chemistry for materials engineering", Polytechnic University of Milan, 2018.

[5] A. D. Roberts, Natural rubber science and technology, Oxford University Press, (1988).

[6] T. Kakub, A. Matsuura, S. Kawahara, Y. Tanaka, Rubber Chem. Technol., 71, (1998).

Chapter 6
The world of tires

6.1 Introduction

A pneumatic tire is a toroidal, high performances composite exhibiting characteristics of flexible membrane pressure container with load carrying, cushioning and road handling capabilities.[1] To enhanced traction a uniform pressure distribution on road contact area is required. To achieve this condition, it is necessary to design a pneumatic with good ground adherence and deformability to face street irregularities with a special focus on the optimization of the rolling resistance.[2] This last, briefly defined as the energy dissipated per unit of length, is proportional to the hysteresis that has to be minimized in dry conditions to reduce fuel consumption, while in wet traction higher values are required to have more grip. To tune this parameter Tan(δ), defined as the ratio of G" and G' described in the chapter 5, can be managed by choosing the right materials for tire compound. Said this, it is easily understood that tire is not made by just a single type of rubber, which is also too weak and flexible, but by a combination of different rubber types, fillers and reinforcing structures.[1]

6.2 Structure of a radial tire

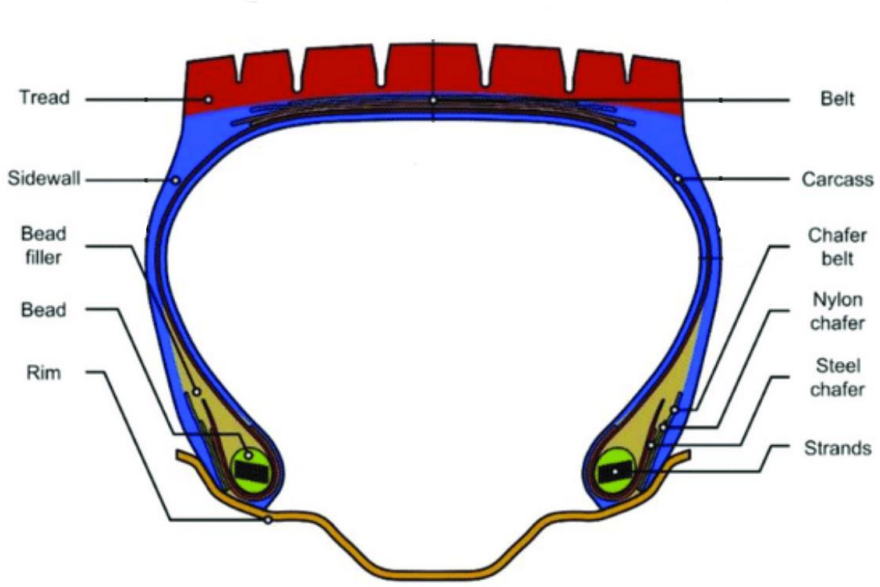

Figure 6.1 Cross section of a radial tire

Figure 6.1 represents a section of a common tire whose main parts are described in the following list.

- *Tread*: it is the part in contact with the road so it is made by a mixture of SBR, for low hysteresis at high temperature and high rolling resistance at low temperature, BR, to increase the life time of the pneumatic, and NR, whose high strain induced crystallization promotes tear resistance.[3] Also CB (for lower hysteresis), silica (to improve rolling resistance behaviour) and plasticizers (to modulate hardness and stiffness) are added.[4]
- *Carcass*: it is the primary reinforcing structure made by a series of plies of cord of steel, polyesters and other textile materials. In the past it ran diagonally in opposite directions, inclined by 25 to 40 degrees angle. Nowadays it extends transversally from bead to bead allowing large radial deflections and minimal lateral stiffness.
- *Belt*: also called steel or restraining belt, it is placed above the carcass to prevent radial growth and directional stability. It is composed by steel, aramid and inorganic glass fibers cords coated by rubber to reduce buildup of heat and improve handling and abrasion resistance.[1]
- *Sidewall*: it starts from the tread and goes to the bead. Its aim is to protect the carcass by giving lateral stability and aging and fatigue resistance. It is made, therefore, by NR/BR loaded with CB of type N660 or N550 for low hysteresis and aromatic amines to protect from O_3 degradation.
- *Liner*: it is a thin layer of butyl-rubber with halogenated derivatives placed under the carcass to promote air impermeability (thanks to silica or addition) and compressed gases retention.[4]
- *Bead*: this is the part in contact with the rim whose main purpose is to prevent air leakage and transfer the load. For these reasons high structured carbon black, low amount of silica and phenolic resins are mixed with natural rubber or NR/BR compound to have a material with high tensile strength and abrasion resistance and low thermoplasticity.
- *Chafer*: it is a narrow strip of rubberized cord reinforced with nylon or steel whose aim is to avoid penetration of impurities in the tire to protect the carcass.[1]

References

[1] M. Galimberti, Course of "Chemistry for elastomer composites", Polytechnic University of Milan, 2020.

[2] G.R. Hamed, Rubb. Chem. Technol., 2000, 73, 524.

[3] W. Meyer and J. Walter, eds., Frictional Interaction of Tire and Pavement. West Conshohocken, PA: ASTM International, 1983.

[4] T. Sabu, Non-linear viscoelasticity of rubber composite and nanocomposites, 2014, 281-282.

Section II – Synthesis and results

Chapter 7

Preparation of CB-SP adduct

7.1 Introduction

In this chapter the preparation of the functionalized filler is described. N326 grade carbon black was used as provided by Birla carbon S.p.a. without any purification and serinol pyrrole was added through the "pyrrole methodology" previously reported. According to this procedure the Diels-Alder reaction occurred between SP, which acted as dienophile, and the edge of CB graphitic layer without application of catalysts or solvents.[1] This method resulted as an easy, effective and viable process to modify CB surface with OH functional groups. This process was applied as developed in the research group where this thesis work was done.

At the end of the functionalization, the adduct was washed to remove the amount of pyrrole not reacted and characterized by means of TGA and SP mass losses based analysis.

7.2 CB-SP adduct process synthesis

7.2.1 *Feedstock preparation and reaction*

Serinol-pyrrole was weighed in a vial and diluted in acetone. CB N326 beads was weighed in a single-neck round bottom flask. The SP/acetone solution and other acetone were added till all the CB was covered by the liquid phase. The flask with solution was sonicate for 15 min. To remove acetone from CB/pyrrole compound the Rotavapor was used (40 °C for the bath, from 550 mbar to 50 mbar going down 50 by 50 mbar). The remaining compound without acetone was transferred in a 2-nek 250 ml round bottom flask that was equipped with a magnetic stirrer. In one neck some cotton was applied to retain possible pour losses. In the other was closed with the tube for the compressed air. The flask was inserted in an oil bath preheated at 160 °C. The stirring velocity was set at 235 rpm. The temperature of the bath went down a little. When the temperature came back to the set point the compressed air was started. The reaction took 2 hours in a temperature range between 160 °C and 180 °C. A scheme of the overall procedure is reported in the following **Figure 7.1**.

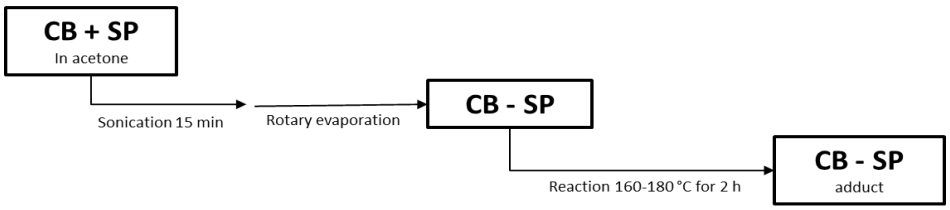

Figure 7.1 Schematic procedure of the CB-SP adduct preparation

The next **Figure 7.2** shows the reaction equipment used for the previous reaction.

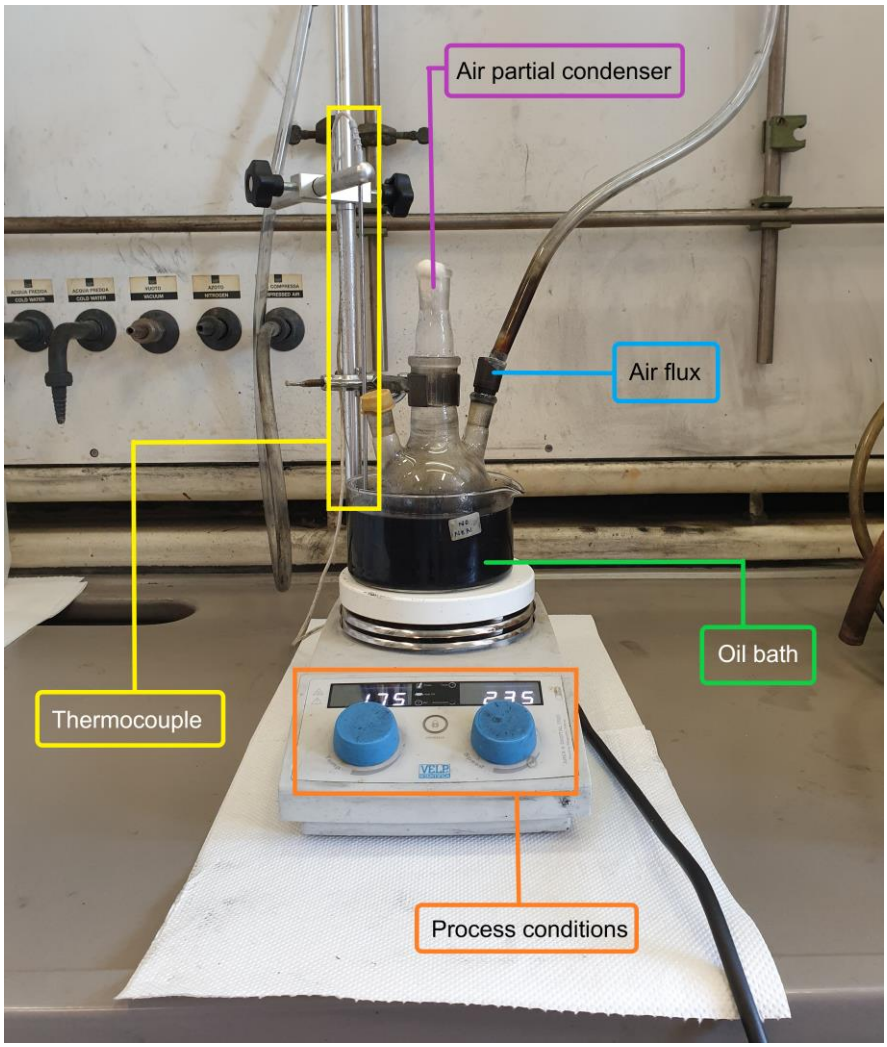

Figure 7.2 CB-SP reaction apparatus

7.2.2 *Extraction of unreacted SP*

The product of the reaction was put in a 1000 ml becher and about 300 ml of acetone was added. Stirring slowly to extract all the unreacted pyrrole. After about 30 min the compound was filtered on a tailed flask connected to a vacuum pump set at 450 mbar. Three washing with acetone were performed. To remove completely the acetone the product was inserted in an oven at 80 °C for an hour.

7.2.3 *Materials and reaction conditions*

The following **Table 7.1** reports the main process parameters.

Table 7.1 Reagents and reactions conditions for the synthesis of CB N326-SP adduct

Adduct		Reagents	Weight [g]	Temperature[a]	Reaction time	Stirring
1°	**CB-SP**	CB N326	32.28	175 °C	2 h	235 rpm
		SP	3.23			
2°	**CB-SP**	CB N326	31.25			
		SP	3.13			

[a] Temperature measured in the oil bath

7.3 Characterization

The value of **phc** (per hundred carbon black) of the adducts listed in **Table 7.1** was evaluated through two different analyses. First, it was calculated by a method based on the evaluation of the mass of the unreacted SP extracted by washing of the synthesized adduct (the procedure is indicated in detail in the Experimental Section). Then, the same data was estimated by the thermogravimetric analysis (TGA).

The degree of functionalization was calculated first on the basis of the SP mass losses based analysis ($\boldsymbol{\eta_{CB-SP;\%}}$). This value is the difference between the serinol pyrrole's mass at the beginning of the experiment ($m_{SP\ initial}$) and the mass of the un-reacted SP as for the phc calculation above, divided by $m_{SP\ initial}$ and multiplied by 100. Then, the degree of functionalization was evaluated on the basis of the mass losses obtained by TGA. In this last case it is called $\boldsymbol{\eta_{TGA}}$.

7.3.1 *Characterization method based on un-reacted SP mass*

The value **phc** (per hundred carbon black) of the adducts listed in **Table 7.**1 can be evaluated through the **Equation (1)**.

$$\boldsymbol{phc} = \frac{\Delta m}{m_{SP\ initial}} \times \frac{m_{CB}}{m_{SP}^{initial}} \quad (1)$$

In **Equation (1)** the value of the phc is calculated on the basis of the following parameters: m_{CB} and $m_{SP}^{initial}$ are, respectively, the total mass of the carbon black and serinol pyrrole weighted at the beginning of the functionalization reaction. While, Δm, which represents the mass of the reacted SP, is the difference between the mass of the initial amount of SP and the mass of the un-reacted pyrrole after washing. This last parameter was obtained by weighting the residual compound remained after the rotary evaporation of the acetone.

The values obtained are reported in **Table 7.2**.

Table 7.2 phc of the adducts calculated with **Equation (1)**

Adduct		phc
1°	**CB-SP**	8,6
2°	**CB-SP**	7,7

7.3.2 *Thermogravimetric analysis (TGA)*

This analysis was performed on the dried powder (instrumentation details are reported in the Experimental Section).

The mass losses of the samples of the adducts analyzed in percentages are reported in the following **Table 7.3** and in the thermogram in **Figure 7.3** and **7.4**.

Table 7.3 Mass losses of CB-SP adducts according to thermogravimetric analysis

Adduct		Mass loss (%) for T<150 °C	Mass loss (%) for 150 <T<900 °C	Mass loss (%) for T> 900 °C
1°	**CB-SP**	0,4	6,3	93,3
2°	**CB-SP**	0,6	4,8	94,6

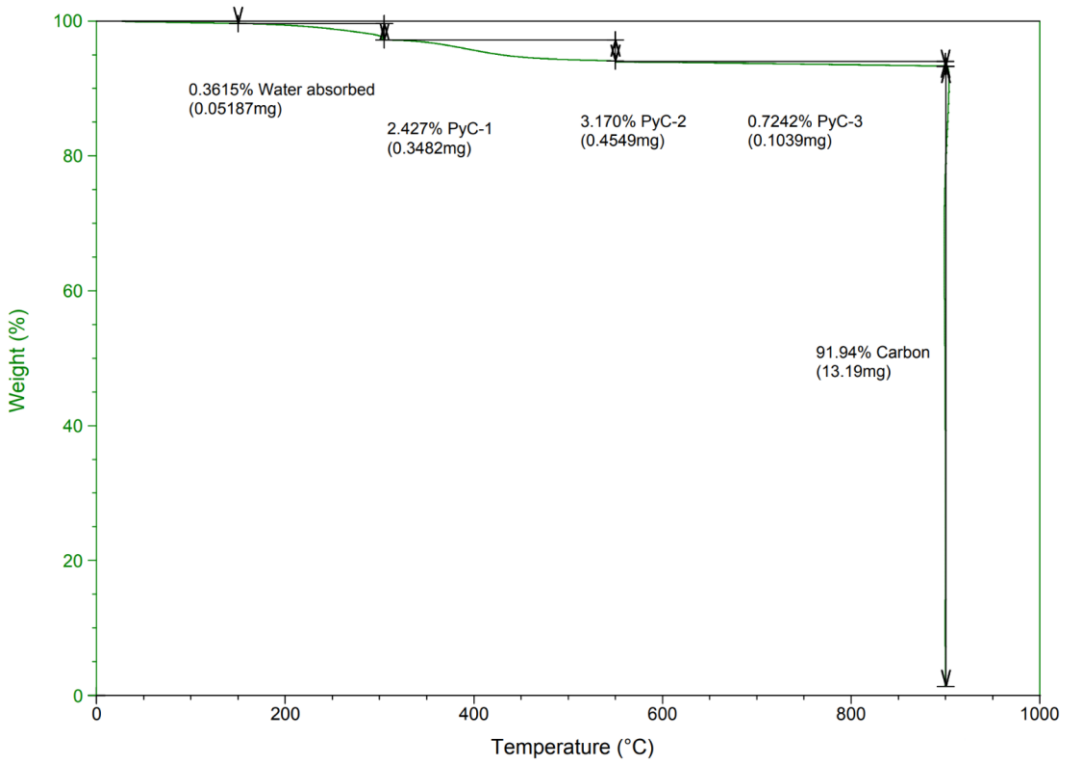

Figure 7.3 TGA weight (%) vs temperature of the dried 1° CB-SP adduct powder

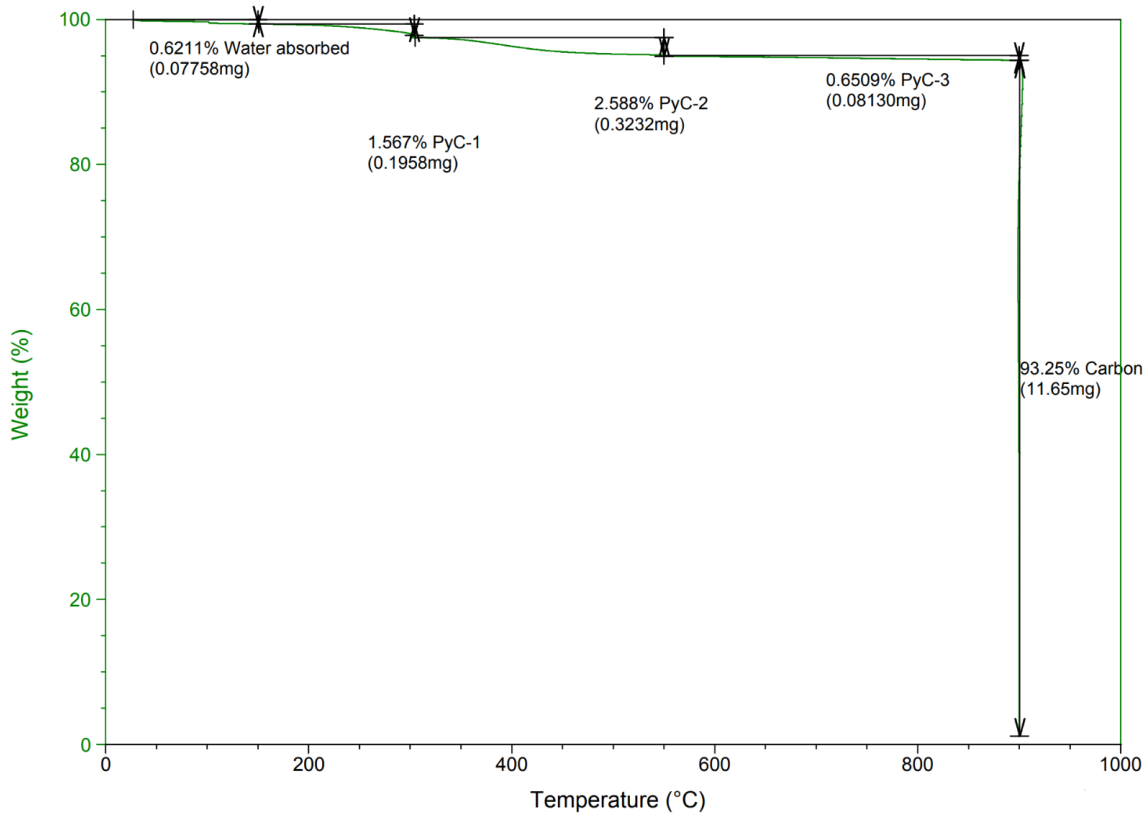

Figure 7.4 TGA weight (%) vs temperature of the dried 2° CB-SP adduct powder

Three temperature ranges are highlighted by these curves. The first one is from 0 to 150 °C in which it is possible to see the desorption of water and organic impurities. Then, the second, from 150 to 900 °C, is the one of interest for the calculation of the phc and also of the degree of functionalization because in this range the decomposition of serinol pyrrole occurs. Finally, at temperature above 900 °C, the complete decomposition of CB is represented.

The value of **phc** (per hundred carbon black) of the adducts listed in **Table 7.1** can be calculated through the **Equation (2)**.

$$\boldsymbol{phc} = \frac{w_{150\rightarrow900°C}^{CB-SP\ adduct} - w_{150\rightarrow900°C}^{CB\ pristine}}{w_{900°C}^{CB}} \times 100 \qquad \textbf{(2)}$$

In the **Equation (2)**, the values of w are related to the 150-900°C interval. The desorption of water and organic impurities was not taken into account because it usually occurs arround the interval from 100 °C to 120 °C.

The phc calculated are reported in **Table 7.4**.

Table 7.4 phc of the CB-SP adducts estimated by TGA

Adduct		phc
1°	**CB-SP**	6,9
2°	**CB-SP**	5,2

7.3.3 *Calculation of the Degree of functionalization*

In the end, the degree of functionalization can be calculated in two ways. In **Equation (3)** it is estimated on the basis of the mass balance of the reacted and un-reacted SP, while the **Equation (4)** explain how to calculate $\boldsymbol{\eta_{TGA}}$ according to the values given by TGA.

$$\boldsymbol{\eta_{CB-SP;\%}} = \frac{\Delta m}{m_{SP\ initial}} \times 100 \quad \textbf{(3)}$$

$$\boldsymbol{\eta_{TGA}} = \frac{w_{150\rightarrow 900°C}^{CB-SP\ adduct} - w_{150\rightarrow 900°C}^{CB\ pristine}}{w_{900°C}^{CB}} \times \frac{m_{CB}}{m_{SP}^{initial}} \times 100 \quad \textbf{(4)}$$

In the **Equation (3)**, the values of $\boldsymbol{\eta_{CB-SP;\%}}$ are evaluated as the fraction, in percentage, of the mass of the reacted SP, calculated as in **Equation (1)**, and the total amount of serinol pyrrole weighted at the beginning of the reaction. This parameter can be considered as a sort of yield of the functionalization reaction. On the other side, in **Equation (4)** m_{CB} and $m_{SP}^{initial}$ are, respectively, the carbon black and the serinol pyrrole masses weighted at the beginning of the experiment, while every w value is the mass loss of the sample from TGA. The interval chosen for the calculation was the 150-900°C because it represents the temperature range in which the decomposition of pyrrole compounds occurred and doesn't take into account for water and organic impurities desorption.

The values of the degree of functionalization estimated are reported in **Table 7.5**.

Table 7.4 $\boldsymbol{\eta_{CB-SP;\%}}$ and $\boldsymbol{\eta_{TGA}}$ of the CB-SP adducts estimated by **Equation (1)** and by TGA, respectively

Adduct		Degree of functionalization	
		$\boldsymbol{\eta_{CB-SP;\%}}$	$\boldsymbol{\eta_{TGA}}$
1°	**CB-SP**	87 %	69 %
2°	**CB-SP**	78 %	52 %

The values of $\eta_{CB-SP;\%}$ are higher than the ones of η_{TGA} mainly due to the fact that in the weighing of the residual SP after rotary evaporation, some impurities were still present and so the value of the degree of functionalization calculated by **Equation (3)** was overestimated.

7.4 Conclusion

The functionalization reaction between pristine CB and serinol pyrrole was made by the pyrrole methodology[1] described in paragraph 7.2. According to this procedure the Diels-Alder reaction occurred between SP and the edge of CB graphitic layer without application of dangerous or noxious reagents.[1] This method resulted as an easy, effective and viable process to modify CB surface with OH functional groups. The adducts obtained were characterized by TGA and through the mass balance of the reacted and un-reacted pyrrole.

The phc calculated through these two analyses are:

- First sample of CB-SP adduct, 6,9 from TGA and 8,6 on the basis of the mass balance method.
- Second sample of CB-SP adduct: 5,2 from TGA and 7,7 on the basis of the mass balance method.

Data from TGA are considered more reliable, as they are not affected by experimental aspects as the presence of volatile substances, such as water and acetone.

However, it is possible to underline that the pyrrole methodology[1] allowed to prepare functionalized adducts of CB-SP with more than 5 phc of pyrrole on the filler.

The yield of functionalization, lower than the one obtained in the Group with few layer graphene and carbon nanotubes could be attributed to the moderate surface area of CB.

References

[1] Barbera, V., Brambilla, L., Milani, A., Palazzolo, A., Castiglioni, C., Vitale, A., ... & Galimberti, M. (2019). Domino Reaction for the Sustainable Functionalization of Few-Layer Graphene. Nanomaterials, 9(1), 44.

Chapter 8
Flocculation study of CB and CB-SP in rubber matrix

8.1 Introduction

This chapter is about the study of the flocculation of CB-SP in a rubber matrix. The rubber matrix was based on isoprene rubber (IR) loaded with CB and the CB-SP adduct was the one previously described. IR is the synthetic poly(1,4-cis-isoprene), from Ziegler-Natta catalysis, carbon black is the N326 provided by Birla carbon and CB-SP is the one described in Chapter 7. Other ingredients were not present in the composite material.

Isoprene rubber is applied in many fields from tire industry to belts, hose, footwear and coatings, but, especially for the first case, it requires to be reinforced to achieve dynamic-mechanical properties to satisfy the application needs.

Main objective of the flocculation study was to study the self assembling ability of CB-SP, in comparison with CB. This was done by evaluating the dynamic-mechanical properties of IR/filler composites, loaded with pristine CB and with the CB-SP adduct, before vulcanization.

The flocculation study was carried out according to the Tunnicliffe[1] methodology, which is explained in detail in paragraph 8.3.

The preparation of the composites was done by melt blending in a Brabender® type internal mixer.

Dynamic-mechanical properties were analyzed by applying sinusoidal stresses, at constant frequency, both in axial and shear direction to determine the storage modulus G'.

8.2 Preparation of IR-based composites filled with CB and CB-SP

IR-based compounds with carbon black as filler, were prepared without the vulcanization agents to study the flocculation of un-crosslinked composites.

The amount of filler was maintained constant at 50 phr (per hundred rubber). CB was replaced with various amounts of CB-SP.

The recipes in phr of the elastomeric compounds are reported in **Table 8.1**.

Table 8.1 Recipes of IR-based compounds with CB or CB/SP as fillers

Recipes in phr	CB-SP 0 % [phr]	CB-SP 25 % [phr]	CB-SP 50% [phr]	CB-SP 75% [phr]	CB-SP 100% [phr]
IR	100	100	100	100	100
CB N326	50	37.5	25	12.5	0
CB N326 - SP	0	12.5	25	37.5	50
N326	0	12.175	24.25	36.25	47.5
SP	0	0.325	0.75	1.25	2.5

In the **Table 8.2**, for each composite, the content of serinol pyrrole and the values of surface area in the filler system are reported. These parameters were calculated as the weighted average of the values of the pristine CB and the pure CB-SP. The amount of SP of these lasts was evaluated by TGA, while the surface area values were obtained through BET analysis[2]. The parameters related to the pristine CB are the one in the "0%" column of **Table 8.2**, while, the data of the CB-SP adduct are reported in the "100%" column of the same **Table 8.2**.

Table 8.2 Serinol pyrrole content and values of surface area in the filler system obtained with TGA and BET analysis[2]

	CB/SP content in the filler system[a,b]				
	0%	**25%**	**50%**	**75%**	**100%**
SP content in the filler system [phc][c]	0	1.1	1.9	3.3	4.8
surface area of the filler system NSA [m^2/g]	77	72	68	65	60
External surface area of the filler system STSA [m^2/g]	75	68	62	56	50

[a] filler system = CB + CB/SP, [b] SP content in CB-SP = 4.8, [c] phc = per hundred carbon

To prepare the composites, the procedure, described in **Figure 8.1**, was applied.

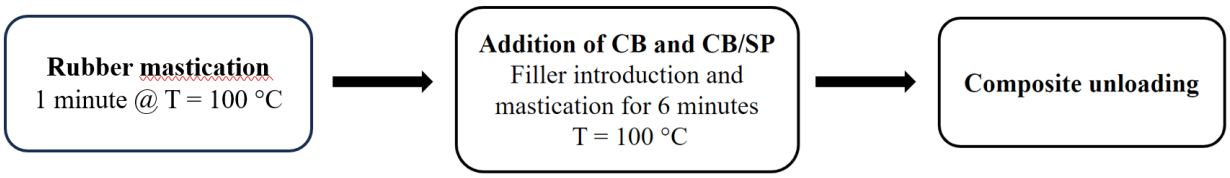

Figure 8.1 Mixing procedure for un-crosslinked IR composites

A 50-cc chamber Brabender® type internal mixer was used with a fill factor equal to 55%.
In the following **Figure 8.2**, the plastograms for the preparation of the composites were collected. They show the variation of torque (Fig. 8.2.a) and of the temperature (Fig. 8.2.b) during the mixing process.

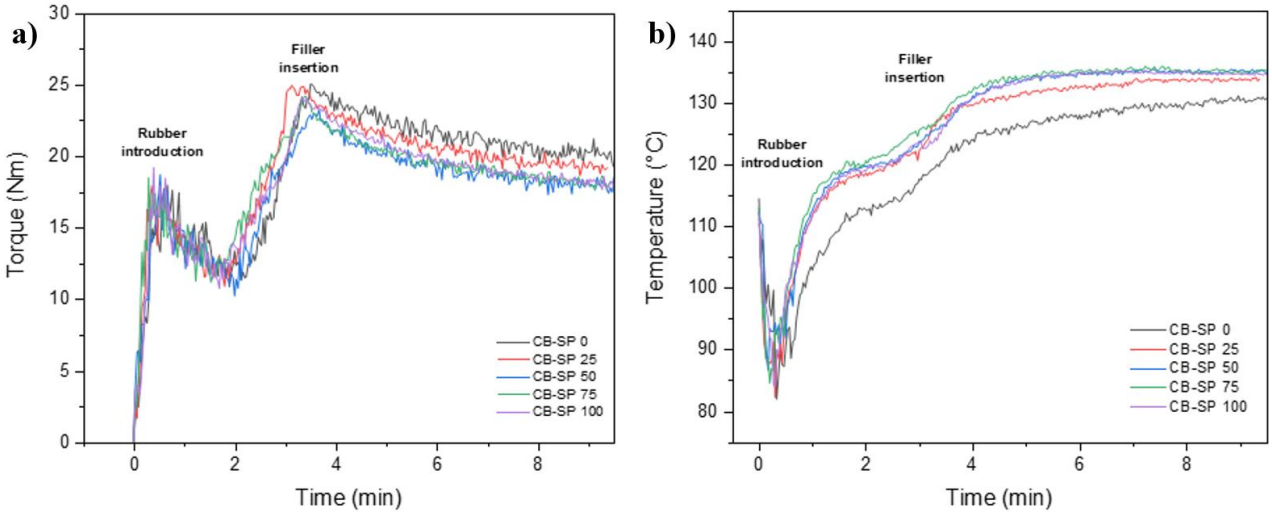

Figure 8.2 Plastograms of the mixing of un-crosslinked IR composites: Torque vs time (a), T vs time (b)

It seems that the introduction of CB-SP (at every loading) reduces the torque registered in the mixing chamber while there is a slight increase of the temperature in the mixing chamber. The first effect could be related to the decreasing values of the superficial area reported in **Table 8.2**.

8.3 Flocculation study

Viscoelastic properties of the sample were characterized in oscillatory shear using a Dynamic Rubber Process Analyzer. The procedure applied was the one proposed by Tunnicliffe[1] that is divided in

three phases, as reported in **Figure 8.3**, and the whole analysis was repeated on three different portions of each sample.

In the first phase the composite was kept at 150 °C for 10 minutes, in order to eliminate any possible influence of the thermal history of each sample.

In the second phase, a strain sweep test was performed: a strain from 0.1 % to 10 % was applied at 150 °C with a constant value of frequency, fixed at 1 Hz. The shear dynamic mechanical modulus as a function of the strain was measured. The extent of the filler network and its breakdown are studied.

In the last phase, each sample was kept at constant temperature (150 °C), frequency (1 Hz) and strain (0.1 %), to inspect the re-formation of the filler network. The values of G' were collected over 20 minutes.

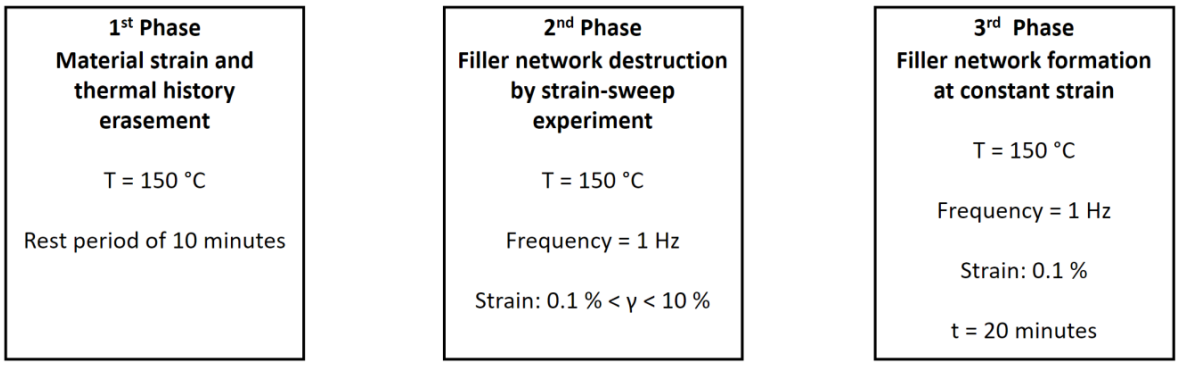

Figure 8.3 Block diagram of the procedure adopted for the flocculation study

Three specimens were analyzed for each sample. The arithmetic average and the standard deviation were calculated for the G' values determined in Phase 2 and in Phase 3.

The storage modulus at minimum strain (G' γ min), the storage modulus at 10% of strain (G' γ max), their difference (ΔG') and their difference normalized with respect to the values of G' γ min (ΔG'/G' γ min) are reported in **Table 8.3.** These data were taken from Phase 2.

Table 8.3 G' γ min, G' γ max, ΔG' and ΔG'/ G' γ min from Phase 2 of the strain sweep experiments on Samples of Table 8.1

Property	**Composite**				
	CB/SP 0%	**CB/SP 25%**	**CB/SP 50%**	**CB/SP 75%**	**CB/SP 100%**
G' γ min (kPa)	618.8	540.4	536.3	594.7	719.7
G' γ max (kPa)	235.1	270.8	311.0	358.7	413.6
ΔG' (kPa)	383.6	269.7	225.2	235.9	306.1
ΔG'/G' γ min	0.620	0.499	0.420	0.397	0.425

In **Table 8.4**, the storage modulus measured at the beginning of the experiment, (G' MIN), the storage modulus after 20 min (G' MAX), their difference (ΔG') and their difference normalized with respect to the values of G' MAX are resumed. These data were obtained in Phase 3.

Table 8.4 G' MIN, G' MAX, ΔG' and ΔG'/ G' MAX of each sample of the filler network re-formation

	CB/SP 0%	CB/SP 25%	CB/SP 50%	CB/SP 75%	CB/SP 100%
$G'_{t=20\ min}$ (kPa) [= G' MAX]	656.0	543.6	527.6	582.5	697.5
G'_{t0}(kPa) [=G' MIN]	395.8	392.2	418.8	478.7	568.9
ΔG' (kPa)	260.2	151.4	108.8	103.8	128.5
$\Delta G' / G'_{t=20\ min}$	0.397	0.279	0.206	0.178	0.184

G' vs strain determined in Phase 2 and G' vs time determined in Phase 3 are in **Figure 8.4**, Fig. 8.4a and Fig. 8.4b respectively.

In particular, in **Figure 8.4a**, the modulus G' at minimum strain (G' γ min) was obtained at the end of the Phase 1, so after 10 min at 150 °C while the values at high strain (G' γ max) were registered at the end of the strain sweep, so at the end of Phase 2.

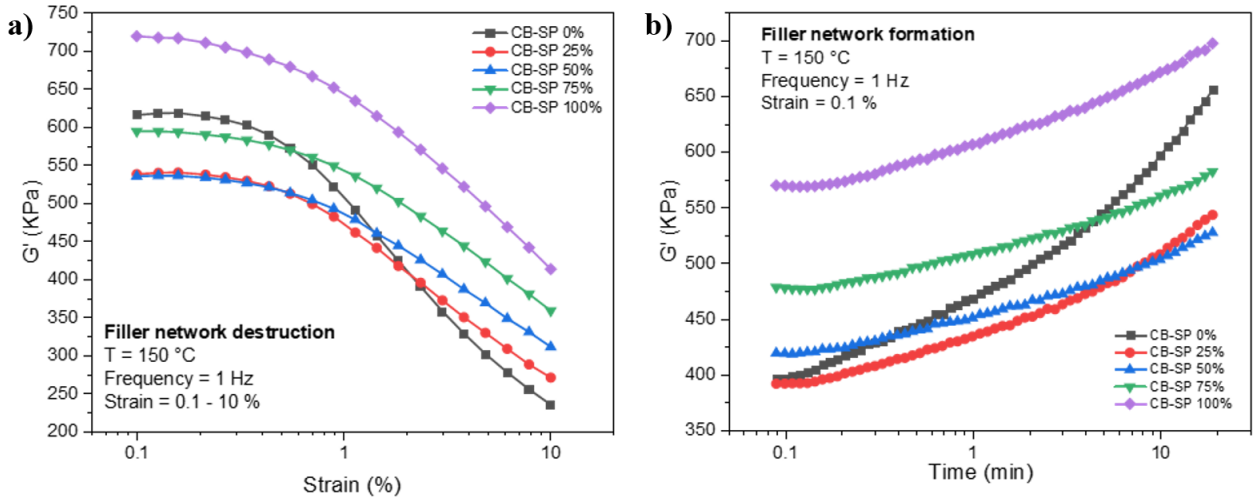

Figure 8.4 Flocculation study on samples of Table 8.1. (see Fig. 8.3). G' vs strain from Phase 2 (a), G' vs time from Phase 3 (b)

By exploring the results of Phase 2 of the flocculation study it can be commented as follow. There is no monotonic trend of the value of G' vs strain with respect to the content of SP. In fact, the composites with 25% and 50% of CB-SP (the red and blue lines) show a significant reduction in G' γ min compared to the compound with only CB (the black one). The composite with 75% CB-SP (the green line) shows little decrease in G' γ min while, on the other side, the composite with 100% CB-SP shows a higher G' γ min value than that of the composite with CB. A possible interpretation is the following: for composites with small amount of functionalized filler, the reduction of the surface area plays the main role, while, for the composites with high content of the filler it seems that the interactions among the OH groups prevail. To support this interpretation, the ΔG'/G' γ min was plotted vs the surface area of the filler and the graph is shown in **Figure 8.5**. The surface area of the filler was calculated as the weighted average of the values of the pristine CB and the pure CB-SP. One can observe a monotonic decrease of ΔG'/ G' γ min for the samples with the CB/CB-SP mixtures, whereas the value increase for the composite with only CB-SP.

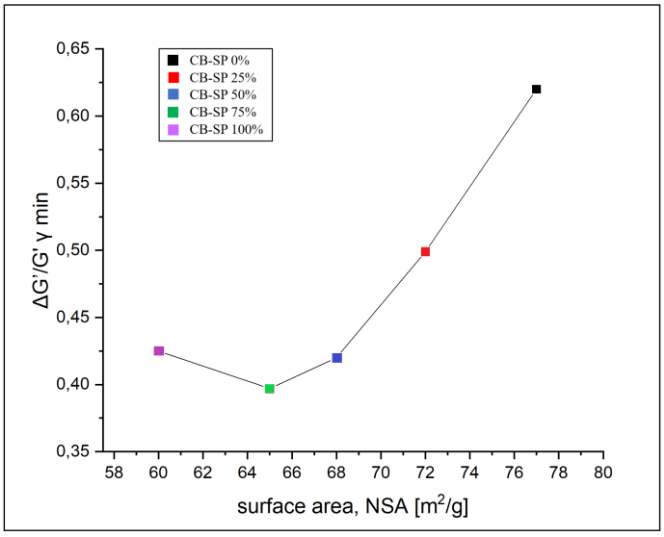

Figure 8.5 ΔG'/ G' γ min vs surface area NSA of the fillers, calculated as explained in the text

On the other side, at the end of Phase 2, the registered moduli show a monotonic increment: the value of storage modulus at high strain (G' γ max) increases with the content of SP (**Figure 8.4a)**. This can be related to fact that the filler network built by CB-SP is more stable and so it would be required a higher strain to remove it.

In the **Figure 8.4b**, the values of G' MIN are collected at the beginning of the Phase 3, while, G' MAX values are obtained after 20 minutes, by keeping each sample at 150 °C, at 0.1 % of strain and a frequency of 1 Hz. The difference between these two values, normalized with respect to the value of G' MAX, can be considered to evaluate the slope of the curve of each composite. Therefore, in the

following **Figure 8.6**, the values of ΔG'/ G' MAX are correlated to the surface area of the filler, which was calculated, as above, as the arithmetic mean of the surface area of CB and CB-SP, taking into account their amount.

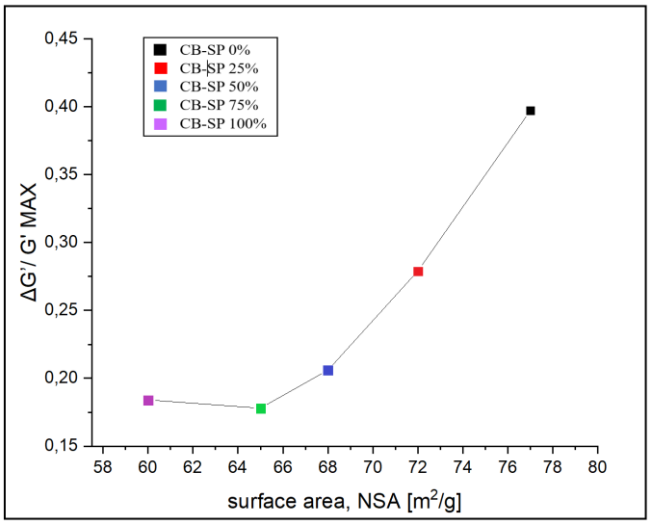

Figure 8.6 ΔG'/ G' MAX vs surface area NSA of adducts, calculated as explained in the text

Also for the data coming from Phase 3, the surface area seems to have the prevailing affect. In fact, the slope of the curves appears to depend on the surface area. Only for the composite with 100% of CB-SP, the effect of the polar groups on the CB surface appears to balance the reduction of the surface area.

8.4 Conclusions

Composites at different loading of CB/CB-SP were prepared by melt blending in an internal Brabender® type mixer.

A study on the filler flocculation was performed in order to evaluate the self assembling ability of CB, either pristine or functionalized. The attention was paid on the storage modulus G' registered, for each composite, both during the strain sweep test (named Phase 2) and then, during the re-formation of the filler network (Phase 3).

The results highlighted the prevailing effect of the surface area, with respect to the interaction of the OH groups on the CB surface. The surface area of the filler system was calculated from the surface area of CB and CB-SP, taking into account their relative amount. A correlation was found between the reduction of the surface area of the filler, due to the increase of the functional group, and the storage moduli of the composites. Only the composite prepared with 100% of CB-SP revealed a higher flocculation ability of the filler, due to the interaction of the OH-groups.

Therefore, CB functionalized with OH does not give rise to a stronger filler-filler interaction, with respect to pristine CB. This could be a positive result: the viscosity of the composites is not expected to increase. However, the reduction of surface area could lead to weaker interactions with the polymer chains and thus to lower reinforcement. To overcome this problem, one should rely on the chemical reactivity of the OH groups.

References

[1] Tunnicliffe, L.B.; Kadlcak, J.; Morris, M.D.; Shi, Y.; Thomas, A.G.; Busfield, J.J.C. Flocculation and viscoelastic behaviour in carbon black-filled natural rubber. Macromol. Mater. Eng. 2014, 299, 1474–1483, doi:10.1002/mame.201400117.

[2] F. Moriggi, M. Galimberti. Adduct of sp2 carbon allotropes. From a DFT study to their use as reinforcing filler for elastomer nanocomposites and substrates for single atom catalyst. 2023.

Chapter 9
Flocculation study of CB and CB-SP in oil matrix

9.1 Introduction

Aim of the work discussed in this Chapter was to perform the flocculation of CB and CB/SP in oil. The oil should simulate the lipohilic environment of the rubber matrix. The use of the oil in place of the rubber had two main objectives:

(i) to investigate the reproducibility of the filler networking phenomenon in different matrices. This would indicate the prevailing role played by the filler, either pristine or functionalized

(ii) to avoid the preparation of the rubber composite. This would make easier and quicker the investigation on CB/PyC adducts. Indeed, the pyrrole methodology allows the preparation of many pyrrole compounds and thus of many CB/PyC adducts.

The development of a quick test to analyze the composite materials draws inspiration from the high-throughput screening (HTS), which is a method for scientific discovery which allows a researcher to quickly conduct a great number of experiments. Actually, in the fields of materials science, chemistry, biology, and drug discovery the HTS method allows to conduct millions of tests. To goal in this case was evidently more modest.

The flocculation of CB in oil was first proposed by Robertson[1], who prepared and studied dispersions of CB of different types and at different parts per weight. The results obtained from the oil dispersions, for example the non linearity of the storage modulus, known as Payne Effect[1],[4], were similar to those obtained in the rubber matrix.[1]

With the same technique, Tunnicliffe[2] studied the filler networking phenomenon of composites containing CB in rubber matrix. In particular, he studied the effect of CB graphitization on reinforcing fillers with different structure.

In the present thesis, the viscoelastic properties of the oil-CB mixture were characterized by performing strain sweep tests at constant temperature and frequency[2] using a Dynamic Rubber Process Analyzer. This was done in order to understand if the behaviour of the fillers in the oil matrix could be comparable to the one of the same fillers in rubber.

Paraffin oil was used as the oil matrix.

The CB used for preparing the dispersions was the same used in the rubber matrix (see Chapter 8) and was CBN326 provided by Birla Carbon

The CB-SP was the same used for the flocculation study described in chapter 8, synthesized through the pyrrole methodology, as shown in Chapter 7.

To prepare the dispersions of CB and CB-SP in oil, a speed mixer was used. The main technical problem to be faced was the dispersibility of the CB-SP adduct in the oil matrix. An *ad hoc* procedure was developed.

Moreover, also the procedure for the experiments in the Rubber Process Analyzer had to be changed. In particular, the temperature had to be reduced, with respect to the one used by Tunnicliffe[2].

9.2 Dispersions in oil of CB and CB-SP. Preparation procedure 1

9.2.1 The oil dispersions

Dispersions based on oil and containing either CB or CB-SP had a total filler content of 50 pho (per hundred oil). This level was kept constant. CB was replaced with an increasing amount of CB-SP, obtaining five binary mixtures with a content of the functionalized filler from 0 % (the pristine carbon black) to 100 % (only CB-SP).

The recipes in pho of the compounds are reported in **Table 9.1**.

Table 9.1 Recipes of oil based composites with CB or CB/SP as fillers, prepared with procedure 1

Ingredient	**Composite**				
	CB-SP 0 % [pho]	**CB-SP 25 % [pho]**	**CB-SP 50% [pho]**	**CB-SP 75% [pho]**	**CB-SP 100% [pho]**
Paraffin oil	100	100	100	100	100
CB N326	50	37.5	25	12.5	0
CB N326 - SP	0	12.5	25	37.5	50
N326	0	12.175	24.25	36.25	47.5
SP	0	0.325	0.75	1.25	2.5

In the following **Table 9.2**, the content of serinol pyrrole and the surface area of each filler system, calculated as described in Chapter 8, are reported. These calculations are based on the weighted average of the parameters of pristine CB and CB-SP. The amount of SP in CB-SP was evaluated by TGA, while, the surface area was obtained by BET[3]. The amount of serinol pyrrole and the value of surface area in pristine CB were 0 phc and 77 m^2/g, respectively. The relative values in CB-SP were 4.8 phc and 60 m^2/g (see **Table 9.2**).

Table 9.2 SP content and surface area of each filler system obtained with TGA and BET[3]

	CB/SP content in the filler system[a,b]				
	0%	**25%**	**50%**	**75%**	**100%**
SP content in the filler system [phc][c]	0	1.1	1.9	3.3	4.8
surface area of the filler system NSA [m^2/g]	77	72	68	65	60

[a] filler system = CB + CB/SP, [b] SP content in CB-SP = 4.8, [c] phc = per hundred carbon

9.2.2 Preparation procedure according to Robertson. Procedure 1

Dispersions of CB and CB-SP adducts in oil matrix, whose recipes were shown in **Table 9.1**, were prepared according to the procedure proposed in **Figure 9.1**, which reproduces the procedure published by Robertson[1].

The blended filler of each dispersion was obtained by simply placing together the relative quantities of CB and CB-SP adducts in the speed mixer cups (**Figure 9.2a**). Then, the paraffin oil was directly added to the cups and the mixtures were mixed by allowing the cups to rotate in the Hauschild Speedmixer DAC-150 (**Figure 9.2b**). The mixing steps were three: 1 minute at 800 rpm, then 1 minute at 2200 rpm and, finally, 3 minutes at 3100 rpm (**Figure 9.1**).

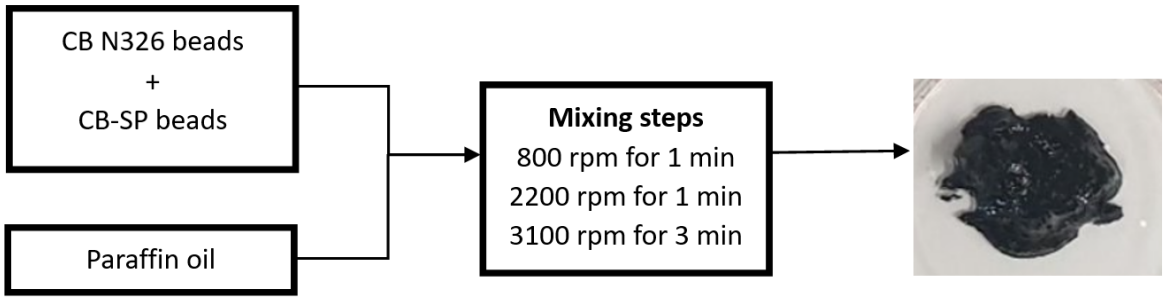

Figure 9.1 Procedure for preparing dispersion of CB/CB-SP in oil, according to Robertson [1]

a) b)

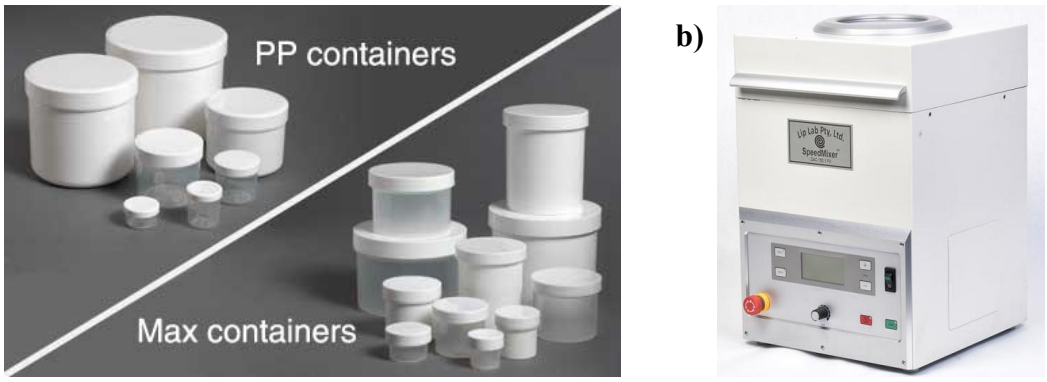

Figure 9.2 Mixing apparatus: Polypropylene containers (a), Hauschild Speedmixer DAC-150 (b)

9.2.3 *Characterization of the dispersions prepared with Procedure 1*

Viscoelastic properties of the sample were characterized in oscillatory shear using a Dynamic Rubber Process Analyzer. The procedure involved was the one proposed by Tunnicliffe[2] and it is divided in three phases as reported in the **Figure 9.3**.

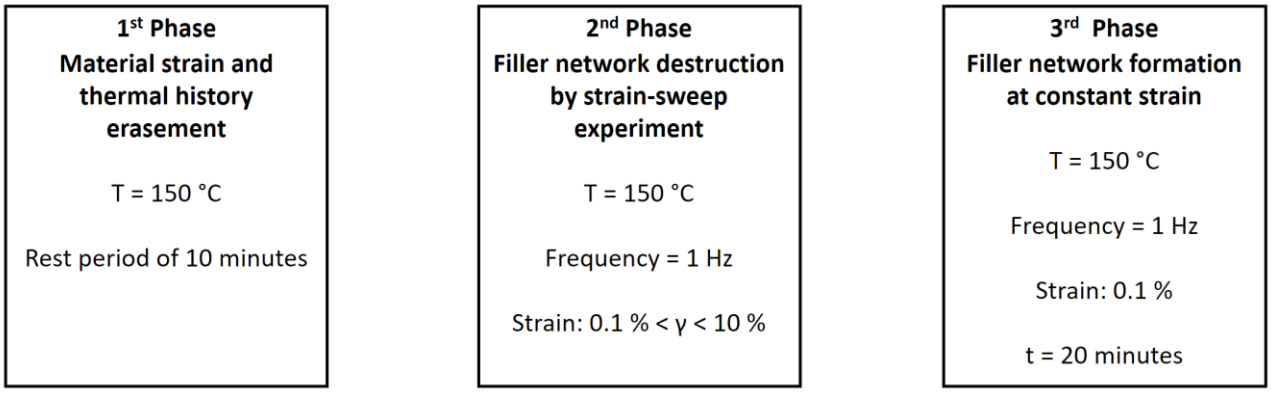

Figure 9.3 Block diagram of the procedure adopted for the flocculation study

In the first phase (named Phase 1) the composite was kept at 150 °C for 10 minutes, in order to eliminate any possible influence of the thermal history of each sample.

In the second phase, a strain sweep test was performed: a strain from 0.1 % to 10 % was applied at 150 °C with a constant value of frequency, fixed at 1 Hz. The shear dynamic mechanical modulus as a function of the strain was measured. The extent of the filler network and its breakdown are studied.

In the last phase, each sample was kept at constant temperature (150 °C), frequency (1 Hz) and strain (0.1 %), to inspect the re-formation of the filler network. The values of G' were collected over 20 minutes.

Three specimens were analyzed for each sample. The arithmetic average and the standard deviation were calculated for the G' values determined in Phase 2 and in Phase 3.

The loss modulus at minimum strain (G' γ min), the loss modulus at 10% of strain (G' γ max), their difference (ΔG') and their difference normalized with respect to the values of G' γ min (ΔG'/G' γ min) are reported in **Table 9.3.** These data were taken from Phase 2.

Table 9.3 G' γ min, G' γ max, ΔG' and ΔG'/ G' γ min from Phase 2 of the strain sweep experiments on samples of Table 9.1

	CB/SP 0%	**CB/SP 25%**	**CB/SP 50%**	**CB/SP 75%**	**CB/SP 100%**
G' γ min (kPa)	785.1	1804.6	3327.5	4964.2	7159.6
G' γ max (kPa)	7.1	37.9	83.6	82.1	130.2
ΔG' (kPa)	778.1	1766.8	3243.9	4882.1	7029.4
ΔG'/G' γ min	0.991	0.979	0.975	0.983	0.982

In **Table 9.4**, the loss modulus measured at the beginning of the experiment, (G' MIN), the loss modulus after 20 min (G' MAX), their difference (ΔG') and their difference normalized with respect to the values of G' MAX are resumed. These data were obtained in Phase 3.

Table 9.4 G' MIN, G' MAX, ΔG' and ΔG'/ G' MAX of each sample of the filler network re-formation

	CB/SP 0%	**CB/SP 25%**	**CB/SP 50%**	**CB/SP 75%**	**CB/SP 100%**
$G'_{t=20\ min}$ (kPa) [= G' MAX]	922.7	1465.3	2659.5	3273.7	5670.5
G'_{t0}(kPa) [=G' MIN]	119.9	943.7	1993.0	2342.2	4095.7
ΔG' (kPa)	802.7	521.5	666.5	931.5	1574.7
ΔG' /$G'_{t=20\ min}$	0.870	0.356	0.251	0.285	0.278

The mean values of G' vs strain determined in Phase 2 and the ones of G' vs time determined in Phase 3 are in **Figure 9.4**, Fig. 9.4a and Fig. 9.4b respectively. In particular, in **Figure 9.4a**, the modulus G' at minimum strain (G' γ min) was obtained at the end of the Phase 1, so after 10 min at 150 °C while

the values at high strain (G' γ max) were registered at the end of the strain sweep, so at the end of Phase 2.

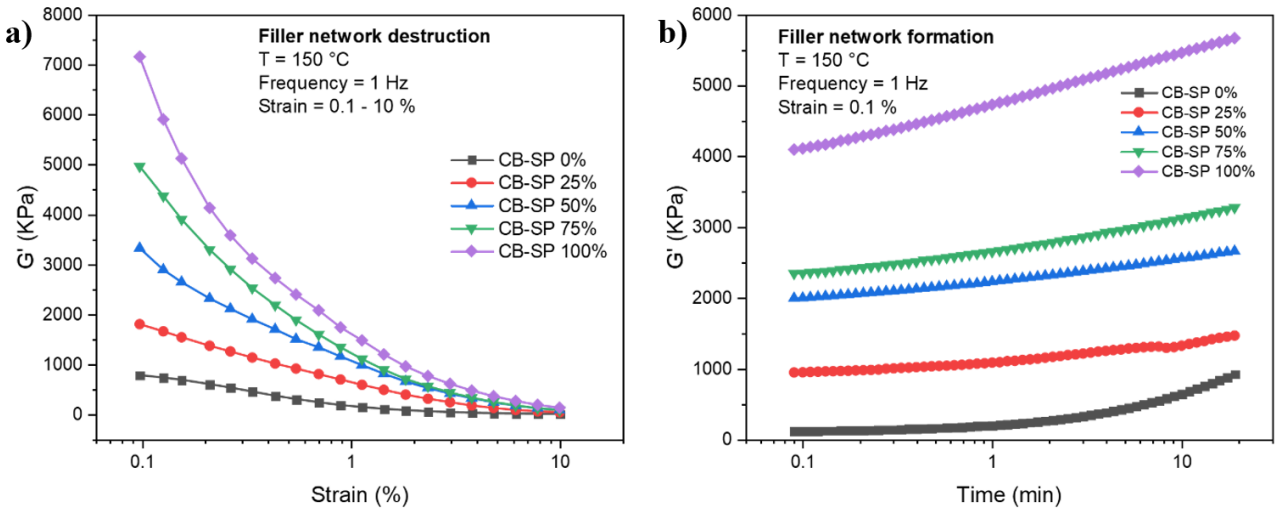

Figure 9.4 Flocculation study on samples of Table 9.1. (see Fig. 9.3). G' vs strain from Phase 2 (a), G' vs time from Phase 3 (b)

By exploring the **Figure 9.4a**, there is a monotonic trend of the value of G' vs strain with respect to the content of SP. In fact, for all the composites, the higher the content of SP in the filler system is, the higher the values of the loss modulus are. in the **Figure 9.4b**, it is possible to observe that the values of G' monotonically increase with the content of SP during the whole filler network re-formation phase. These results are different from what has been observed in the rubber composites in Chapter 8. The slope of the curves of **Figure 9.4b** decreases with the increasing of the CB-SP amount. This was observed also in the Phase 3 of the flocculation study of rubber composites described in Chapter 8,

A possible interpretation for the differences observed is the following. The behaviour of each composite is essentially governed by the physical-chemical characteristics of the filler. The interaction with the matrix appears to play a minor role. If that were true, one could also hypothesize that the oil was squeezed out during the rheological test, performed at 150°C in the rubber process analyzer.

In the **Figure 9.5**, for each composite, the mean values of G' vs strain determined in Phase 2 and the ones of G' vs time determined in Phase 3 are represented with their relative range of experimental error (the vertical lines related to each point). This interval was evaluated by the representation of the positive and negative value of the standard deviation calculated for each value.

In particular, in **Figure 9.5 a,c,e,g,i**, the modulus G' at minimum strain (G' γ min) was obtained at the end of the Phase 1, so after 10 min at 150 °C while the values at high strain (G' γ max) were registered at the end of the strain sweep, so at the end of Phase 2.

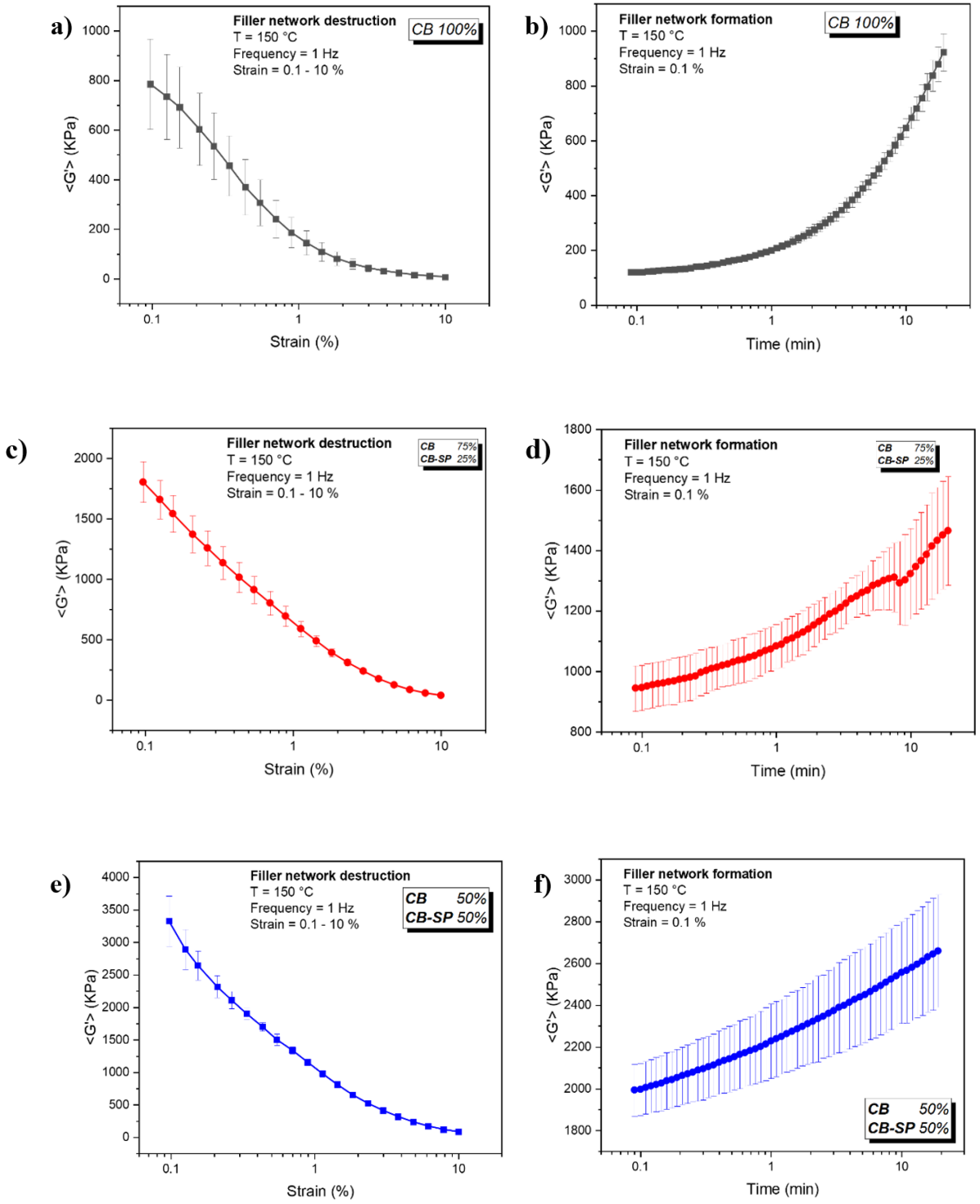

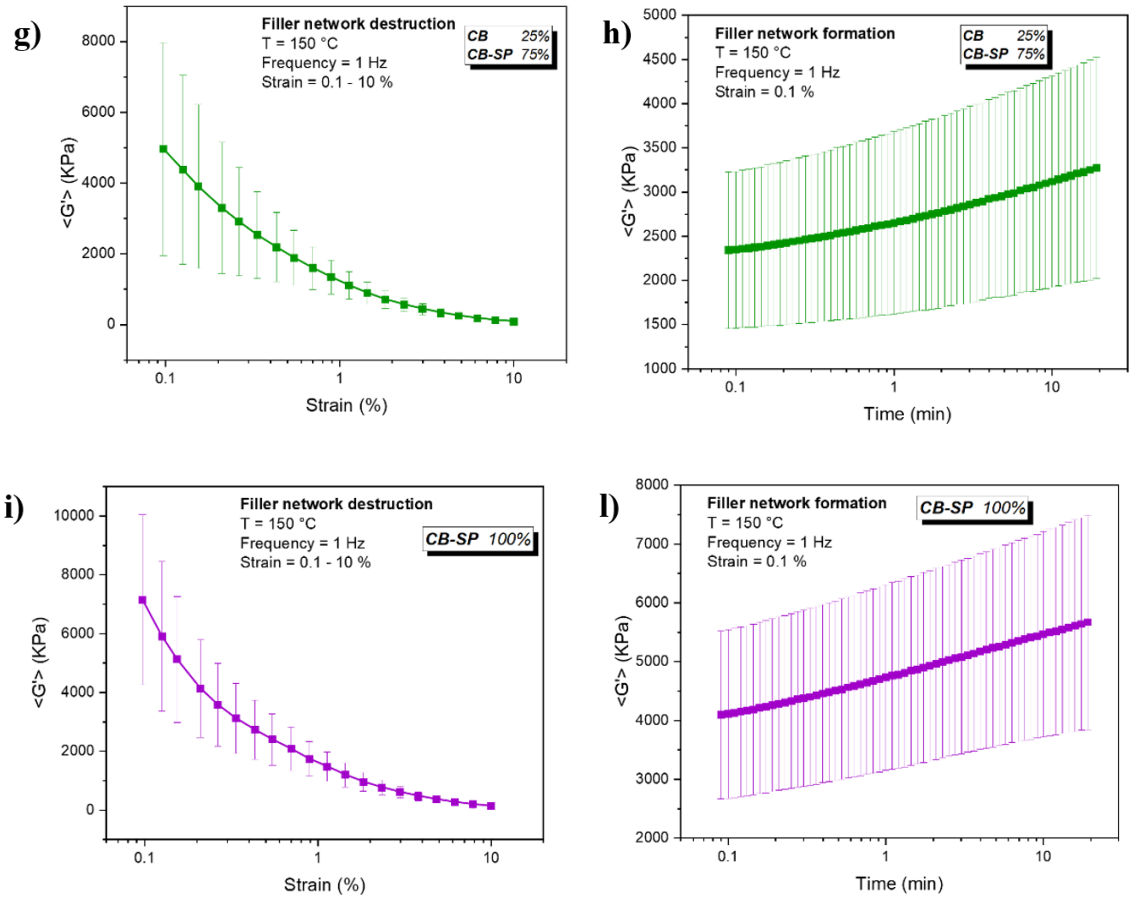

Figure 9.5 Flocculation study on samples of Table 9.1. (see Fig. 9.3).

G' vs strain of CB-SP 0% from Phase 2 with relative standard deviation (a), G' vs time of CB-SP 0% from Phase 3 with relative standard deviation (b), G' vs strain of CB-SP 25% from Phase 2 with relative standard deviation (c), G' vs time of CB-SP 25% from Phase 3 with relative standard deviation (d), G' vs strain of CB-SP 50% from Phase 2 with relative standard deviation (e), G' vs time of CB-SP 50% from Phase 3 with relative standard deviation (f), G' vs strain of CB-SP 75% from Phase 2 with relative standard deviation (g), G' vs time of CB-SP 75% from Phase 3 with relative standard deviation (h), G' vs strain of CB-SP 100% from Phase 2 with relative standard deviation (i), G' vs time of CB-SP 100% from Phase 3 with relative standard deviation (l).

The standard deviations, represented by the vertical lines in **Figure 9.5**, increase with the content of CB-SP. In particular, for filler systems with high content of SP, these values are of the same order of magnitude of the mean values of the G'. This trend is too high to be accepted and a possible interpretation of this result is that the oil based dispersions were not homogeneous enough. In fact, it could be possible that the energy, given to each sample by the rotational mixing in the speed mixer, was not enough to break the agglomerates of CB-SP. This evidence suggested that a modification of the procedure used to prepare the composites, whose recipes is reported in **Table 1,** is required. Therefore, in the next paragraph 9.3, an *ad hoc* procedure, developed at Polimi, is described.

9.3 Dispersions in oil of CB and CB-SP. Preparation Procedure 2

9.3.1 The oil dispersions

Dispersions based on oil and containing either CB or CB-SP had a total filler content of 50 pho (per hundred oil). This level was kept constant as in the procedure 1. Also in this case, CB was replaced with an increasing amount of CB-SP. In this study, only four binary mixtures were prepared. The functionalized filler contents were 0 % (the pristine carbon black), 33%, 66 % and 100 % (only CB-SP).

The recipes in pho of the compounds are reported in **Table 9.5**.

Table 9.5 Recipes of oil based dispersions with CB or CB/SP as fillers prepared with procedure 2

	Composite			
Ingredient	**CB-SP 0 % [pho]**	**CB-SP 33 % [pho]**	**CB-SP 66% [pho]**	**CB-SP 100% [pho]**
Paraffin oil	100	100	100	100
CB N326	50	33	17	0
CB N326 - SP	0	17	33	50
N326	0	16.15	31.35	47.5
SP	0	0.85	1.65	2.5

9.3.2 The new dispersion procedure developed at Polimi. Procedure 2

As anticipated in the previous paragraph 9.2, the procedure to prepare the oil-filler composites required the introduction of a pre-mixing step to improve the dispersibility of the filler in the oil matrix.

The new dispersion procedure (named Procedure 2) was developed at Polimi and it is sketched in the block diagram in **Figure 9.6**. First, in order to reduce the size of the CB/CB-SP agglomerates, the dry mixture was grinded into powder using a Moulinex® blender. This additional step required 20 seconds for the pristine CB while the grinding of CB-SP took 2 minutes. Then, the blended filler of each dispersion, whose recipes are reported in **Table 9.5**, was obtained by simply placing together the relative quantities of CB and CB-SP adducts in the speed mixer cups. After this, the paraffin oil was added to each cup and the mixtures were rotary mixed in the Hauschild Speedmixer DAC-150 (see Fig 9.2). The mixing steps in this case were two: 1 minute at 800 rpm, then 15 minutes at 3100 rpm (**Figure 9.6**).

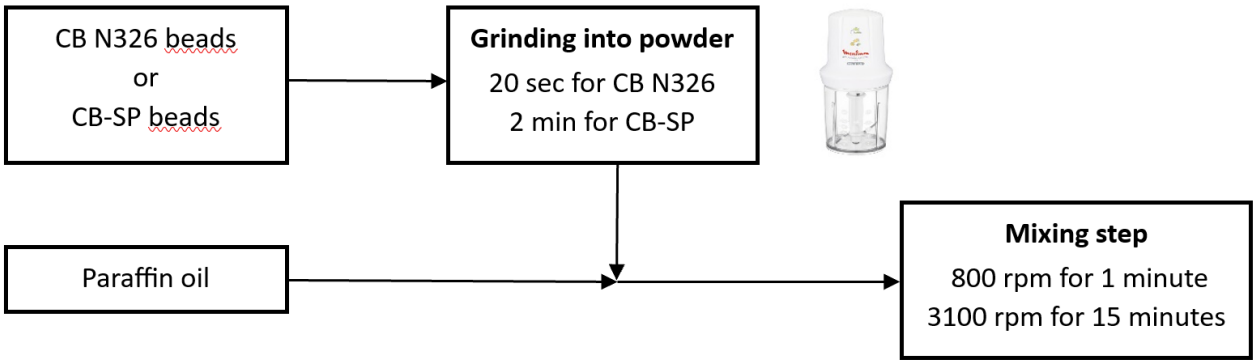

Figure 9.6 Procedure for preparing dispersion of CB/CB-SP in oil, according to Procedure 2

9.3.3 *Characterization of the composites prepared with Procedure 2*

Viscoelastic properties of the sample were characterized in oscillatory shear using a Dynamic Rubber Process Analyzer. An important change of the procedure was made. The three phases of the procedure proposed by Tunnicliffe[2] were performed at 50 °C instead of 150 °C. This was done in order to reduce the scattering of the results, particularly in the light of the hypothesis that the oil could be squeezed out from the oil/filler mixture. Also the length of the phases was changed: it was reduced to 2 min for Phase 1 and to 5 min for Phase 3. The phases of the new procedure are reported in **Figure 9.7**.

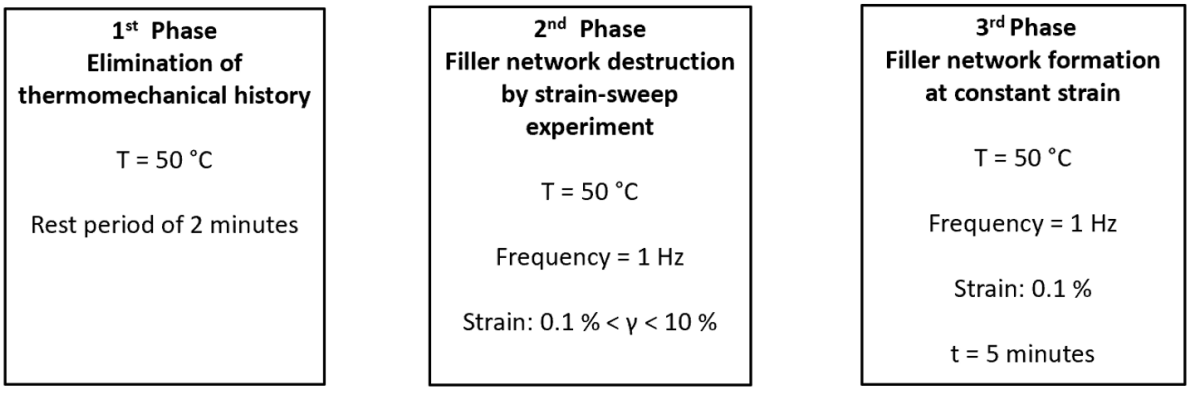

Figure 9.7 Block diagram of the procedure adopted for the flocculation study of composites prepared with Procedure 2

In the first phase (named Phase 1) the composite was kept at 50 °C for 2 minutes, in order to eliminate any possible influence of the thermal history of each sample. In the second phase, a strain sweep test was performed: a strain from 0.1 % to 10 % was applied at 50 °C with a constant value of frequency,

fixed at 1 Hz. The shear dynamic mechanical modulus as a function of the strain was measured. The extent of the filler network and its breakdown are studied.

In the last phase, each sample was kept at constant temperature (50 °C), frequency (1 Hz) and strain (0.1 %), to inspect the re-formation of the filler network. The values of G' were collected over 5 minutes.

Five specimens were analyzed for each sample. The arithmetic average and the standard deviation were calculated for the G' values determined in Phase 2 and in Phase 3.

The loss modulus at minimum strain (G' γ min), the loss modulus at 10% of strain (G' γ max), their difference (ΔG') and their difference normalized with respect to the values of G' γ min (ΔG'/G' γ min) are reported in **Table 9.6.** These data were taken from Phase 2.

Table 9.6 G' γ min, G' γ max, ΔG' and ΔG'/ G' γ min from Phase 2 of the strain sweep experiments on samples of Table 9.5

	CB/SP 0%	**CB/SP 33%**	**CB/SP 66%**	**CB/SP 100%**
G' γ min (kPa)	495.7	279.7	278,1	661.0
G' γ max (kPa)	2.9	0.9	12.9	2.3
ΔG' (kPa)	492.8	277.8	265.2	658.7
ΔG'/ G' γ min	0.994	0.993	0.954	0.997

In **Table 9.7**, the loss modulus measured at the beginning of the experiment, (G' MIN), the loss modulus after 5 min (G' MAX), their difference (ΔG') and their difference normalized with respect to the values of G' MAX are resumed. These data were obtained in Phase 3.

Table 9.7 G' MIN, G' MAX, ΔG' and ΔG'/ G' MAX of each sample of the filler network re-formation

	CB/SP 0%	**CB/SP 33%**	**CB/SP 66%**	**CB/SP 100%**
$G'_{t=5\ min}$ (kPa) [= G' MAX]	333.4	242.1	323.7	466.4
G'_{t0}(kPa) [=G' MIN]	186.3	65.4	121.9	389.6
ΔG' (kPa)	147.1	176.7	201,8	76.8
ΔG' / $G'_{t=5\ min}$	0.441	0.703	0.623	0.165

The mean values of G' vs strain determined in Phase 2 and the ones of G' vs time determined in Phase 3 are in **Figure 9.8**, Fig. 9.8a and Fig. 9.8b respectively.

In particular, in **Figure 9.8a**, the modulus G' at minimum strain (G' γ min) was obtained at the end of the Phase 1, so after 2 min at 50 °C while the values at high strain (G' γ max) were registered at the end of the strain sweep, so at the end of Phase 2.

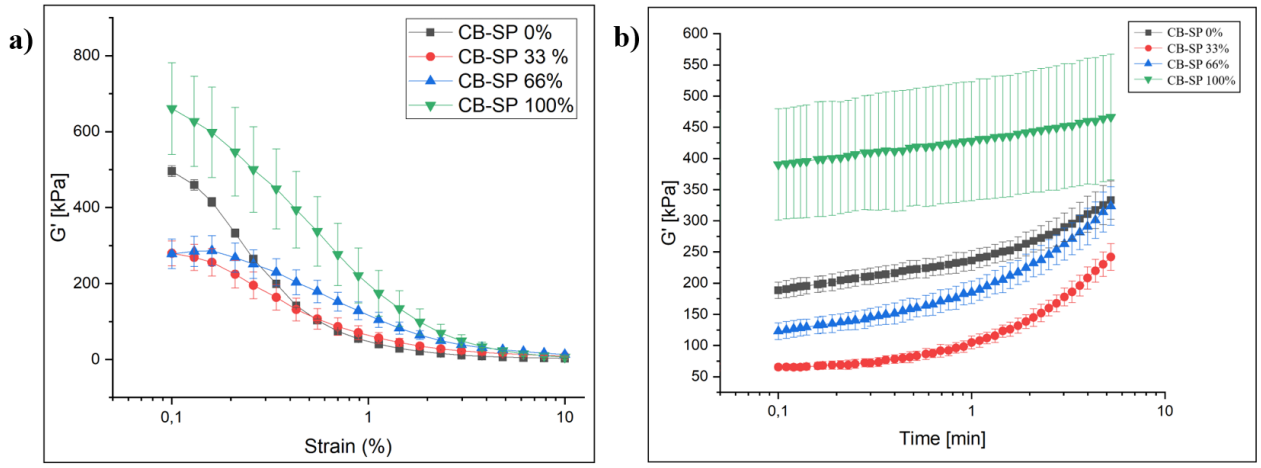

Figure 9.8 Flocculation study on samples of Table 9.5. (see Fig. 9.7). G' vs strain from Phase 2 (a), G' vs time from Phase 3 (b)

As shown in **Figure 9.8**, the standard deviation is lower than the one of the composites prepared with Procedure 1 (**Figure 9.5**). In particular, the value of the standard deviation was reduced, at least, of one order of magnitude, for each compound, in both Phase 2 and 3.

By exploring the results of Phase 2 of the flocculation study it can be commented as follow. There is no monotonic behaviour of the value of G' vs strain with respect to the content of SP. In fact, the composites with 33% and 66% of CB-SP (the red and blue lines) show a significant reduction in G' γ min compared to the compound with only CB (the black one). On the other side, the composite with 100% CB-SP (the green line) shows a higher G' γ min value than that of the composite with CB. Also in this case, a possible interpretation is the following: for composites with small amount of functionalized filler, the reduction of the surface area plays the main role, while, for the composites with high content of the filler it seems that the interactions among the OH groups prevail.

It is indeed worth commenting that this behaviour and trend are the same observed for the rubber composites analyzed in Chapter 8, as if, with the modified procedure, the oil could remain in the composite and could act as the matrix of the composite, analogously to the rubber.

9.4 Conclusions

Dispersions of CB and CB-SP in paraffin oil were prepared by using the procedure proposed by Robertson[1]. They were then analyzed in a rubber process analyzer by using two procedures: (i) the one described by Tunnicliffe[2], (ii) a procedure developed at Polimi. The procedure developed at Polimi was aimed at improving the filler dispersion and maintaining constant the composition of the composite during the measurement, preventing the migration of the oil, squeezed out from the disk in the rheometer. It is worth reminding that the aim of this work was to investigate the filler networking phenomenon promoted by CB and by CB-SP, by using a quick analytical method.

On the basis of the results of this Chapter 9, some conclusions can be drawn. They should be seen as working hypotheses, which should be confirmed by further experiments. They can be summarized as follows:

- The method discussed in this Chapter highlights that the functionalization of CB with SP strongly influences the rheological behaviour of the composites
- The results of the rheological measurements depend heavily on the experimental protocol adopted. In particular: grinding of the filler is recommended to reduce the particle size and to favor the dispersion of the filler. Moreover, a low temperature could be used for the rheological experiments, to prevent the oil migration
- The rheological results obtained by simply using the Robertson – Tunnicliffe protocol, without any modification, are affected by a large standard deviation, particularly by increasing the amount of CB-SP in the composite
- The same results observed with the rubber composites (see Chapter 8), with an acceptable standard deviation, were obtained by grinding the filler powder and by using 50°C as the temperature for the rheological experiments. Thes experimental conditions could favor the analysis of a homogenous oil/filler composite.
- "The same results" written in the previous point means that the rheological behaviour seems to depend on the surface area of the filler as well as on the interactive ability of the OH groups on its surface: the latter aspect prevails at large functionalization extent, by using 100% of CB-SP. Moreover, the trends in **Figure 9.8** can be compared with the ones obtained in rubber matrix (**Figure 8.4**). Also the values of the loss modulus of the oil based composites show the competition of the effects of the reduction of the filler system surface area and the increasing of OH-groups.
- By examining the results obtained by using the Robertson – Tunnicliffe protocol, without any modification, although in the presence of a large standard deviation, one can observe that the

filler networking phenomenon occurs in the presence of a larger amount of SP on the CB surface.

Final comments could be made.

The Robertson – Tunnicliffe protocol could allow the direct interaction of the filler particles: a filler cake is analyzed, with the oil squeezed out form the disk in the rheometer. An inhomogeneity of the composite must be expected (moreover, the filler was not grinded). However, this procedure could allow to highlight the interactive ability of the functional groups grafted on the CB surface by the pyrrole methodology.

The modified procedure applied on the oil based composites could be used, in place of the procedure applied on the rubber composites, achieving comparable results, thus allowing a quicker investigation of novel composite materials.

References

[1] N. Warasitthinon, A.C. Genix, M. Sztucki, J. Oberdisse, C. G. Robertson; The Payne Effect: Primarily Polymer-Related Or Filler-Related Phenomenon?. Rubber Chemistry and Technology 1 October 2019; 92 (4): 599–611

[2] Tunnicliffe, L. B. et al. Flocculation and viscoelastic behaviour in carbon black-filled natural rubber. Macromol. Mater. Eng. 299, 1474–1483 (2014).

[3] F. Moriggi, M. Galimberti. Adduct of sp2 carbon allotropes. From a DFT study to their use as reinforcing filler for elastomer nanocomposites and substrates for single atom catalyst. 2023.

[4] M. Galimberti, Course of "Chemistry for elastomer composites", Polytechnic University of Milan, 2020.

Chapter 10
Functionalized carbon black in rubber compound

10.1 Introduction

This chapter is about the study of elastomeric composites based on isoprene rubber (IR) reinforced with CB and CB-SP adduct and cured with a sulphur based system.

IR is poly(1,4-cis-isoprene), carbon black is the N326 provided by Birla Carbon and functionalized CB is the one described in Chapter 7. The sulphur based system was based on sulfur and activators and accelerators such as ZnO and a sulphenamide.

Pristine carbon black filler was replaced with an increasing amount of the CB-SP adduct and the composites' properties were studied before and after vulcanization.

The preparation of the composites was done by melt bending in a Brabender® type internal mixer.

The flocculation study was performed first with RPA 2000 instrument at 150 °C for 10 minutes to prevent vulcanization, then composites were vulcanized at 170 °C for 10 minutes in the same apparatus.

Dynamic-mechanical properties were analyzed by applying sinusoidal stresses, at constant frequency, both in axial and shear direction to determine E', E'' and Tan Delta.

10.2 Preparation of IR-based composites filled with CB and CB-SP at different relative ratios

IR-based compounds were prepared with carbon black content of 50 phr (per hundred rubber). The amount of filler was maintained constant in all the composites. Hence CB was replaced by different amounts of CB-SP from 0 % (the pristine carbon black) to 100 % (in absence of non-functionalized filler).

The composites were with a conventional vulcanization system with a ratio of sulphur to accelerator equal to 2.9.[1]

The recipes are in **Table 10.1.**

Table 10.1 Recipes of IR-based compounds with CB or CB/SP as fillers

Recipes in phr	CB-SP 0 % [phr]	CB-SP 25 % [phr]	CB-SP 50% [phr]	CB-SP 75% [phr]	CB-SP 100% [phr]
IR	100	100	100	100	100
CB N326	50	37.5	25	12.5	0
CB N326 - SP	0	12.5	25	37.5	50
N326	0	12.175	24.25	36.25	47.5
SP	0	0.325	0.75	1.25	2.5
Stearic acid	2	2	2	2	2
ZnO	4	4	4	4	4
6-PPD	2	2	2	2	2
TBBS	1.8	1.8	1.8	1.8	1.8
Sulphur	2	2	2	2	2

In the **Table 10.2**, for each composite, the content of serinol pyrrole and the values of surface area in the filler system are reported. These parameters were calculated as the weighted average of the values of the pristine CB and the pure CB-SP. The amount of SP in CB-SP was evaluated by TGA, while the surface area values were obtained through BET analysis[2]. The parameters related to the pristine CB are the one in the "0%" column of **Table 10.2**, while, the data of the CB-SP adduct are reported in the "100%" column of the same **Table 10.2**.

Table 10.2 Serinol pyrrole content and values of surface area in the filler system obtained with TGA and BET analysis[2]

	CB/SP content in the filler system[a,b]				
	0%	**25%**	**50%**	**75%**	**100%**
SP content in the filler system [phc][c]	0	1.1	1.9	3.3	4.8
surface area of the filler system NSA [m^2/g]	77	72	68	65	60

[a] filler system = CB + CB/SP, [b] SP content in CB-SP = 4.8, [c] phc = per hundred carbon

10.2.1 *Preparation procedure*

Starting from the composites analyzed in Chapter 8, that are also called "Masterbatch", the anti-ozonant, the activators and the curing agents were added in the same Brabender® type internal mixer. The chamber was heated at 50 °C and then the Masterbatch was inserted and mixed for 1 min to prepare the compound for the addition of the ingredients. They were added in two steps keeping the temperature fixed at 50 °C. First, ZnO, Stearic acid and 6-PPD were inserted, then TBBS and sulphur were added. After both the additions, 2 minutes mixing was carried out. The whole mixing procedure is reported in **Figure 10.1**.

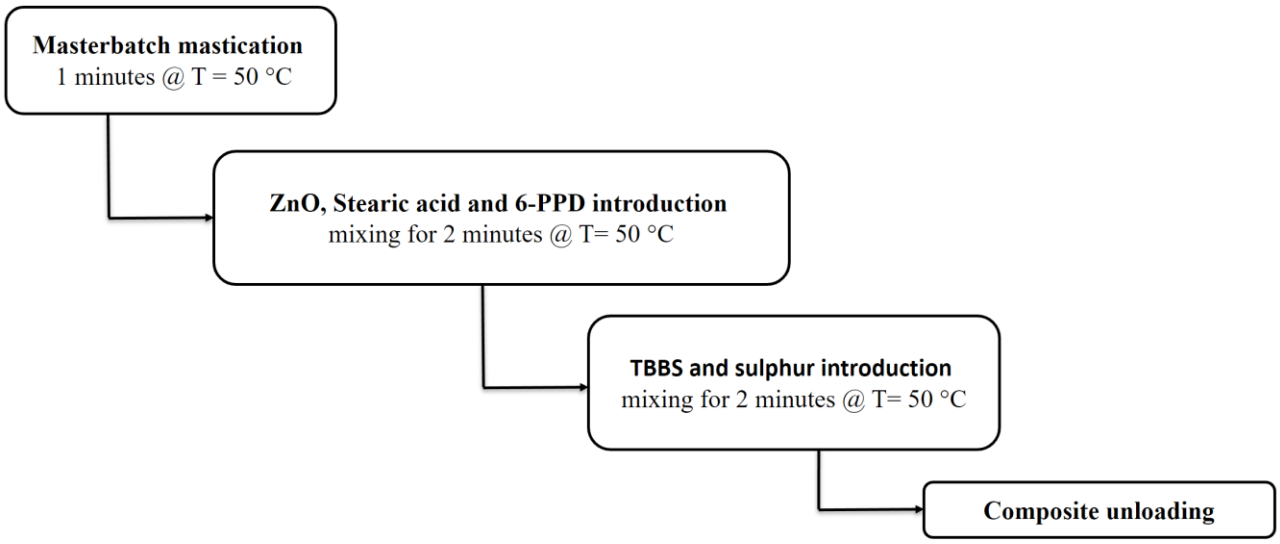

Figure 10.1 Mixing procedure for un-crosslinked IR composites with curing agents

10.3. Flocculation study on un-crosslinked composites

Viscoelastic properties of the sample were characterized in oscillatory shear using a Dynamic Rubber Process Analyzer (RPA). The procedure applied was the one proposed by Tunnicliffe[3], used in Chapter 8, at a lower temperature, 100°C, to prevent vulcanization.

After 10 minutes at 100 °C (Phase 1), in order to eliminate the influence of the thermo-mechanical history of the sample, a strain sweep test (Phase 2) was performed, from 0.1 % to 10 % strain at 100 °C, with a constant value of frequency, fixed at 1 Hz, to inspect the non linearity of G' modulus, i.e. the disruption of the filler network. Then, in the Phase 3, each sample was kept at constant temperature (100 °C), frequency (1 Hz) and strain (0.1 %). The re-formation of the filler network was analyzed, over 20 minutes, measuring the values of G'.

Three specimens were analyzed for each sample. The arithmetic average and the standard deviation were calculated for the G' values determined in Phase 2 and in Phase 3.

The storage modulus at minimum strain (G' γmin), the storage modulus at 10% of strain (G' γ max), their difference (ΔG') and their difference normalized with respect to the values of G' γ min (ΔG'/G' γ min) are reported in **Table 10.3**. These data were taken from Phase 2.

Table 10.3 G' γ min, G' γ max, ΔG' and ΔG'/ G' γ min from Phase 2 of the strain sweep experiments on Samples of Table 10.1

	CB/SP 0%	**CB/SP 25%**	**CB/SP 50%**	**CB/SP 75%**	**CB/SP 100%**
G' γ min (kPa)	643.2	600.9	589.9	633.9	589.1
G' γ max (kPa)	194.4	199.4	201.0	210.6	210.7
ΔG' (kPa)	448.8	401.6	388.9	423.3	378.3
ΔG'/G' γ min	0.698	0.668	0.659	0.668	0.642

In **Table 10.4**, the storage modulus measured at the beginning of the experiment, (G' MIN), the storage modulus after 20 min (G' MAX), their difference (ΔG') and their difference normalized with respect to the values of G' MAX are resumed. These data were obtained in Phase 3.

Table 10.4 G' MIN, G' MAX, ΔG' and ΔG'/ G' MAX of each sample of the filler network re-formation in Phase 3

	CB/SP 0%	**CB/SP 25%**	**CB/SP 50%**	**CB/SP 75%**	**CB/SP 100%**
$G'_{t=20\ min}$(kPa) [= G' MAX]	739.2	709.1	678.0	725.4	650.8
G'_{t0} (kPa) [= G' MIN]	353.0	334.3	320.1	323.9	315.4
ΔG' (kPa)	386.1	374.9	357.9	401.5	335.4
$\Delta G'/G'_{t=20\ min}$	0.522	0.529	0.528	0.554	0.515

G' vs strain determined in Phase 2 and G' vs time determined in Phase 3 are in **Figure 10.2**, Fig. 10.2a and Fig. 10.2b respectively.

In particular, in **Figure 10.2a**, the modulus G' at minimum strain (G' γ min) was obtained at the end of the Phase 1, so after 10 min at 100 °C while the values at high strain (G' γ max) were registered at the end of the strain sweep, so at the end of Phase 2.

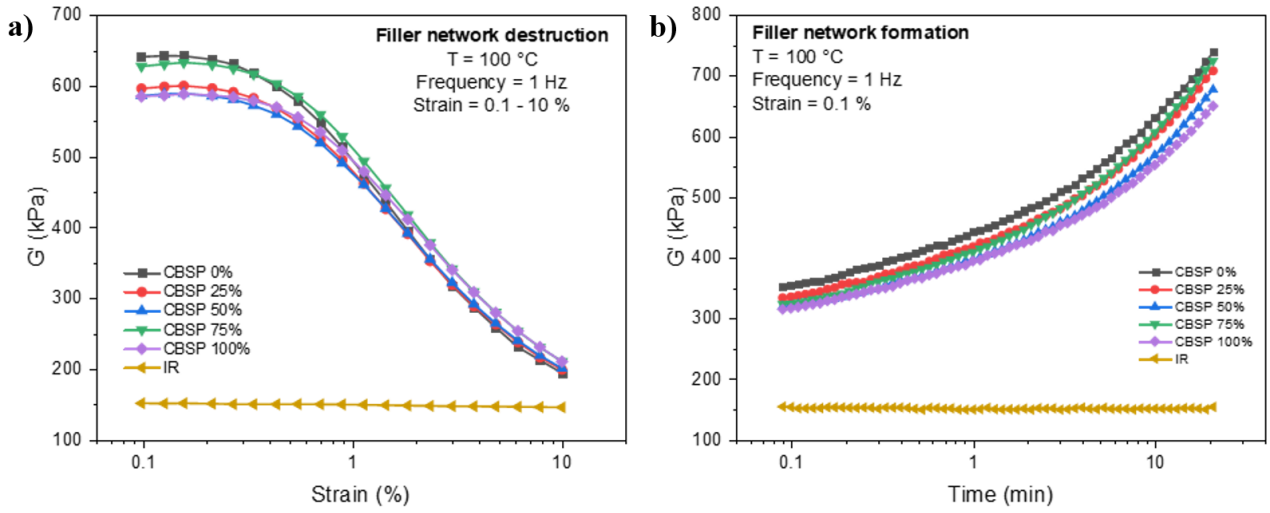

Figure 10.2 Flocculation experiment. G' vs strain % from Phase 2 (a), G' vs time from Phase 3 (b)

For all the composites (except the CB-SP 100 %), the value of $G'_{\gamma\ min}$ and the ratio $\Delta G'/G'_{\gamma\ min}$ monotonically decrease by increasing the amount of SP, and the curves of re-formation of the filler network (**Figure 10.2b)** show the same trend. Such behaviour is different from the one observed in Chapter 8, where tests were performed on masterbatches in the absence of low molecular weight ingredients, activators and vulcanizers. This difference can be attributed to the low molecular weight ingredients, which can interact with the OH groups on the CB surface and thus promote the dispersion of CB-SP.

10.4 Crosslinked IR-based composites filled with CB and CB-SP

10.4.1 Crosslinking

The composites were vulcanized withy the sulphur based system at 170 °C for 10 minutes in RPA 2000 instrument and analyzed with the methodology proposed in the following **Figure 10.3**.

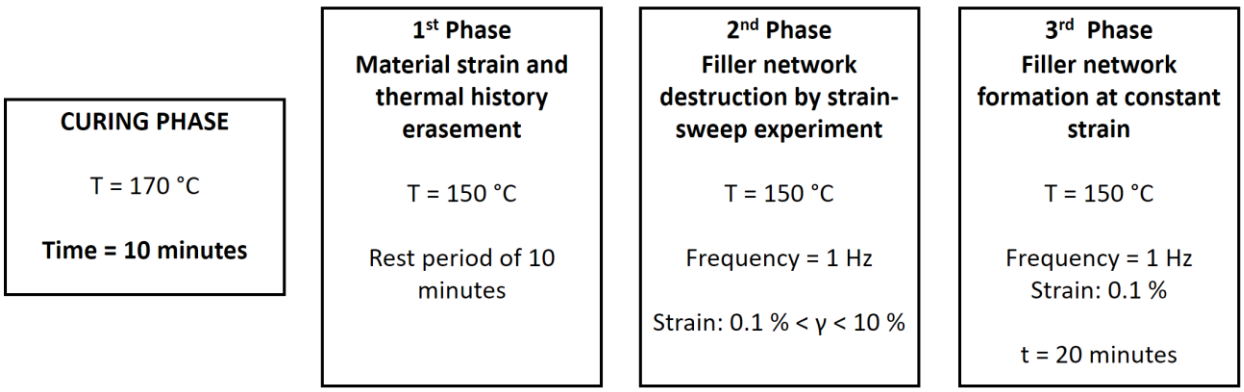

Figure 10.3 Block diagram of the procedure adopted for the flocculation study[3] including curing

The next **Table 10.5** reports the parameters obtained during the Curing Phase (**Figure 10.4a**). M_H is the highest achieved torque. It represents the highest crosslinking level reached in this phase. M_L is the lowest achieved torque. t_{S1} is the scorch time. It is the time required to increase the torque value of 1 dN/m. t_{90} is the time after which the 90 % of the maximum torque is achieved. It is also called optimum cure time. The curing rate parameter is calculated as the ratio between the (M_H - M_L) difference of the (t_{90} - t_{S1}) difference.

Table 10.5 Torque values, induction times (t_{s1}) and times to achieve the optimum level of vulcanization (t_{90}) obtained for rubber composites

	CB/SP 0%	**CB/SP 25%**	**CB/SP 50%**	**CB/SP 75%**	**CB/SP 100%**
M_H (dNm)	18.68	18.34	18.75	18.66	19.26
M_L (dNm)	2.02	2.12	2.16	2.22	2.18
M_H - M_L (dNm)	16.66	16.22	16.59	16.44	17.08
t_{S1} (min)	1.01	0.96	0.88	0.80	0.76
t_{90} (min)	2.26	2.05	1.87	1.68	1.62
Curing rate (dNm/min)	13.33	14.88	16.75	18.68	19.86

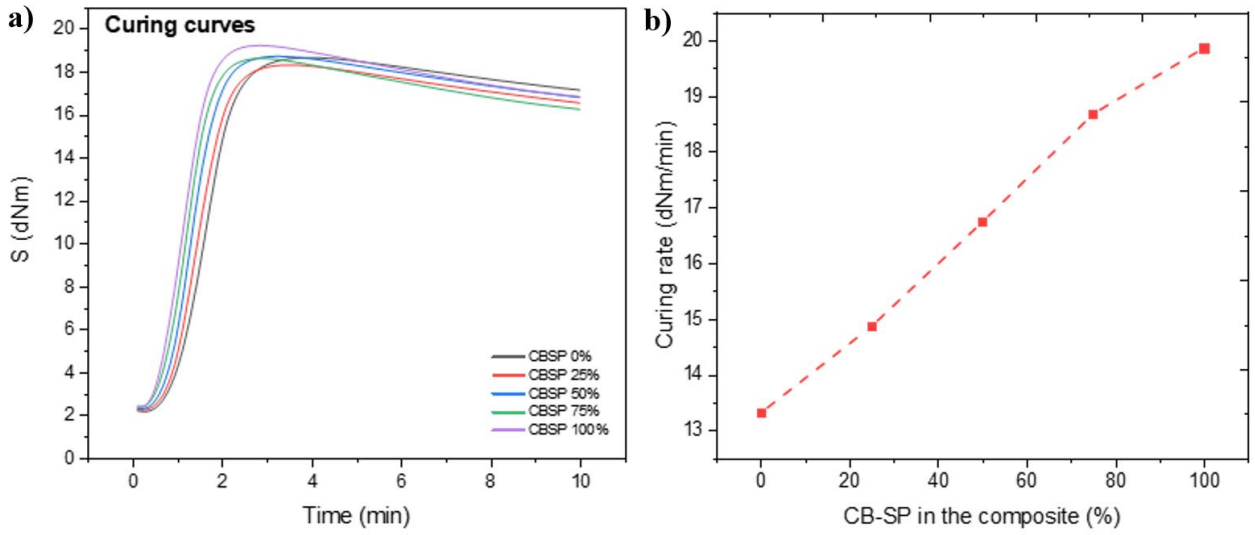

Figure 10.4 Rheometric curves: torque vs time (a) and Curing rate vs % CB-SP (b)

The values of M_L and M_H are very similar for the composites with and without CB-SP, with an appreciable increase for the composite with 100% CB-SP. Hence, serinol pyrrole did not led to higher viscosity and to higher crosslinking degree.

The presence of serinol pyrrole caused faster vulcanization kinetics, associated to lower t_{S1} and t_{90} values. The higher the amount of functionalized filler was, the more these trends were pronounced. Moreover, as shown in **Figure 10.4b**, curing rate increases linearly with the CB-SP content in the composite. The faster vulcanization could be ascribed to the presence of the basic nitrogen.
The reversion of vulcanization is evident in Figure 10.4a, in spite of the traditionally high amount of ZnO used. This could be due to the vulcanization temperature. Reversion is more pronounced for composites filled with CB-SP, which are characterized by a faster crosslinking.

10.4.2 Shear dynamic mechanical properties. Flocculation study

In order to study the flocculation of the vulcanized composites, Phase 1, 2 and 3 of the Tunnicliffe's procedure[3] sketched in the **Figure 10.3** were performed. After 10 minutes at 100 °C (Phase 1), in order to eliminate the influence of the thermo-mechanical history of the sample, a strain sweep test (Phase 2) was performed, from 0.1 % to 10 % strain at 100 °C, with a constant value of frequency, fixed at 1 Hz, to inspect the non linearity of G' modulus, i.e. the disruption of the filler network. Then, in the Phase 3, each sample was kept at constant temperature (100 °C), frequency (1 Hz) and strain (0.1 %). The re-formation of the filler network was analyzed, over 20 minutes, measuring the values of G'.
Three specimens were analyzed for each sample. The arithmetic average and the standard deviation were calculated for the G' values determined in Phase 2 and in Phase 3.
The storage modulus at minimum strain (G' γ min), the storage modulus at 10% of strain (G' γ max), their difference (ΔG') and their difference normalized with respect to the values of G' γ min (ΔG'/G' γ min) are reported in **Table 10.6**. These data were taken from Phase 2.

Table 10.6 G' γ min, G' γ max, ΔG' and ΔG'/ G' γ min from Phase 2 of the strain sweep experiments on Samples of Table 10.1 after curing

	CB/SP 0%	**CB/SP 25%**	**CB/SP 50%**	**CB/SP 75%**	**CB/SP 100%**
G' γ min (kPa)	2017.7	1948.4	1952.8	1847.2	1827.1
G' γ max (kPa)	1249.3	1215.5	1245.2	1201.9	1249.7
ΔG' (kPa)	768.4	732.9	707.5	645.3	577.4
ΔG'/G' γ min	0.381	0.376	0.362	0.349	0.316

In **Table 10.7**, for the vulcanized composites, the storage modulus measured at the beginning of the experiment, (G' MIN), the storage modulus after 20 min (G' MAX), their difference (ΔG') and their

difference normalized with respect to the values of G' MAX are resumed. These data were obtained in Phase 3.

Table 10.7 G' MIN, G' MAX, ΔG' and ΔG'/ G' MAX of each sample from Phase 3 of the filler network re-formation

	CB/SP 0%	**CB/SP 25%**	**CB/SP 50%**	**CB/SP 75%**	**CB/SP 100%**
$G'_{t=20\ min}$(kPa) [= G' MAX]	2009.8	1947.8	1951.5	1832.0	1813.7
G'_{t0} (kPa) [= G' MIN]	1745.7	1692.5	1715.3	1624.4	1648.6
ΔG' (kPa)	264.1	255.3	236.2	207.7	165.1
$\Delta G'/G'_{t=20\ min}$	0.131	0.131	0.121	0.113	0.091

G' vs strain determined in Phase 2 and G' vs time determined in Phase 3 are in **Figure 10.5**, Fig. 10.5a and Fig. 10.5b respectively.

In particular, in **Figure 10.5a**, the modulus G' at minimum strain (G' γ min) was obtained at the end of the Phase 1, so after 10 min at 150 °C while the values at high strain (G' γ max) were registered at the end of the strain sweep, so at the end of Phase 2.

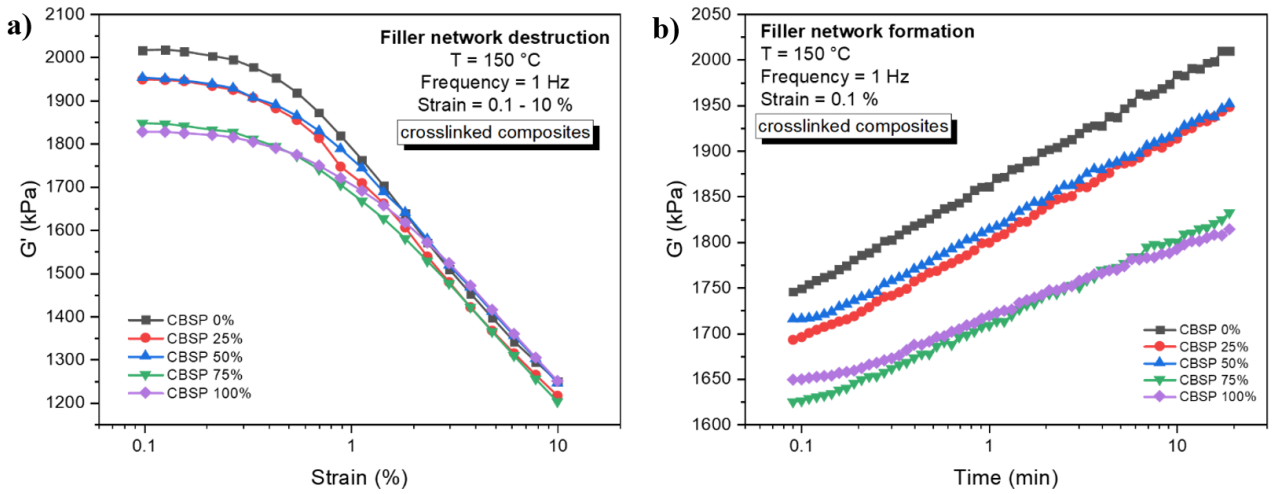

Figure 10.5 Flocculation studies G' vs strain % from Phase 2 (a), G' vs time from Phase 3 (b)

Looking at the graph in **Figure 10.5a**, it is clear that the crosslinked composites containing CB-SP show a reduction of the Payne effect[3] compared to the composite containing pristine CB. The reduction is more pronounced as the content of CB-SP increases.

In **Figure 10.6** a comparison is shown among the graphs from Phase 2 for the masterbatches discussed in Chapter 8 (Fig. 10.6a) for the composites of the present Chapter, uncrosslinked (Fig. 10.6b) and crosslinked (Fig. 10.6c).

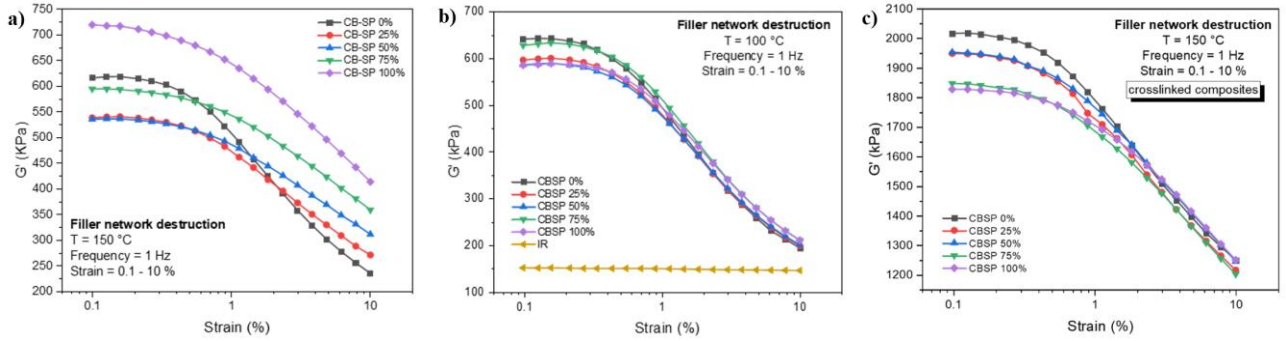

Figure 10.6 G' vs strain % of Masterbatches (see Fig. 8.4a) (**a**), G' vs strain % of un-crosslinked Masterbatches with vulcanization agents (see Fig. 10.2a) (**b**), G' versus strain % of cured composites (see Fig. 10.5a) (**c**)

It is evident that the dependence of G' vs strain is different for the three classes of composites. The composites with 100% CB-SP give the maximum value of G' γ min in the masterbatch without other ingredients and the minimum value of G' γ min in the composites with other ingredients, particularly after vulcanization.

Also the graphic of the curves obtained from Phase 3 is different for the masterbatch and for the composites, as it is shown in Figure 10.7.

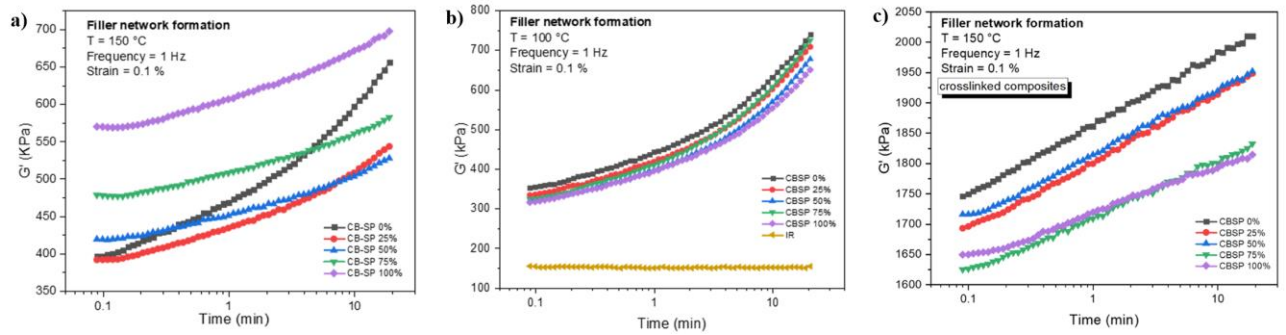

Figure 10.7 G' vs time of Masterbatches (see Fig. 8.4b) (**a**), G' vs time of un-crosslinked Masterbatches with vulcanization agents (see Fig. 10.2b) (**b**), G' versus time of cured composites (see Fig. 10.5b) (**c**)

This is a clear indication that the presence of other ingredients and, in particular, the vulcanization help the dispersion of CB-SP. Moreover, it could be hypothesized that the basic nitrogen can lead to

more efficient interactions of CB with the polymer chains, reacting with the sulphur chains and favoring the formation of chemical bonds between sulphur and the surface of CB, as hypothesized by the Group[5] where this thesis was done.

10.4.3 *Dynamic-mechanical properties from axial compression tests*

The dynamic-mechanical properties of the cured composites in **Table 10.1** were evaluated by axial compression tests. The values of E', E'' and Tan Delta were calculated at three different values of frequency (1, 10 and 100 Hz) and at three different values of temperature (10 °C, 23 °C and 70 °C). The detailed procedure applied for their calculations is described in the Experimental Section of Chapter 11.

The data obtained at 1, 10 and 100 Hz are reported in the following **Table 10.8**, **Table 10.9**, and **Table 10.10**, respectively.

Table 10.8 E', E'' and Tan Delta evaluated for each composite at 10, 23 and 70 °C through axial compression tests at 1 Hz

	CB/SP 0%	**CB/SP 25%**	**CB/SP 50%**	**CB/SP 75%**	**CB/SP 100%**
E'@10°C	4.31	4.06	4.14	4.16	4.45
E"@10°C	0.52	0.51	0.52	0.54	0.52
Tan Delta@10°C	0.12	0.12	0.12	0.13	0.12
E'@23°C	4.13	3.88	3.95	3.97	4.23
E"@23°C	0.46	0.44	0.45	0.47	0.47
Tan Delta@23°C	0.11	0.11	0.12	0.12	0.11
E'@70°C	4.10	3.81	3.87	3.87	4.16
E"@70°C	0,35	0.34	0.36	0.37	0.38
Tan Delta@70°C	0.09	0.09	0.09	0.09	0.09
ΔE' (E'@10°C -E'@70°C)	0.22	0.25	0.27	0.29	0.29

Table 10.9 E', E'' and Tan Delta evaluated for each composite at 10, 23 and 70 °C through axial compression tests at 10 Hz

	CB/SP 0%	**CB/SP 25%**	**CB/SP 50%**	**CB/SP 75%**	**CB/SP 100%**
E'@10°C	4.71	4.45	4.53	4.59	4.85
E"@10°C	0.69	0.68	0.69	0.70	0.67
Tan Delta@10°C	0.15	0.15	0.15	0.15	0.14
E'@23°C	4.45	4.19	4.25	4.30	4.57
E"@23°C	0.56	0.56	0.57	0.58	0.57
Tan Delta@23°C	0.13	0.13	0.13	0.14	0.12
E'@70°C	4.32	4.02	4.07	4.10	4.39
E"@70°C	0.39	0.39	0.40	0.42	0.42
Tan Delta@70°C	0.09	0.10	0.10	0.10	0.10
ΔE' (E'@10°C -E'@70°C)	0.39	0.43	0.46	0.48	0.47

Table 10.9 E', E'' and Tan Delta evaluated for each composite at 10, 23 and 70 °C through axial compression tests at 100 Hz

	CB/SP 0%	**CB/SP 25%**	**CB/SP 50%**	**CB/SP 75%**	**CB/SP 100%**
E'@10°C	5.32	5.05	5.13	5.21	5.46
E"@10°C	1.19	1.16	1.17	1.19	1.17
Tan Delta@10°C	0.22	0.23	0.23	0.23	0.21
E'@23°C	4.90	4.62	4.67	4.74	4.99
E"@23°C	0.87	0.85	0.86	0.88	0.85
Tan Delta@23°C	0.18	0.19	0.19	0.19	0.17
E'@70°C	4.56	4.27	4.32	4.39	4.66
E"@70°C	0.53	0.53	0.55	0.57	0.56
Tan Delta@70°C	0.12	0.12	0.13	0.13	0.12
ΔE' (E'@10°C -E'@70°C)	0.77	0.78	0.81	0.82	0.79

The difference between the values in the above Tables is subtle indeed.

The functionalization of CB with SP leaves substantially unaltered the axial dynamic mechanical properties of the composites. It can be observed that higher dynamic rigidity was obtained with CB-SP 100%.

In the following **Figure 10.6**, the values of the elastic modulus versus the frequency are reported for each temperature.

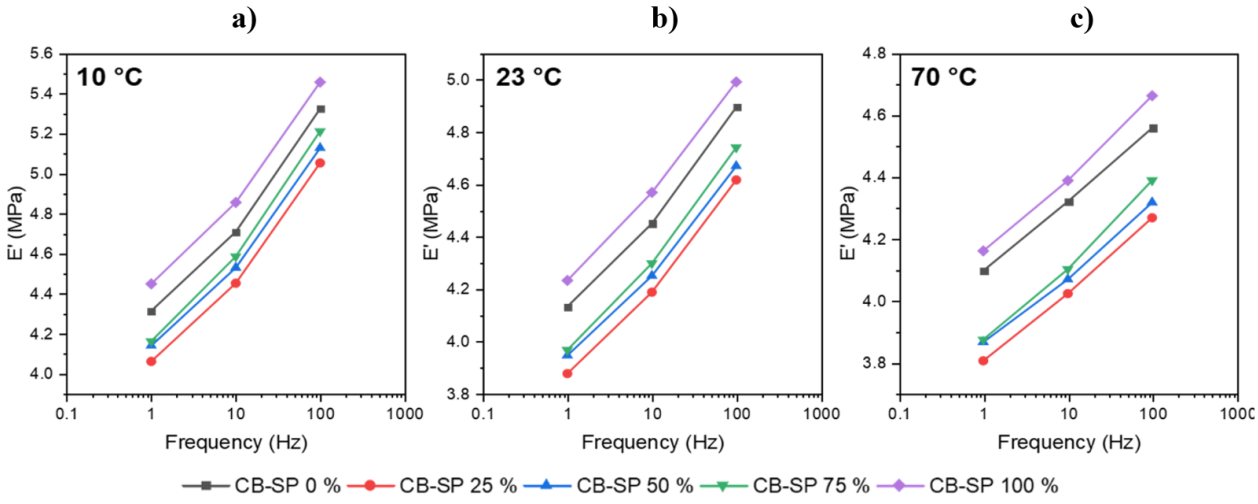

Figure 10.6 E' vs frequency at 10 °C (a), at 23 °C (b) and at 70 °C (c)

In the **Figure 10.6**, there is a monotonic trend of the E' with respect to the frequency. In fact, for each temperature, the elastic modulus of every composite increases with the frequency. Moreover, it is possible to underline that the highest values are registered for the lowest temperature and for the highest frequency (**Figure 10.6a**). The graphs confirm what was commented above: higher dynamic rigidity is observed with CB-SP 100%.

The values of Tan Delta versus the frequency are reported for each temperature in the following **Figure 10.7**.

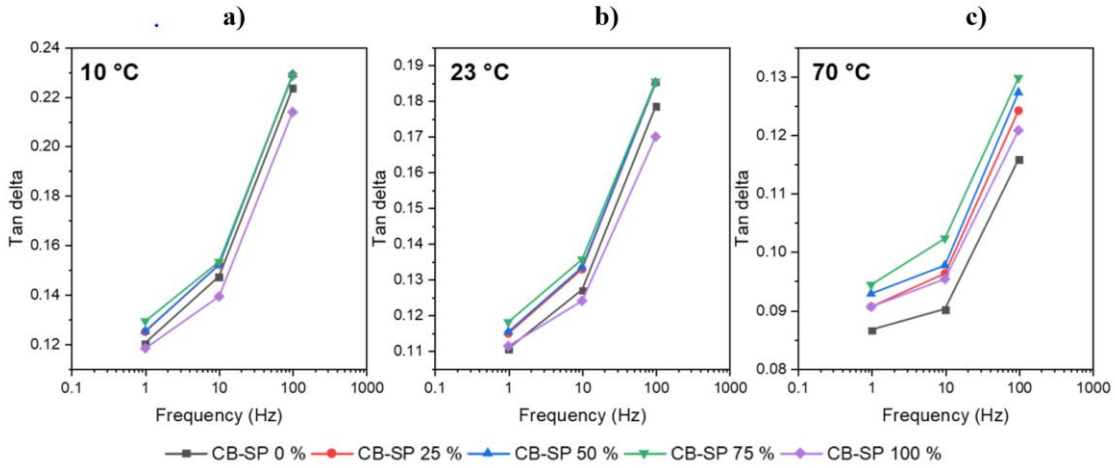

Figure 10.7 Tan Delta vs frequency at 10 °C (a), at 23 °C (b) and at 70 °C (c)

Also here in **Figure 10.7**, the values on the Y-axis increase monotonically with the frequency for each temperature. Indeed, the highest Tan Delta for all the composites is registered at the lowest temperature (10 °C) and at the highest frequency (100 Hz). The composite with CB-SP 100% shows the lowest hysteresis or a hysteresis close to that of the composite with CB pristine.

In the following **Figure 10.8**, the trends of E', E'' and Tan Delta (tan δ) versus the temperature are reported at 100 Hz.

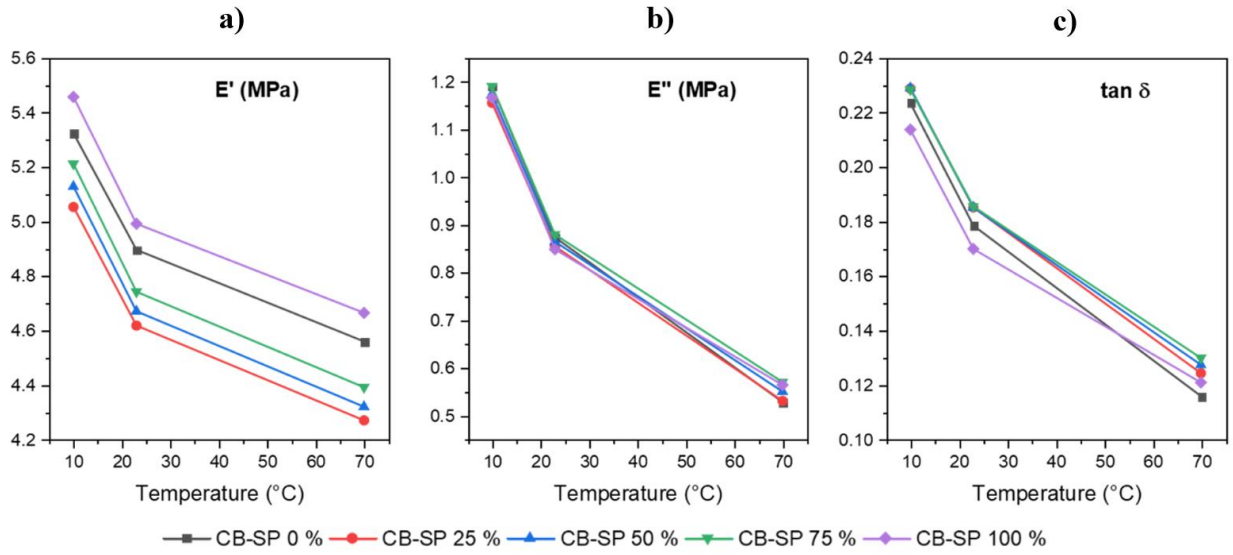

Figure 10.8 E' versus T (a), E'' versus T (b) and Tan Delta versus T (c) calculated at 100 Hz

By exploring the **Figure 10.8**, for each composite all the parameters decrease monotonically with the increasing of the temperature. The decrease of E' is obviously not due to the entropic elasticity but to the presence of the filler network.

Considering the values of the elastic modulus (**Figure 10.8a**), the composite with 100% CB-SP adduct shows the highest values of E' at each temperature. On the other hand, the composites prepared with the blended fillers have lower elastic modulus than the compound made with pristine CB. In this case, the lower is the amount of SP, the lower is the value of E'. However, the differences can be considered not remarkable. As already commented, the reduction of E' with CB-SP could be attributed to the reduction of surface area, whereas the increase with CB-SP 100% could be attributed to the prevailing effect of the OH functional groups.

In the **Figure 10.8c**, it appears that the composites with CB-SP 100% (the violet line) shows lower Tan Delta with respect to the composite prepared with the pristine CB at low temperatures and similar/higher at the highest temperature. The composites with mixtures of fillers (CB-SP 25 %, CB-SP 50 % and CB-SP 75 %) have always higher values of Tan Delta than the composite with pristine

CB. These results are in line with the values of E'. Also for the avlues of Tan delta, the differences are not remarkable.

10.5 Conclusions

Composites based on isoprene rubber (IR) were prepared by adding vulcanization agents, as described in **Table 10.1**, to the "Masterbatch" analyzed in chapter 8 using a Brabender® type mixer.

The aim of the work was to investigate the influence of so called small ingredients of a rubber compound, in particular polar species such as ZnO and stearic acid, on the behavior of Cb functionalized with OH groups.

Flocculation studies were performed before and after curing in a rubber process analyzer, following Tunnicliffe's procedure[3]. The flocculation studies were performed at two temperatures: at 100 °C to prevent vulcanization, then at 150 °C after vulcanization. Shear rheological experiments were performed.

The dynamic-mechanical properties of the vulcanized IR-composites were also analyzed by axial compression tests.

Some conclusions can be summarized as follows:

- So called small ingredients, likely in particular polar compounds (such as ZnO and stearic acid) acted as dispersing agents of CB-SP. In fact, the value of G' γ min of the CB-SP 100% was the highest in the Masterbatch, while it was the lowest for the composites charged with vulcanization agents (**Figure 10.6**).
- The reduction of the Payne effect[4] was registered both for the pre- and post-curing IR composites.
- the composite with 100% CB-SP adduct showed the highest values of E' at each temperature

In conclusion, the presence of OH groups grafted on the CB surface were beneficial for the composite properties.

So called small ingredients, likely in particular the polar ingredients, can interact with the OH groups on the CB surface.

In the composites discussed in this chapter, specific coupling agents were not used for CB-SP. In spite of that, the interesting/positive results mentioned above were obtained. Therefore, the OH functional groups could be better exploited by using a suitable coupling agent to link the filler with the polymer chains through covalent bonds.

References

[1] F. N.Linhares at. Al. Effect of different sulphur-based crosslink networks on the nitrile rubber resistance to biodiesel. Fuel.Vol.191, 130-139, 2017.

[2] F. Moriggi, M. Galimberti. Adduct of sp2 carbon allotropes. From a DFT study to their use as reinforcing filler for elastomer nanocomposites and substrates for single atom catalyst. 2023.

[3] Tunnicliffe, L.B.; Kadlcak, J.; Morris, M.D.; Shi, Y.; Thomas, A.G.; Busfield, J.J.C. Flocculation and viscoelastic behaviour in carbon black-filled natural rubber. Macromol. Mater. Eng. 2014, 299, 1474–1483, doi:10.1002/mame.201400117.

[4] M. Galimberti, Course of "Chemistry for elastomer composites", Polytechnic University of Milan, 2020.

[5] Musto, S., Barbera, V., Cipolletti, V., Citterio, A., & Galimberti, M. (2017). Master curves for the sulphur assisted crosslinking reaction of natural rubber in the presence of nano-and nano-structured sp2 carbon allotropes. *eXPRESS Polymer Letters*, *11*(6), 435-448.

Section III – Experimental part

Chapter 11

Experimental part

11.1 Materials

11.1.1. *Carbon Black*

Carbon Black (CB) N326 was from Birla Carbon S.p.a..

11.1.2. *Reagents and solvents*

Paraffin oil, tetrahydrofuran (THF), 2-propanol, methanol, distilled water, acetone, hexane, and ethyl acetate (all from Sigma-Aldrich, used as received) were used for the dispersions' tests.

11.1.3. Rubbers

Isoprene rubber (cis-1,4-polyisoprene)

11.1.4. *For rubber compounds preparation*

The following ingredients were used as received: ZnO (Zinc Oxide), Stearic acid (Sogis), (1,3-dimethyl butyl)-N'-Phenyl-p-phenylenediamine (6PPD) (Crompton), sulphur (Solfotecnica), N–tert-butyl-2-benzothiazyl sulfenamide (TBBS).

11.2 Functionalization of carbon black with serinol pyrrole

11.2.1 *General procedure*

Serinol-pyrrole was weighed in a vial and diluted in acetone. CB N326 beads was weighed in a single-neck round bottom flask. The SP/acetone solution and other acetone were added till all the CB was covered by the liquid phase. The flask with solution was sonicate for 15 min at room temperature with a 2 L ultrasonic bath (260 W). To remove acetone from CB/pyrrole compound the Rotavapor was used (40 °C for the bath, from 550 mbar to 50 mbar going down 50 by 50 mbar). The remaining compound without acetone was transferred in a 2-nek 250 ml round bottom flask that was equipped with a magnetic stirrer. In one neck some cotton was applied to retain possible pour losses. In the other was closed with the tube for the compressed air. The flask was inserted in an oil bath preheated at 160 °C. The stirring velocity was set at 235 rpm. The temperature of the bath went down a little. When the temperature came back to the set point the compressed air was started. The reaction took 2 hours. After this time the product was weighed.

The compound was put in a 1000 ml becher and about 300 ml of acetone was added. Stirring slowly to extract all the unreacted pyrrole. After about 30 min the compound was filtered with a filter on a tailed flask connected to a vacuum pump set at 450 mbar. 3 washing with acetone were performed. To remove completely the acetone the product was inserted in an oven at 80 °C for an hour.
Finally, the dry product was weighted.
In the following **Table 11.1** the materials and the reaction conditions of each CB-PyC adducts synthesis reaction are reported:

Table 11.1 Reagents and reactions conditions for the synthesis of CB N326-SP adduct

Adduct		**Reagents**	**Weight [g]**	**Temperature**[a]	**Reaction time**	**Stirring**
1°	**CB-SP**	CB N326	32.28	175 °C	2 h	235 rpm
		SP	3.23			
2°	**CB-SP**	CB N326	31.25			
		SP	3.13			

[a] Temperature measured in the oil bath

11.3 Dispersion of CB and CB-SP in oil matrices

11.3.1 *Initial procedure*

At the beginning of the test the procedure involved was the one proposed by Robertson et al.[1]. First of all, the paraffin oil was weighted in a polypropylene cup and CB and/or CB-SP. Then the fillers made of pure CB or CB-SP or the blend composition of each case were weighted and added to the same cup previously filled with the oil. The total amount of filler was maintained at a value of 50 p.h.o.
The compounds were then mixed for 1 min at 800 rpm, then for 1 min at 2200 rpm and in the end for 3 min at 3100 rpm without discharging the resulting dispersion. The mixing equipment was the Hauschild Speedmixer DAC-150.

11.3.2 *Optimized procedure*

The optimized procedure used was made by a preliminary step of manual grinding of CB and CB-SP with amethyst mortar to reduce as possible the dimension of the agglomerates of the fillers. Then the grinded fillers were weighted as for the initial procedure, but before the addition of the paraffin oil they were mixed in the Hauschild Speedmixer DAC-150 for 30 sec at 1000 rpm and then for 30 sec at 2000 rpm. After this the cup was discharged and the oil added by reaching also here the amount of

50 p.h.o. Finally, the compounds were then mixed for 1 min at 800 rpm, then for 1 min at 2200 rpm and in the end for 3 min at 3100 rpm in the same speedmixer.

11.4 Preparation of rubber composites

11.4.1 *IR-based composites*

100 phr of isoprene rubber (IR) were inserted into the brabender® internal chamber type mixer at temperature equal to 100°C for 1 minute. Then CB N326 (pristine or functionalized with SP) was added and mixed for 6 min at 100°C. The composite was then discharged. At this point, the internal mixer chamber's temperature was lowered at 50°C. The compound previously unloaded was added and mixed for 1 min. After that, stearic acid, ZnO and 6PPD were added and mixed for 2 min at 50°C. Then TBBS and sulfur were added and mixed for 2 min at T = 50°C. Finally, the compound was discharged at 50°C. The round per minute (rpm) of the mixer was set at a value of 60 for all the duration of the mixing.

11.5 Characterization techniques

11.5.1 *Thermogravimetric analysis*

According to the standard methodology ISO9924-1, TGA were performed under flowing N2 (60 mL/min) with a Mettler TGA SDTA/851 instrument. Samples were heated from 30 °C to 300 °C at 10 °C/min, maintained at 300 °C for 10 min and then heated up to 550 °C at 20 °C/min. After being kept at 550 °C for 15 min, they were further heated up to 900 °C at 10°C/min and kept at 900 °C for 30 min under flowing air (60 mL/min).

11.5.2 *Curing*

Curing was performed at 170 °C for 10 min. Monsanto oscillating disc rheometer (MDR 2000) (Alpha Technologies, Swindon, UK) was used to determine M_L (the minimum torque modulus), M_H (the maximum one), the modulus M_{final} at the end of the vulcanization, t_{S1} (the time required to have a torque equal to M_L + 1) and the time t_{90} required to achieve 90 % of the maximum modulus M_H, and therefore to achieve the optimum crosslinking network.

11.5.3 *Dynamic-mechanical test: Strain Sweep*

These tests were performed using a Monsanto R.P.A. 2000 rheometer in the torsion mode. The procedure applied is the following: RPA was charged with 5.0 g of crude compound and a first strain sweep (0.1 -25% shear strain amplitude) was performed at 50 °C and 1 Hz. Then, the sample was crosslinked at 170°C for 10 min at 17 Hz of frequency and, at the end of the formation of crosslinking

network, it was kept at 50°C for 10 minutes. Shear dynamic-mechanical properties were measured applying a 0.1-25% strain sweep at 10 Hz. Rubbers' dynamic-mechanical properties were evaluated calculating G', G'' and consequently Tan Delta.

11.5.4 *Axial compression tests*

Dynamic-mechanical properties in traction-compression mode were measured using an Instron dynamic device. A cured test piece with a cylindrical shape (length = 25 mm; diameter = 12 mm) was kept at set temperature (10°C, 23°C and 70°C) for the whole duration of the test. The sample underwent to compression-preloaded up to a 25% longitudinal deformation with respect to the initial length and then it was submitted to a dynamic sinusoidal strain with an amplitude of ± 3.5% with respect to the length under pre-load, with a 1 Hz frequency. The tests were repeated also at 10 and 100 Hz frequency. The rubber's dynamic-mechanical properties in compression were calculated in terms of dynamic storage modulus (E'), dynamic loss modulus (E'') and consequently loss factor (Tan Delta) values.

References

[1] N. Warasitthinon, A. C. Genix, M. Sztucki, J. Oberdisse, C. G. Robertson. The Payne Effect: Primarily Polymer-Related Or Filler-Related Phenomenon?. Rubber Chemistry and Technology 1 October 2019; 92 (4): 599–611

Chapter 12
Conclusions

The main objective of this thesis was to study a functionalized furnace CB, CBN326, with OH groups on its surface, as filler of elastomer nanocomposites.
The functionalized CB was conceived as a polar filler potentially suitable to reproduce the advantages of silica avoiding its drawbacks.

Pristine CB was functionalized with serinol pyrrole (SP), whose chemical structure is in Figure 12.1.

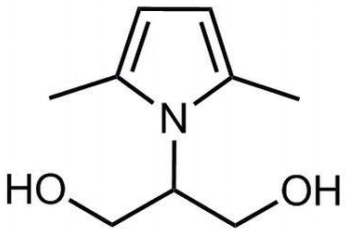

Figure 12.1 Chemical structure of serinol pyrrole

The synthesis of SP and the preparation of CB-SP adducts were performed without the use of solvents (a solvent was used at the lab scale to prepare the homogenous CB/SP mixture) and catalysts and were characterized by high atom efficiency and almost by the absence of wastes.
In particular, the functionalization of CB was performed with so called “pyrrole methodology”, inspired by the principles of green chemistry, just mixing CB and SP and giving thermal energy.
CB-SP adducts were investigated by means of thermogravimetric analysis. Values of phc (SP per hundred carbon) > 5 were evaluated and a degree of functionalization > 60% was calculated.
The BET measurements led to reveal the reduction of the surface area after the functionalization. The larger the amount of SP, the lower the value of the surface area.

The CB-SP adducts were used as fillers in elastomer composites. Poly-isoprene rubber (IR) was selected as elastomer.
Flocculation studied were performed, in the rubber matrix and in oil as the matrix.
The results can be summarized as follows.

IR-based composites with CB and CB-SP as fillers, in the absence of other ingredients. Flocculation studies

CB and CB-SP were used, as such or in mixture, as filler in the isoprene rubber matrix, in the absence of other ingredients.

Flocculation studies were performed, by applying a protocol available in the literature, proposed by Tunnicliffe[2], monitoring the G' modulus in three phases: after storage at high temperature, performing a strain sweep test and keeping the samples at high temperature. The results were taken as indication of the formation, disruption and re-formation of the filler network.

The filler networking was observed to increase by using CB-SP in place of CB and to decrease by using mixtures of this filler. The interpretation is that the reduction of surface area prevails over the interaction between the OH groups, unless CB-SP is being used as the only filler.

Paraffin oil based composites with CB and CB-SP as filler

Masterbatches were prepared in paraffin oil, by applying a protocol available in the literature, proposed by Robertson[1].

Flocculation studies were performed by applying a protocol available in the literature, proposed by Tunnicliffe[2], analogously to what reported above.

Results similar to those obtained in isoprene rubber were obtained by applying a modified protocol: CB and CB/SP were grinded and a moderate temperature was used for the tests, to avoid the migration of oil.

A monotonous increase of the G' values with the SP amount in the filler system was observed when the same protocol used in the rubber mixture was used. This could be due to the migration of oil, which leads to a direct contact among the filler particles.

In brief, the flocculation in oil highlights that the functionalization of CB with SP strongly influences the rheological behaviour of the composites. Moreover, the results of the rheological measurements depend heavily on the experimental protocol adopted.

IR-based composites with CB and CB-SP as fillers, in the presence of the other composite's ingredients

Composites based on isoprene rubber (IR) were prepared with CB and CB-SP, either as such or in mixture, in the presence of the other composite's ingredients.

Flocculation studies were performed on the uncured and cured composites. The following picture, taken from Figure 10.6 in Chapter 10, summarizes the effect of the composite's ingredients (from (a) to (b)) and then of the vulcanization (from (b) to (c)).

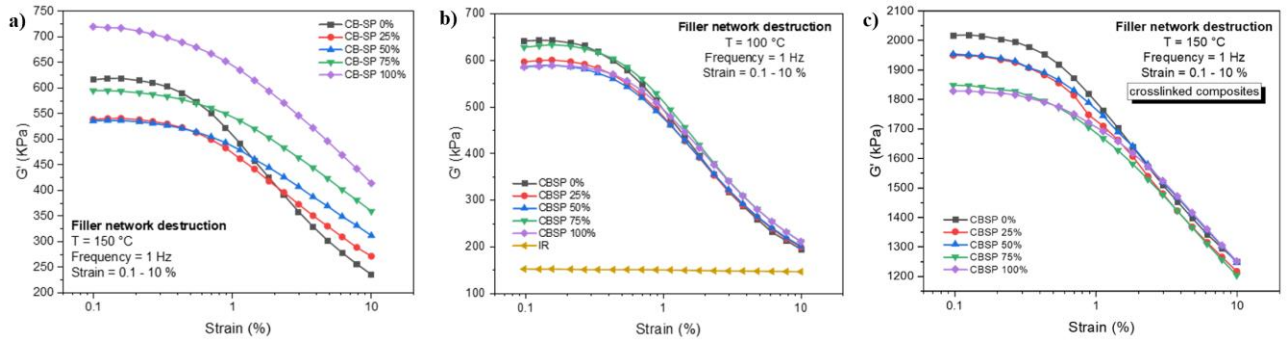

The Payne effect decreases from (a) to (b) to (c) and, in (c), the composite with CB-SP clearly becomes the composite with the lowest Payne Effect. It is worth underlining that

The composite with 100% CB-SP adduct showed the highest values of E' at each temperature. Hence, in spite of the lower surface area, the composite with CB-SP revealed the higher dynamic rigidity.

In a nutshell

The functionalization of CB with SP has a clear effect on the properties of a rubber composite and, more in general, of a composite based on a lipophilic matrix.

The introduction of OH functional groups onto the CB surface modifies the properties and the behavior of CB.

The functionalization reduces the surface area of CB. The reduction of surface area appears to have the prevailing effect up to a certain level of SP: reduction of Payne Effect.

The effect of the OH groups becomes evident above a certain level of SP.

The mentioned level of SP likely depends on the type of CB and of the matrix.

The effect of SP on the composite's properties depends on the chemical composition of the surrounding: so called small ingredients of the composite, in particular the polar ingredients, promote the reduction of the Payne effect, particularly in the vulcanized composite, which shows also the highest dynamic rigidity.

This thesis reveals the potentiality of the OH groups grafted on the CB surface. The next step appears to be the identification of a suitable coupling agent, to covalently link CB and the polymer chains.

References

[1] N. Warasitthinon, A.C. Genix, M. Sztucki, J. Oberdisse, C. G. Robertson. The Payne Effect: Primarily Polymer-Related Or Filler-Related Phenomenon? Rubber Chemistry and Technology 1 October 2019; 92 (4): 599–611

[2] Tunnicliffe, L.B.; Kadlcak, J.; Morris, M.D.; Shi, Y.; Thomas, A.G.; Busfield, J.J.C. Flocculation and viscoelastic behaviour in carbon black-filled natural rubber. Macromol. Mater. Eng. 2014, 299, 1474–1483, doi:10.1002/mame.201400117.

Ringraziamenti

First of all, I would like to thank prof. Maurizio Galimberti for having accepted the role of supervisor. Thank you very much, for your support because the work done during the thesis' period has been a great experience for me. I am very pleased for the opportunity you gave to me, I learned a lot. Thanks for your kind cooperation: my work wouldn't be so constructive without your competence and your guide in every situation. I am grateful for the opportunity to have worked with someone as talented as you.

A special thanks goes to Francesco Moriggi for the attention and interest with which he guided me in this research activity with the role of co-supervisor. I would express my sincere gratitude for your kind help. Your hard work to follow me step by step has been a great source to learn more about this project we started together. Thank for your assistance in all the difficulties I met during my work. I really appreciate your help in solving all problems I faced.

I would like to thank my family for their constant support, trust and love given me during all university years. In particular, I want to thank mom Cristina and dad Elio for having financed my studies, without ever underlining it or making it weigh.

A dutiful thanks goes to my girlfriend, Alice. Thank you for all the love and the support with which you have allowed me to face the most difficult challenges. I want to thank you for always believing in me, for always being by my side and for your constant support given. Also, you taught me to believe in myself more, thus allowing me to realize better than my I can ever imagine.

Last thanks to Politecnico of Milan for the places where I have studied in these years. The structure of the university allows me to grow both as engineer and as human.